

Spring 5-12-1961

# Practical Analysis of Blocking Oscillators

Richard D. Griffith

Follow this and additional works at: [https://digitalrepository.unm.edu/ece\\_etds](https://digitalrepository.unm.edu/ece_etds)



Part of the [Electrical and Computer Engineering Commons](#)

---

## Recommended Citation

Griffith, Richard D.. "Practical Analysis of Blocking Oscillators." (1961). [https://digitalrepository.unm.edu/ece\\_etds/327](https://digitalrepository.unm.edu/ece_etds/327)

This Thesis is brought to you for free and open access by the Engineering ETDs at UNM Digital Repository. It has been accepted for inclusion in Electrical and Computer Engineering ETDs by an authorized administrator of UNM Digital Repository. For more information, please contact [disc@unm.edu](mailto:disc@unm.edu).

UNIVERSITY OF NEW MEXICO-UNIVERSITY LIBRARIES



A14429 085363

PRACTICAL  
ANALYSIS OF  
BLOCKING  
OSCILLATIONS

---

GRIFFITH

378.789  
Un3Ogri  
1961  
cop. 2

THE LIBRARY  
UNIVERSITY OF NEW MEXICO



Call No.

378.789  
Un30gri  
1961  
cop.2

Accession  
Number

274113



UNIVERSITY OF TORONTO

LIBRARY  
OF  
THE  
UNIVERSITY OF TORONTO  
128  
ST. GEORGE STREET  
TORONTO, CANADA

UNIVERSITY OF NEW MEXICO LIBRARY

MANUSCRIPT THESES

Unpublished theses submitted for the Master's and Doctor's degrees and deposited in the University of New Mexico Library are open for inspection, but are to be used only with due regard to the rights of the authors. Bibliographical references may be noted, but passages may be copied only with the permission of the authors, and proper credit must be given in subsequent written or published work. Extensive copying or publication of the thesis in whole or in part requires also the consent of the Dean of the Graduate School of the University of New Mexico.

This thesis by ...Richard D. Griffith.....  
has been used by the following persons, whose signatures attest their acceptance of the above restrictions.

A Library which borrows this thesis for use by its patrons is expected to secure the signature of each user.

NAME AND ADDRESS

DATE

---

MANUSCRIPT

Unpublished theses submitted for the degree of Master of Arts and deposited in the University of New Mexico Library are open for inspection, but are to be read only with regard to the rights of the authors. Bibliographical references may be made, but passages may be copied only with the permission of the author, and proper credit must be given in subsequent works or abstracts of work. Extensive copying or publication of the thesis in whole or in part requires also the consent of the Dean of the Graduate School of the University of New Mexico.

This thesis by \_\_\_\_\_, Richard D. \_\_\_\_\_, has been used by the following persons whose names are given in acceptance of the above restrictions:

A library which borrows this thesis for use by its patrons is expected to secure the signature of each user.

NAME AND ADDRESS \_\_\_\_\_  
DATE \_\_\_\_\_



PRACTICAL ANALYSIS  
OF  
BLOCKING OSCILLATORS



By

Richard D. Griffith

A Thesis

Submitted in Partial Fulfillment of the  
Requirements for the Degree of  
Master of Science in Electrical Engineering

The University of New Mexico

1961



This thesis, directed and approved by the candidate's committee, has been accepted by the Graduate Committee of the University of New Mexico in partial fulfillment of the requirements for the degree of

MASTER OF SCIENCE

*E. H. Castetter*  
Dean

*May 12, 1961*  
Date

Thesis committee

*W. W. Grammann*  
Chairman

*Ruben L. Kelly*

*Arnold H. Kochman*

This thesis, directed and supervised by the advisor named  
in the title, has been approved by the Graduate Committee of the  
University of New Mexico in partial fulfillment of the require-  
ments for the degree of

MASTERS IN SCIENCE

\_\_\_\_\_  
Date

\_\_\_\_\_  
Date

Thesis Committee

\_\_\_\_\_  
Chairman

\_\_\_\_\_  
Member

\_\_\_\_\_  
Member

378.789  
Un30gr  
1961  
cop. 2

## ABSTRACT

The analysis and design of both vacuum tube and transistor blocking oscillators are described, with particular emphasis on the quasi-stable region. A relatively simple nonlinear analysis of the vacuum tube circuits is developed in terms of only two tube parameters — a current division factor and a current emission factor. This nonlinear analysis gives a clearer understanding of the role played by the tube in influencing circuit operation, as well as improving the accuracy that can be obtained with a linear analysis. Theoretical and experimental results are compared. Since the transistor is a more linear device, the transistor circuits are studied with a piecewise linear analysis. The approximations used in the analyses are in terms of readily measurable large-signal parameters, and particular attention is given to reducing the effects of variations in these parameters.

The objective is to give a method of treatment of blocking oscillator circuits which will be of practical value for circuit design. An attempt has been made to reach a good compromise between accuracy, generality, and usefulness. The use of statistical methods to complement the mathematical analyses is stressed.

Emphasis is placed on circuits which do not use an input capacitor. It is shown that these are practical circuits for generating high repetition rate and/or nonperiodic pulses. It is shown that the performance of the intrinsic circuits can be considerably improved by modifications, without the addition of an input capacitor, while still maintaining the advantages of the intrinsic circuit.

While the approximations are made for particular types of components and the analyses are performed on specific circuits, the methods employed are general. It is believed, therefore, that this material may be a useful guide for the analysis and design of many other blocking oscillator circuits.

The authors and others have shown that the  
 conditions are essential for the growth of the  
 fungus. A variety of other conditions have been  
 investigated in regard to the growth of the  
 fungus and a certain amount of light is  
 essential for the growth of the fungus. The  
 amount of light required for the growth of the  
 fungus is not known. It is known that the  
 fungus can grow in the dark. It is known  
 that the fungus can grow in the light. It  
 is known that the fungus can grow in the  
 dark. It is known that the fungus can  
 grow in the light. It is known that the  
 fungus can grow in the dark. It is known  
 that the fungus can grow in the light.

The authors have given a series of  
 results which will be published in the  
 Journal of the Royal Microscopical Society.  
 The authors have also made a study of the  
 growth of the fungus in the dark. It is  
 known that the fungus can grow in the  
 dark. It is known that the fungus can  
 grow in the light. It is known that the  
 fungus can grow in the dark. It is known  
 that the fungus can grow in the light.

It is known that the fungus can grow  
 in the dark. It is known that the fungus  
 can grow in the light. It is known that  
 the fungus can grow in the dark. It is  
 known that the fungus can grow in the  
 light. It is known that the fungus can  
 grow in the dark. It is known that the  
 fungus can grow in the light.

## TABLE OF CONTENTS

	Page
CHAPTER I -- INTRODUCTION	1
CHAPTER II -- GENERAL BLOCKING OSCILLATOR THEORY	4
Necessary Conditions	4
Quasi-stable State	5
Recovery Period	8
CHAPTER III -- TRANSFORMER DESIGN	12
The Problem	12
Effect of Rise Time Requirements on Design	12
Basic Transformer Theory	13
Choice of Core Material	19
Uniformity	20
CHAPTER IV -- VACUUM TUBE INTRINSIC BLOCKING OSCILLATORS	23
Graphical Analysis	23
Mathematical Analysis	32
Statistical Verification	45
Operating Life	53
CHAPTER V -- MODIFICATIONS TO THE INTRINSIC BLOCKING OSCILLATOR	59
Capacitive Turnoff	59
Grid-Plate Diode	64
Grid Resistor	65
CHAPTER VI -- TRANSISTOR BLOCKING OSCILLATORS	71
General Considerations	71
Saturated Equivalent Circuit	73
Intrinsic Circuit Analysis	75
Current-Limited Blocking Oscillator	79
CHAPTER VII -- CONCLUSIONS	85
LIST OF REFERENCES	87
APPENDIX A -- TUBE CURVE PLOTTER	89
APPENDIX B -- MEASUREMENTS OF B AND K	91

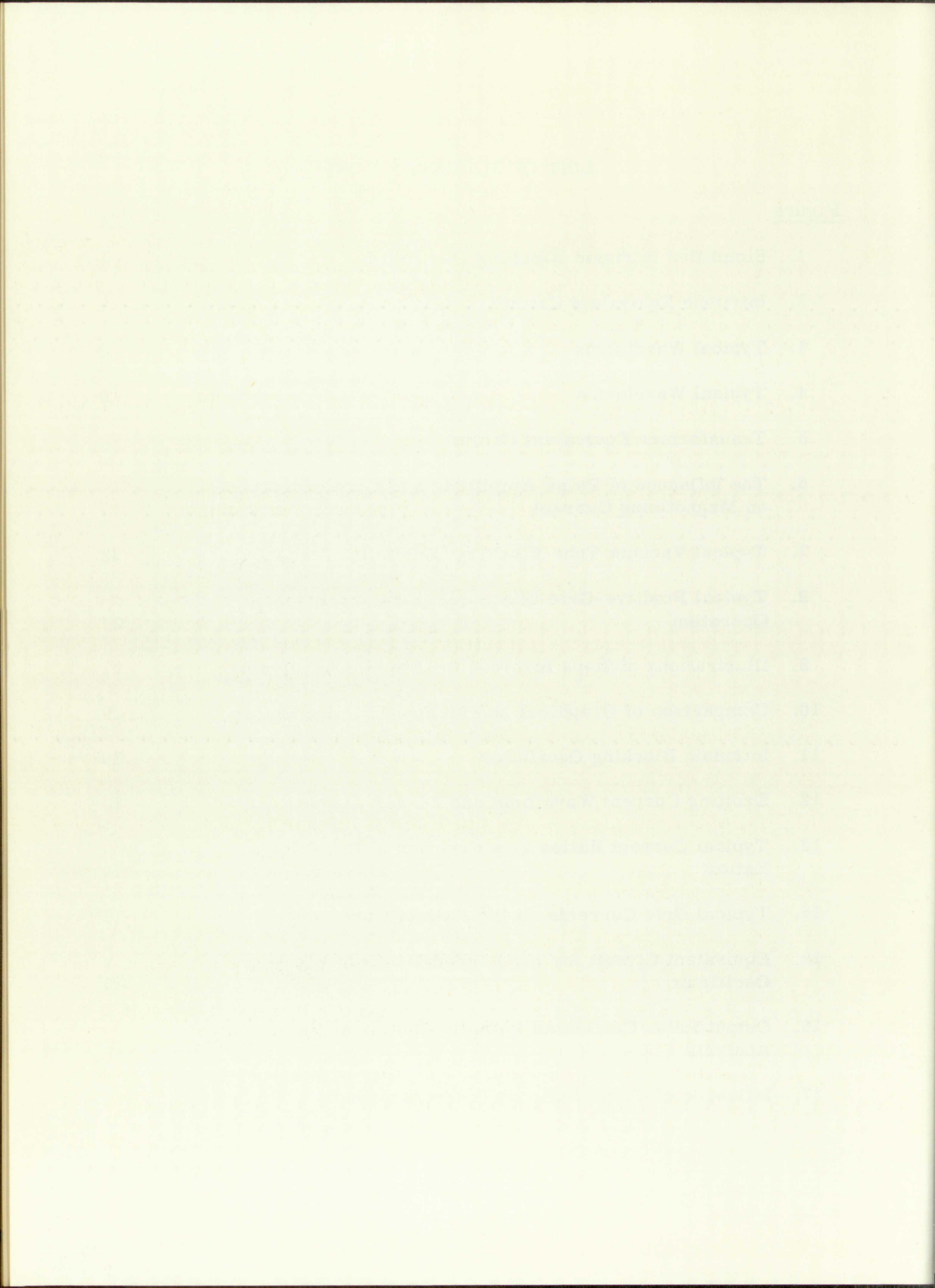
TABLE OF CONTENTS

1	CHAPTER I -- INTRODUCTION
1	CHAPTER II -- GENERAL BLOCKING OSCILLATOR THEORY
2	General Oscillator
3	Blocker Oscillator
4	Blocker Period
11	CHAPTER III -- THE RESONANT CIRCUIT
11	The Theory
12	Resonance in the Parallel Resonance Circuit
13	Series Resonance in the Series Resonance Circuit
14	Quality Factor
15	Coupling Coefficient
16	Impedance
20	CHAPTER IV -- FACTORIAL BLOCKING OSCILLATOR
20	Blocker Oscillator
21	General Oscillator
22	Blocker Oscillator
23	Blocker Period
24	Coupling Coefficient
25	Impedance
26	CHAPTER V -- TRANSISTOR BLOCKING OSCILLATOR
26	Blocker Oscillator
27	General Oscillator
28	Blocker Oscillator
29	Blocker Period
30	Coupling Coefficient
31	Impedance
32	CHAPTER VI -- TRANSISTOR BLOCKING OSCILLATOR
32	General Oscillator
33	Blocker Oscillator
34	Blocker Period
35	Coupling Coefficient
36	Impedance
37	CHAPTER VII -- NON-CIRCULAR
37	Blocker Oscillator
38	General Oscillator
39	Blocker Oscillator
40	Blocker Period
41	Coupling Coefficient
42	Impedance
43	APPENDIX A -- THE TYPICAL BLOCKING OSCILLATOR
44	APPENDIX B -- TRANSISTOR BLOCKING OSCILLATOR



## LIST OF ILLUSTRATIONS

<u>Figure</u>	<u>Page</u>
1. Simplified Intrinsic Blocking Oscillator	5
2. Intrinsic Equivalent Circuit	6
3. Typical Waveforms	9
4. Typical Waveforms	10
5. Transformer Equivalent Circuit	14
6. The Influence of Pulse Amplitude and Core Saturation on Magnetizing Current	17
7. Typical Vacuum Tube Blocking Oscillator Transformers	22
8. Typical Positive-Grid Characteristics and Paths of Operation	24
9. Illustrations of Steps Involved in Graphical Analysis	27
10. Comparison of Graphical and Measured Pulse Shapes	29
11. Intrinsic Blocking Oscillator	30
12. Exciting Current Waveform and Linear Approximation	30
13. Typical Current Ratios as a Function of the Voltage Ratios	34
14. Typical Grid Currents on the Path of Operation	36
15. Equivalent Circuit for the Loaded Intrinsic Blocking Oscillator	40
16. Output Pulse Calculated from the Nonlinear Mathematical Analysis	42
17. Influence of Turns Ratio on Pulse Amplitude	47



## LIST OF ILLUSTRATIONS (cont)

<u>Figure</u>	<u>Page</u>
18. Influence of Turns Ratio on Pulse Width	48
19. Distribution of the Current Division Factor	49
20. Distribution of the Current Emission Factor	50
21. The Effect of the Current Division Factor on Pulse Amplitude	51
22. Influence of the Current Division Factor on Pulse Width	52
23. Dependence of the Pulse Width Upon the Current Emission Factor	54
24. Typical Variation of Pulse Emission with Heater Voltage	57
25. Blocking Oscillator with a Grid Capacitor	60
26. Capacitive Turnoff	62
27. The Effect of the Grid Capacitor on Pulse Width	63
28. Pulse Amplitude Limiting with a Grid-Plate Diode	66
29. Combination of Grid Resistor and Diode	67
30. Alternate Combination	67
31. Distributions of Pulse Amplitude with Various Circuit Modifications	68
32. Common-Emitter Intrinsic Blocking Oscillator	74
33. Typical Collector Characteristic and Path of Operation	74
34. Input Characteristics and Linear Approximation	74
35. Saturated Transistor Equivalent Circuit	74
36. Equivalent Circuit for the Intrinsic Blocking Oscillator	76



## LIST OF ILLUSTRATIONS (cont)

<u>Figure</u>		<u>Page</u>
37.	Current-Limited Blocking Oscillator	79
38.	Equivalent Circuit	79
39.	Typical Variation of Pulse Width with Temperature	84

## LIST OF TABLES

<u>Table</u>		<u>Page</u>
I	Intrinsic Blocking Oscillator with 50-Tube Sample	46
II	The Effects of Circuit Modifications	69
III	Parameter Means for Sample of Ten 2N1613 Transistors	82
IV	Measurements on Sample of 30-2N1613	83



## CHAPTER I -- INTRODUCTION

A conventional blocking oscillator uses capacitance in series with the input circuit of the active device. When appropriate values are chosen for this input capacitor, the circuit operation is relatively insensitive to variations in the characteristics of the active element and the transformer. This tolerance to changes in characteristics enables the empirical design of most circuits, and a thorough understanding of the operation of the circuit is not usually necessary.

Energy is stored in the input capacitor during a pulse, and most of this energy must be dissipated before a new pulse can be generated. The repetition rate of this circuit is limited; and identical pulses cannot be generated unless the pulses are periodic, or unless the capacitor is completely discharged between pulses.

Particular attention will be given to the Intrinsic Blocking Oscillator, defined here as a blocking oscillator having only a transformer and an active device in the feedback loop. There are two reasons for the emphasis on this circuit: (1) The circuit is particularly useful where pulses having high repetition rates and/or nonperiodicity are required, since the recovery time limitations due to the input capacitance are eliminated; (2) Because of its basic nature, a study of this circuit reveals important properties generally applicable even with circuit modifications.

Without an input capacitor, circuit operation is governed by the characteristics of the active device and the transformer. It is shown that there is a considerable variation in these characteristics because of manufacturing tolerances and the effects of environment. Proper design of these circuits requires a good understanding of the operation of the circuit, a knowledge of the effects of the various important parameters, and

## CHAPTER I - INTRODUCTION

A conventional blocking coil, after some capacitor is added to the input circuit of the active device. When appropriate values are chosen for the input capacitor, the current gain of the active device is increased in the characteristic of the active device and the frequency response is improved. This response is changed in a certain manner under the action of the input circuit, and a frequency independent of the operation of the coil is not usually possible.

It is stated in the input capacitor during a pulse, and most of the energy that is dissipated before a new pulse can be generated. The response rate of this circuit is limited; the electrical pulse cannot be generated unless the output is periodic, or unless the capacitor is charged through a feedback path.

Further attention will be given to the bistable Blocking Oscillator, defined here as a blocking oscillator having only a transformer and an active device in the feedback loop. There are two reasons for the study of this circuit: (1) The circuit is particularly useful when a pulse having high repetition rates and/or completely variable pulse widths is required. (2) Because of its basic nature, a study of this circuit reveals important properties which are common to other oscillators.

Without an input capacitor, circuit operation is governed by the characteristics of the active device and the transformer. It is shown that there is a considerable variation in these characteristics because of manufacturing tolerances and the effect of environment. Proper design of these circuits requires a good understanding of the operation of the coil, a knowledge of the effect of the various important parameters, and



control over these parameters such that the circuit will function within its desired limits. Since the objective is to obtain the necessary information, the simplest and most practical means should be employed. The approach used here will be to combine graphical, mathematical, and statistical methods to obtain an over-all understanding of blocking oscillator operation that would be difficult to determine from a single method of study.

A graphical analysis is used primarily to verify that the transformer approximations are valid. It is shown that statistical data are invaluable for evaluating a given design, and for checking a mathematical analysis to determine the effects of approximations on the accuracy of the analysis. It is shown that the main advantages of mathematical analyses are to identify the important circuit parameters, to give an approximate mathematical representation to the relationships between the parameters and the circuit operation, and to indicate possible methods for improving the design.

Pulse termination is shown to occur when the physical requirements necessary to sustain the quasi-stable state can no longer be satisfied. Thus, regeneration in the feedback loop is not responsible for terminating the pulse, a commonly held theory.

The analysis and design of both vacuum tube and transistor blocking oscillators are considered. While emphasis is now on transistor circuits, the vacuum tube is still of interest for certain applications, particularly where there is a high radiation environment.

A piecewise linear analysis of the vacuum tube blocking oscillator in the quasi-stable state can be made by assuming average values for such tube characteristics as the amplification factor, plate resistance, and the grid resistance. However, these parameters are not constant in the positive grid region; they may vary during this so-called piecewise linear region by a factor of two or more. These average values are difficult to

...the results of the analysis are shown in Figure 1. The results show that the model is able to predict the behavior of the system with a high degree of accuracy. The model is based on the assumption that the system is linear and time-invariant. The results of the analysis are shown in Figure 1. The results show that the model is able to predict the behavior of the system with a high degree of accuracy. The model is based on the assumption that the system is linear and time-invariant.

The results of the analysis are shown in Figure 1. The results show that the model is able to predict the behavior of the system with a high degree of accuracy. The model is based on the assumption that the system is linear and time-invariant. The results of the analysis are shown in Figure 1. The results show that the model is able to predict the behavior of the system with a high degree of accuracy. The model is based on the assumption that the system is linear and time-invariant.

The results of the analysis are shown in Figure 1. The results show that the model is able to predict the behavior of the system with a high degree of accuracy. The model is based on the assumption that the system is linear and time-invariant. The results of the analysis are shown in Figure 1. The results show that the model is able to predict the behavior of the system with a high degree of accuracy. The model is based on the assumption that the system is linear and time-invariant.

The results of the analysis are shown in Figure 1. The results show that the model is able to predict the behavior of the system with a high degree of accuracy. The model is based on the assumption that the system is linear and time-invariant. The results of the analysis are shown in Figure 1. The results show that the model is able to predict the behavior of the system with a high degree of accuracy. The model is based on the assumption that the system is linear and time-invariant.

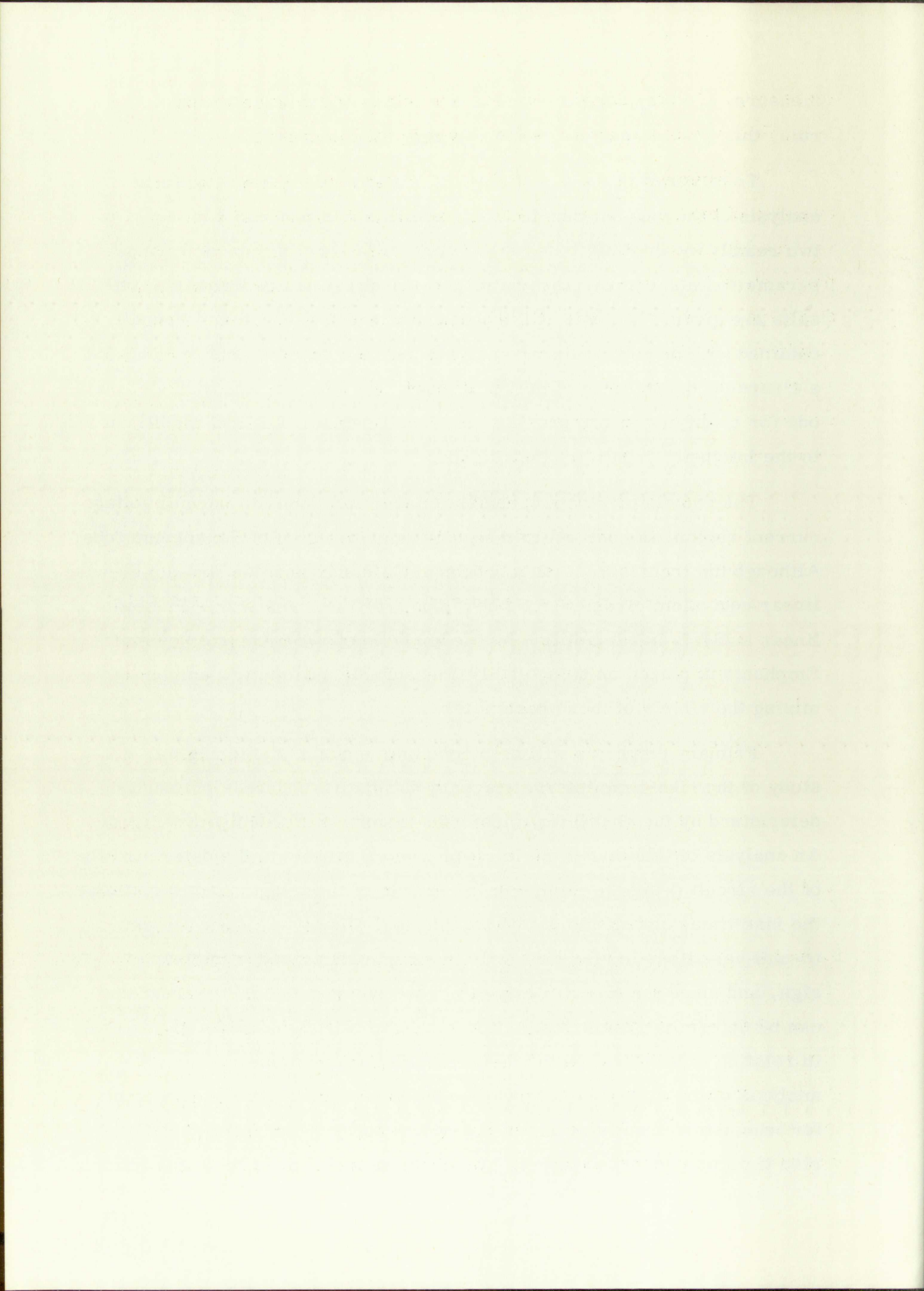
The results of the analysis are shown in Figure 1. The results show that the model is able to predict the behavior of the system with a high degree of accuracy. The model is based on the assumption that the system is linear and time-invariant. The results of the analysis are shown in Figure 1. The results show that the model is able to predict the behavior of the system with a high degree of accuracy. The model is based on the assumption that the system is linear and time-invariant.

measure, and they depend upon the particular operating condition. As a rule, this type of analysis results in very poor accuracy.

To circumvent these difficulties, a relatively simple nonlinear analysis of the vacuum tube blocking oscillator is presented in terms of two readily measurable tube parameters. Methods of measuring these parameters and comparisons between theoretical and experimental results are given. Not only is the agreement much better than is usually obtained with piecewise linear analyses, but the new parameters provide a clearer understanding of the operation of the circuit, and indicate methods for modifying and improving the circuit design. Several modifications to the intrinsic circuit are considered.

The transistor blocking oscillator operates over its normal voltage-current region, in contrast to the positive grid region of the vacuum tube. Although the transistor is also nonlinear, a much more accurate piecewise linear equivalent circuit can be developed for the transistor. Piecewise linear analysis is exemplified by the analysis of two transistor circuits. Emphasis is placed on using easily measurable parameters and on minimizing the effects of these parameters.

Primary emphasis will be placed on the quasi-stable region. A study of the rise-time interval reveals that the rise time is primarily determined by the characteristics of the transformer and by the trigger. An analysis of this rise-time interval can aid greatly in the determination of the circuit design to minimize the effects of the trigger and to optimize the rise time, and should not be underrated. However, since the unit-to-unit variations in rise time will be small with a good transformer design, and since the circuit design for good rise time is fairly broad and can be determined empirically, the rise time will be considered here only in relation to its effect on the design for the quasi-stable region. The analysis of the rise-time interval would become particularly important for transistor circuits which used low-frequency transistors such that the rise time was governed largely by the characteristics of the transistor.



## CHAPTER II -- GENERAL BLOCKING OSCILLATOR THEORY

### Necessary Conditions

The essential components of a blocking oscillator are a three-terminal active device capable of providing power gain, and a transformer. Power gain in the active device is required to overcome circuit losses. Another requirement of the active device is that its output must be controllable at the input under all conditions. The last condition eliminates many breakdown devices, such as thyratrons, from use in blocking oscillators. The active device and transformer are connected together to form a positive feedback loop. Additional components may be included in the feedback loop to obtain a specific circuit operation. In addition, other components are normally required for proper biasing, decoupling, and trigger or sync insertion.

During the pulse, the active device is driven beyond any linear region it may have, as a result of the positive feedback. Thus, the total voltage and current excursions are determined by the large signal characteristics of the device. It is the characterization of this large signal behavior which makes the analysis of blocking oscillators so difficult.

A stable state exists when the current through the active device is zero or nearly so. When the current through the device is increased, by insertion of a trigger pulse, for example, the loop gain becomes greater than unity. The regeneration as a result of the positive feedback causes the large voltage and current excursions. These excursions reach a maximum when the loop gain is reduced to unity by the nonlinear characteristics of the loop. The interval required to reach a unity loop gain is called

Necessary Conditions

The essential ingredients of a blocking oscillator are a device capable of providing power gain and a feedback loop in the active device which is required to maintain constant phase. Another requirement of the active device is that its output must be controllable at the frequency of oscillation. The first condition is satisfied by the active device, such as a triode, when power gain is high. The active device and feedback are connected together in a positive feedback loop. Additional conditions may be required for a feedback loop to obtain a specific frequency response. In addition, other components are required for proper feedback, depending on the nature of the device.

During the pulse, the active device is driven beyond the linear region. The output of the device is limited by the large signal characteristics of the device. It is the characteristic of the large signal behavior which makes the analysis of blocking oscillators an difficult.

A static state exists when the current through the active device is zero or nearly so. When the current through the device is increased by application of a trigger pulse, the energy of the loop gain becomes available. The regeneration is a result of the positive feedback around the large signal and current characteristics. When the excitation ceases, the loop gain is reduced to zero in the negative direction. At the time the feedback is reduced to zero, the energy is again available.

the rise period; the rise time is usually taken as the time required to traverse the 10-to-90 percent points of the amplitude variation during the rise period.

### Quasi-stable State

The interval during which the loop gain is unity is a quasi-stable state which can exist for a desired length of time. The presence of the pulse during this interval causes an exciting current in the transformer, which must be supplied by the active device. This increasing exciting current causes the operating points of the active device to shift in order to maintain a unity loop gain. When the device can no longer supply the required exciting current, the circuit switches from the quasi-stable state back to the stable state. The quasi-stable region is usually referred to as the main part of the pulse and is the interval of primary interest here.

Consider the simplified intrinsic blocking oscillator circuit shown in Figure 1 where components for trigger insertion have been neglected. Assume a further simplification by considering the transformer to consist only of a primary inductance and an ideal transformer having a turns ratio,  $n$ , as shown in Figure 2.

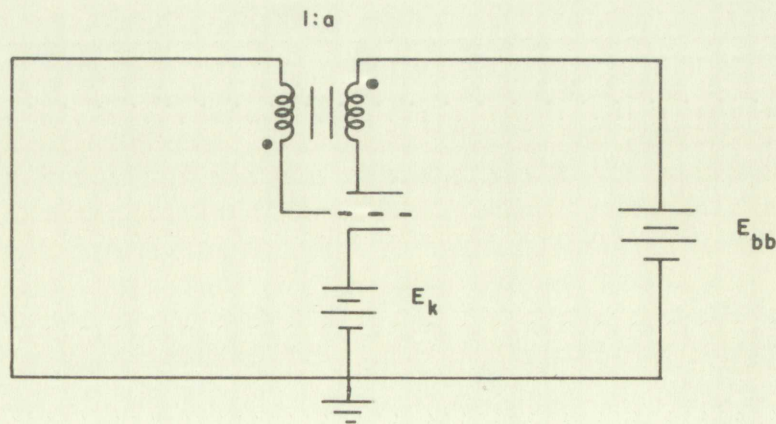


Figure 1. Simplified Intrinsic Blocking Oscillator

The first section, the operating time is usually taken as the time required to  
travel the 10 to 20 percent point of the amplitude variation during the  
start period.

### Quasi-stable State

The interval during which the loop gain is only a quasi-stable  
state which is not for a desired length of time. The presence of the  
noise during this interval causes an excitation current in the test  
which must be supplied by the active device. This increasing excitation  
current causes the operating point of the active device to shift in order  
to maintain a high loop gain. When the device has no longer enough  
excited excitation current, the circuit switches from the quasi-stable  
state to the stable state. The quasi-stable region is usually re-  
ferred to as the quasi-stable state and is the interval of operation  
that is of interest.

Consider the simplified circuit including blocking oscillator circuit shown  
in Figure 1. When comparing the trigger injection has been explained.  
As shown a further simplification by considering the transistor as an  
ideal voltage source and an ideal transformer having a turns  
ratio of  $n$  as shown in Figure 2.

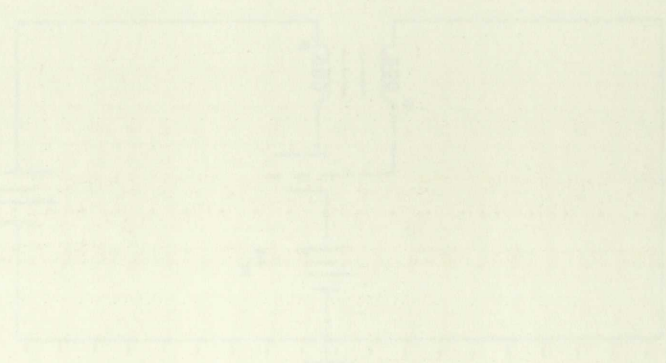


Figure 2. Simplified circuit including blocking oscillator.



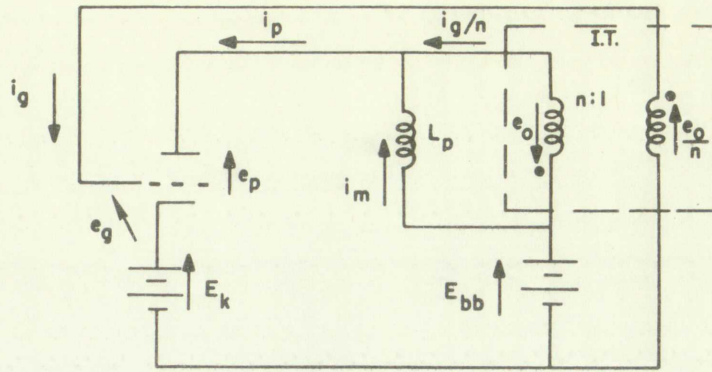


Figure 2. Intrinsic Equivalent Circuit

From Figure 2 the loop voltage equations<sup>1</sup> are

$$E_{bb} = E_k + e_p + e_o \quad (1)$$

and

$$e_g = e_o/n - E_k \quad (2)$$

where  $e_o$  is the pulse voltage across the transformer primary.

These equations result in a voltage loop gain of unity. To have unity power gain, the loop current gain must also be unity. The current gains are found to be

$$\text{Current gain of tube} = \frac{i_p}{i_g},$$

and

$$\text{Current gain of transformer} = \frac{i_g}{i_m + i_g/n}$$

---

<sup>1</sup> $(E_{bb} - E_k)$  in Equation (1) can be considered as the effective plate supply voltage. A negative grid bias can be substituted for the cathode bias, and the only effect will be to modify this effective supply voltage.

Handwritten scribble or signature at the bottom of the page.

Equating the product of the individual current gains to unity results in

$$i_m = i_p - \frac{i_g}{n} = i_g \left( \frac{i_p}{i_g} - \frac{1}{n} \right) \quad (3)$$

It may be noted that the concept of unity loop gain is not necessary to derive Equation (3) since it can be obtained directly from Figure 2 by inspection.

The magnetizing current is a result of the pulse voltage across the transformer, the relationship being

$$e_o = L_p \frac{di_m}{dt} \quad (4)$$

Hence:

$$i_m = \frac{1}{L_p} \int e_o dt \quad (5)$$

Equation (5) shows that the magnetizing current is a function of the time integral of the pulse voltage. Since the plate and grid currents are functions of the plate and grid voltages,  $e_o$  in Equations (1) and (2) may change in order to satisfy Equation (3) as the magnetizing current increases. But the magnetizing current as given in Equation (5) will not increase linearly with time unless the pulse voltage is constant. Any assumption of a linearly increasing magnetizing current should, then, be coupled with an assumption of a constant pulse amplitude.

Equation (3) shows that the magnetizing current can be given in terms of the plate and grid currents or in terms of one current and the ratio of the currents. The best method for approximations is yet to be determined.

The analysis thus far is equally suitable for a transistor blocking oscillator. It would be convenient in a transistor circuit to change the current and voltage subscripts, and for a pnp transistor also to change referenced directions.

$$(1) \quad \frac{d^2 \psi}{dx^2} + \left( \frac{2m}{\hbar^2} (E - V(x)) \right) \psi = 0$$

It may be noted that the concept of energy levels is not necessary in the present theory (2) since it can be obtained directly from Eqs. (1) and (2).

The propagating current is a result of the pulse voltage across the junction, the relationship being

$$(2) \quad I = \frac{e}{h} \frac{\partial \psi}{\partial x} \Big|_{x=0} - \frac{e}{h} \frac{\partial \psi}{\partial x} \Big|_{x=L}$$

Equation (2) shows that the magnitude of the current is a function of the time integral of the pulse voltage, hence the pulse and not the voltage function of the pulse and not voltage,  $\psi$ , in Eqs. (1) and (2) must change in order to satisfy Eqs. (1) as the propagating current increases. But the propagating current is given by Eqs. (1) and (2) which are linearly related with time when the pulse voltage is constant. An assumption of a linearly increasing propagating current should then be coupled with an assumption of a constant pulse amplitude.

Equation (2) shows that the propagating current can be given in terms of the pulse and not voltage or in terms of one current and the other. The first method for calculations is not to be determined. The analysis in (1) is equally suitable for a constant voltage pulse. It would be convenient in a transmission circuit to change the current and voltage separately, and for a propagating current, a constant voltage pulse is required.

Since the active device is nonlinear, nothing can be said, as yet, about the magnitude of the voltages and currents or the manner in which they vary with time. Equations (1) through (4) give the relationships between the voltages and the currents which must be simultaneously satisfied, no matter what these nonlinearities may be. It should be noted that the relationships between voltages and currents depend upon the characteristics of the individual device; and any one analysis, using approximations, may be limited to devices having similar current-voltage characteristics. Thus, a different analysis is needed for tube and transistor circuits; and the approximations may be valid for only a particular type or class of tube or transistor.

The only approximations made thus far have been in characterizing the transformer. It will be shown later that, for a well designed linear transformer, these approximations are valid if the inductance and turns ratio are appropriately chosen. A saturating-type transformer must also include the effects of saturation, however.

Figures 3 and 4 show typical time variations of the plate and grid voltage and currents. For these waveforms the circuit of Figure 1 was used with  $E_{bb} = 150v$ ,  $E_k = 18v$ , and  $a=1$ . Note that the difference in pulse shapes in Figures 3 and 4 is due to the different voltage-current characteristics of the tubes.

### Recovery Period

Immediately after the quasi-stable state, the magnetic field built up in the transformer will start collapsing. The manner in which this field collapses will depend upon the transformer damping. If the transformer is underdamped, damped oscillations or ringing will occur which may re-trigger the blocking oscillator, a usually undesirable condition. A resistor across one of the transformer windings to obtain critical or over-

...the active device is nonlinear, resulting in a non-linear relationship between the input and output of the system in which they are used. (Theoretically, the relationship between the input and the output of a linear system is linear, but in practice, the relationship between the input and the output of a nonlinear system is nonlinear.)

The basic approximation made here is that the input and output of the system are linearly related. This is a well-known approximation, and it is valid for a wide range of conditions. A commonly used approximation is that the input and output of a system are linearly related. This is a well-known approximation, and it is valid for a wide range of conditions.

### Frequency Period

...the frequency of the input signal is much higher than the natural frequency of the system. In this case, the system will respond to the input signal as if it were a linear system. The natural frequency of the system is the frequency at which the system would oscillate if it were not damped.

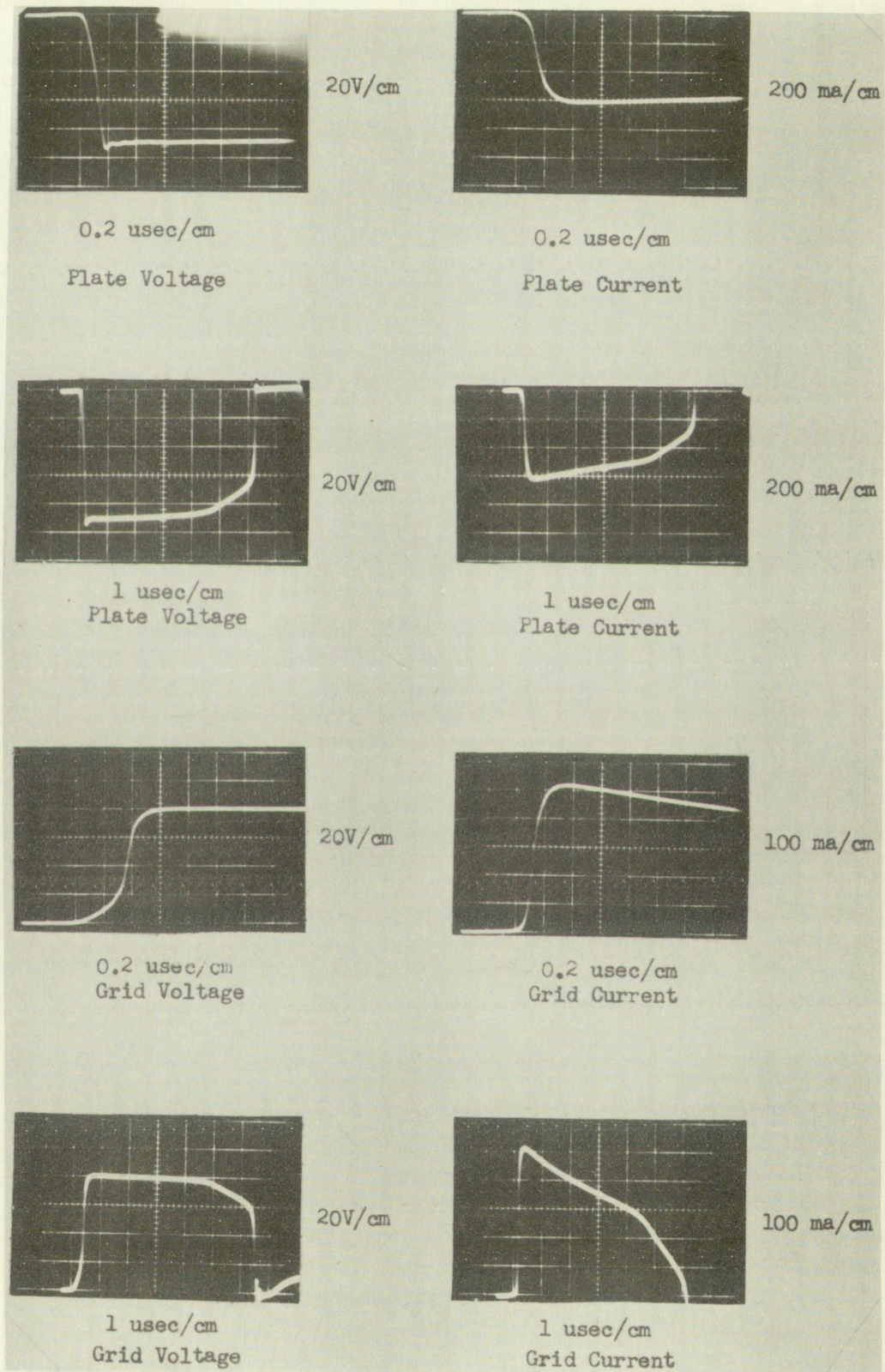


Figure 3. Typical Waveforms





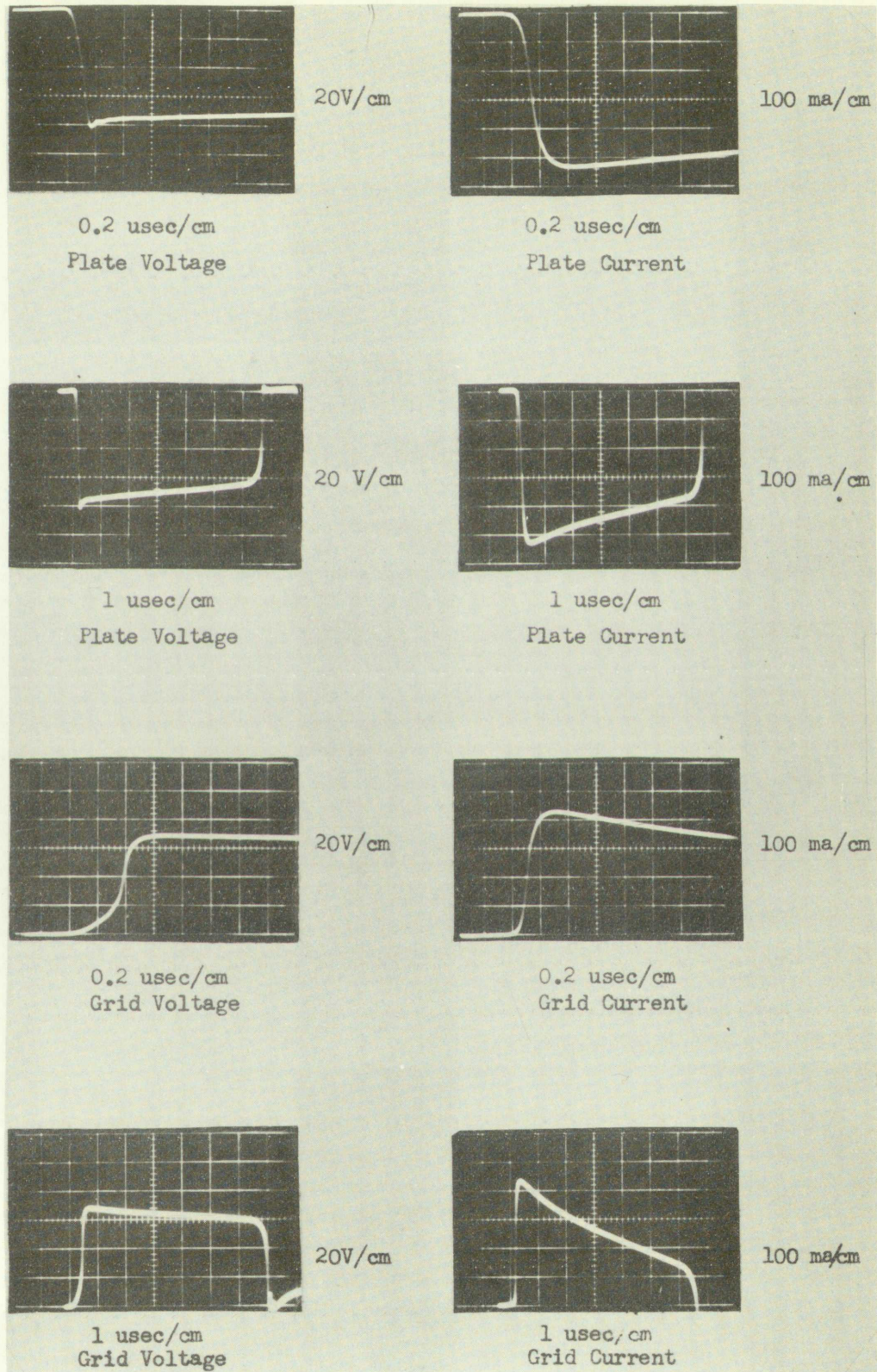
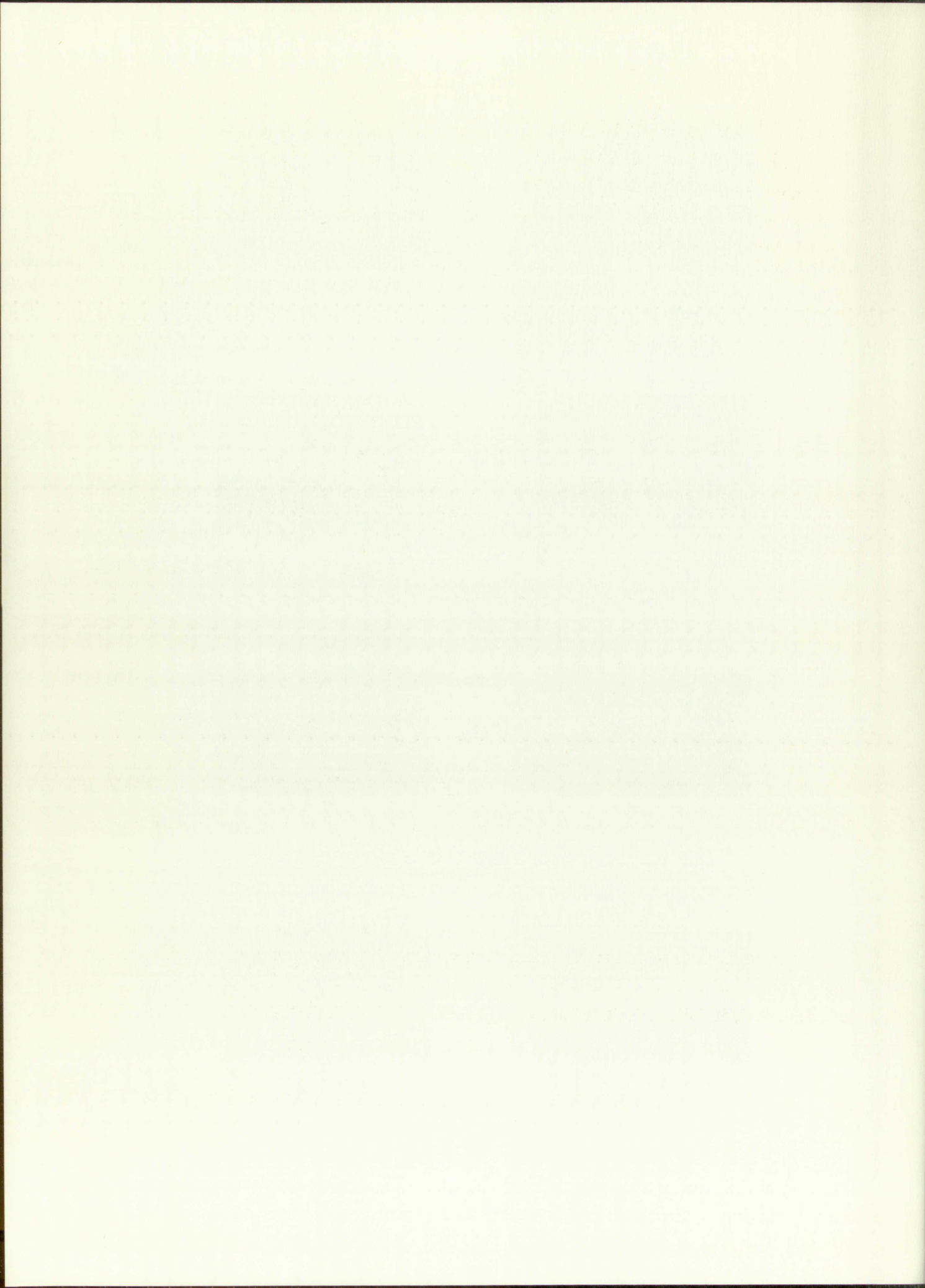


Figure 4. Typical Waveforms



damping will eliminate this effect; the recovery period can be as short as twice the duration of the main pulse. Sometimes the load and transformer losses supply sufficient damping, and no additional resistor is required.

A diode may be connected across one of the transformer windings such that it will conduct during the recovery period. The reverse voltage present during the recovery interval is then limited to the forward drop of the diode, and the rate of collapse of the magnetic field is greatly reduced.<sup>2</sup> This results in a considerable longer recovery time than that obtained with resistive damping. While this method is often used to eliminate the high reverse voltage during the recovery period, it can only be employed where the long recovery time is permissible.

If capacitance is used in the grid circuit of the blocking oscillator, all or part of the energy stored in this capacitance must be dissipated during the recovery period. A path must be supplied for discharging this capacitance, and the resultant time constant usually governs the recovery time.

Many circuit modifications are possible to change the recovery characteristics. A good example is the use of a zener diode to limit the reverse voltage to the breakdown voltage of the diode. This is particularly useful in transistor circuits to limit voltages to within the transistor ratings while still maintaining fast recovery time.

---

<sup>2</sup>This is a result of limiting the voltage in Equation (7) on page 15.

damaging will occur during this period. The recovery period can be as short as  
with the duration of the initial phase. In addition, the load and temperature  
levels which influence damage, and in addition, voltage is required.

A diode may be considered as a case of the semiconductor diode  
and that it will conduct during the recovery period. The reverse voltage  
applied during the recovery period is the voltage which is applied to the  
of the diode, but the rate of change of the magnetic field is usually re-  
duced. This results in a considerably longer recovery time than that  
obtained with resistive damping. While this method is often used to obtain  
into the high reverse voltage during the recovery period, it can only be  
employed when the recovery time is sufficiently

It is important to bear in mind that the rate of change of the magnetic field  
all or part of the energy stored in the capacitor must be dissipated  
during the recovery period. A diode must be supplied for dissipating this  
energy, and the resistance must be constant usually during the recovery  
period.

Many of the applications are possible to change the recovery  
characteristics. A good example is the use of a series diode to limit the  
reverse voltage to the diode during the recovery period. This is possible  
only when a resistor is used to limit voltage to within the limits  
for voltage with this limiting fast recovery type.

## CHAPTER III -- TRANSFORMER DESIGN

### The Problem

The design of a blocking oscillator transformer depends upon the particular circuit under consideration. Different circuit requirements may require considerably different transformer designs, and this is one reason for the relatively few types of commercial transformers on the market.

Transformer design involves the making of important decisions in three major areas: (1) the method of construction, (2) the choice of materials, and (3) the number of turns required on each winding. As is to be expected, these three areas have interrelated requirements, which, in conjunction with the large number of different possible design requirements, make a general design procedure impractical. The method to be followed here will be to discuss the principal design considerations, leaving their final solutions as individual design problems.

### Effect of Rise Time Requirements on Design

The rise time of a blocking oscillator is governed primarily by the trigger and by the leakage inductances and distributed capacitances of the transformer and the capacitance of the tube or transistor. The main difficulty in calculating rise time appears to be in getting accurate equivalent circuit values for small pulse transformers.



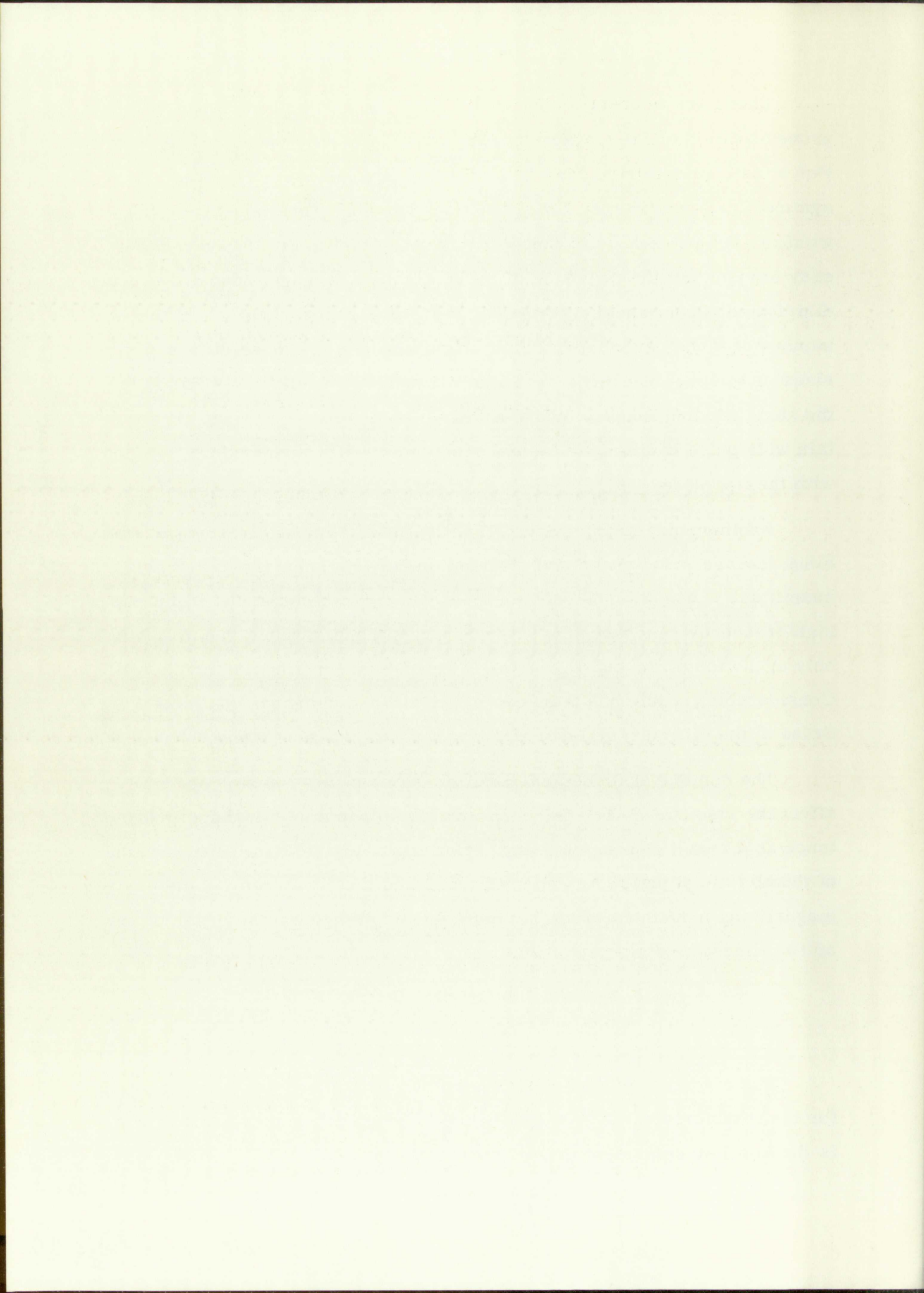
There are a few concepts which can result in a considerable improvement in the rise time response, especially with vacuum tube circuits. For a fast, smooth rise time probably the most important property is symmetrical construction. Single-layer windings, one layer for each winding, are preferable to multiple layers. With multiple layers it is easy to visualize the presence of more complex leakage inductances and distributed capacitances. With single-layer windings having a different number of turns per winding, it is often possible to choose different wire sizes or to space the turns such that all windings occupy approximately the same winding length. While multiple layers may be necessary to obtain wide pulse widths, the fastest rise times will in general be obtained with the fewest layers.

Another undesirable feature, not quite so obvious, is crossed turns. Since leakage inductances and distributed capacitances are distributed quantities, crossed turns can cause asymmetry which results in individual high-frequency resonances. This results in ringing which can occur not only at the top of the pulse, but during the steeply rising portion as well. Considerable trouble has been experienced when using toroidal cores because of the difficulty in layer winding without crossing turns.

The number of turns and the dimensions of the transformer will affect the rise time. Too few turns will result in a high leakage inductance as a result of poor coupling. For solenoidal construction, a rule of thumb is to adjust the number of turns and the core area for the desired magnetizing inductance while having a winding length on the order of one or two times the diameter of the coil.

### Basic Transformer Theory

The circuit in Figure 2 used a greatly simplified equivalent circuit for the transformer. A more accurate, though still approximate, form is the familiar equivalent circuit shown in Figure 5.





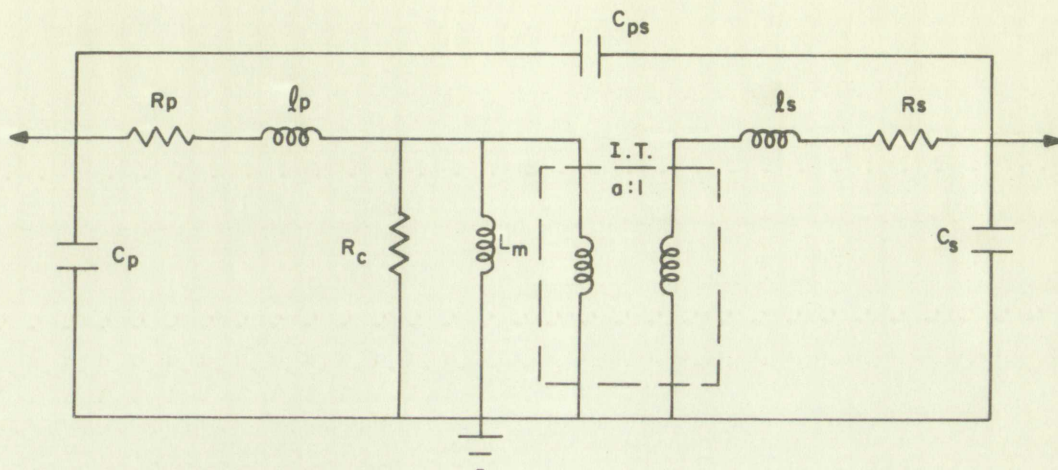


Figure 5. Transformer Equivalent Circuit

It is easy to visualize that the use of an equivalent circuit as complex as this would greatly complicate the solution of nonlinear equations.

During the main part of the pulse, the plate and grid currents as well as the core loss and magnetizing currents, contribute to voltage drops in the leakage inductances. Thus, to generate relatively square pulses the leakage inductances should be small in relation to the magnetizing inductance, indicating the necessity of tight coupling. During this interval when the pulse voltages are changing slowly, the effects of leakage inductances and distributed capacitances are minor with close coupling. The elimination of these components in the circuit of Figure 5 still leaves resistances whose voltage drops depend upon nonlinear currents, a considerable complication to any analysis.

An approximation widely used with power transformers is

$$\frac{E_p}{E_s} = \frac{1}{\sqrt{\eta}} \frac{N_p}{N_s} = \frac{a}{\sqrt{\eta}} \quad (6)$$

where  $a$  is the actual turns ratio from primary to secondary and  $\eta$  is the power efficiency. Considering the turns ratio,  $n$ , in Figure 2, as the right-hand side of this equation, it becomes the effective turns ratio of the transformer. In a transformer with no leakage, the magnetizing

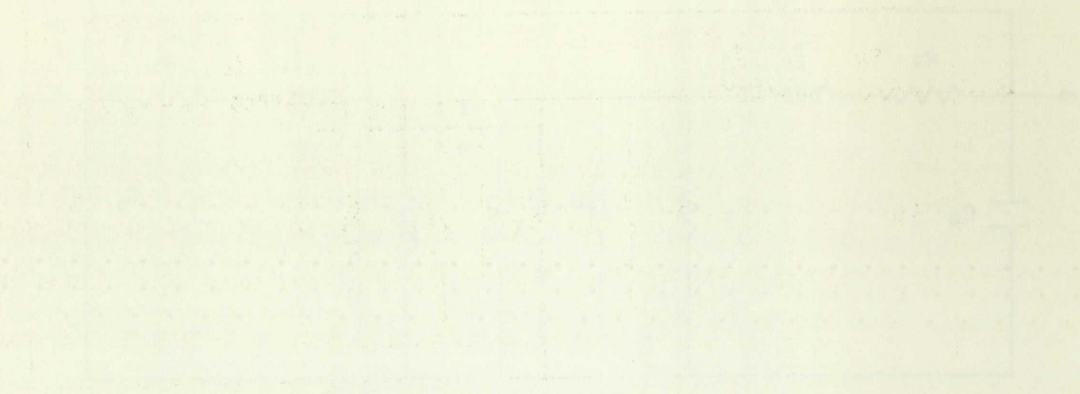


Figure 1. [Illegible text]

[Illegible text block containing several paragraphs of text, likely describing the data shown in the figure above.]

[Illegible text block containing several paragraphs of text, likely continuing the discussion or providing further context.]

inductance is equal to the primary inductance. Thus, the equivalent circuit of Figure 2 considers only the primary inductance and an effective turns ratio.<sup>3</sup> Although this equivalent circuit is highly desirable, its validity has not yet been demonstrated.

Since the primary inductance may be nonlinear, the magnetizing current as given in Equation (5) may strongly depend upon characteristics of the core material over the operating region of flux density. This is particularly true if operation extends into the saturated region. A transformer saturates if its flux density exceeds a given maximum value. The saturation may be gradual as the flux density increases (soft saturation), or it may be sharp (hard saturation), depending upon the type of core material. The effects of core material and operating region may be determined from the relationship between magnetizing current and flux density. Since

$$e = L \frac{di_m}{dt} = N \frac{d\phi}{dt}, \quad (7)$$

therefore:

$$\int_0^T e dt = \int_0^{I_m} L di_m = \int_{\phi_i}^{\phi_m} Nd\phi$$

and assuming  $e$  and  $L$  constant gives

$$ET = L I_m = N (\phi_m - \phi_i),$$

---

<sup>3</sup> Although the transformer turns ratio is modified to agree with the actual voltage ratio, power losses in the transformer are neglected. These losses could be considered by using  $\frac{I_s}{I_m} = n\eta$  for the current ratio, but the accuracy of the following analyses would not be significantly improved.



where  $\phi_i$  is the initial flux at time zero and may be either positive, negative, or zero, depending upon the recovery interval of the previous pulse and the characteristics of the core material.  $\phi_m$  is the maximum flux occurring when the magnetizing current is maximum.

Substituting flux density for flux results in

$$ET = L I_m = NA (B_m - B_i) \quad (8)$$

where A is the effective core area.

Since the relationship between turns, area, and inductance is

$$L \propto \frac{N^2 A}{\frac{l_c}{\Delta\mu} + l_g} \quad (9)$$

where  $l_c$  is the core mean path length

$l_g$  is the effective air gap

$\Delta\mu$  is the incremental permeability of the core,

the substitution of this equation for inductance gives

$$I_m \propto \frac{\frac{l_c}{\Delta\mu} + l_g}{N} (B_m - B_i) \quad (10)$$

The air-gap length and initial flux density can often be assumed to be zero, thus simplifying the equation to

$$I_m \propto \frac{l_c}{N\Delta\mu} B_m \quad (11)$$

In the linear region of the transformer, where the incremental permeability is approximately constant, the magnetizing current is, therefore, proportional to the flux density. In the saturated region where the incremental permeability decreases, the magnetizing current will increase at a faster rate than the flux density.

where  $\rho$  is the initial rate of change and may be either positive or negative, depending upon the density,  $\rho$ , of the population, and the characteristic time of the process,  $\tau$ . The characteristic time is constant when the population is constant.

Substituting the density for that results in

$$\frac{d\rho}{dt} = \rho \left( \frac{1}{\tau} - \rho \right)$$

where  $A$  is the effective growth rate.

Since the relationship between  $\rho$ ,  $\tau$ , and  $A$  is

$$A = \frac{1}{\tau} - \rho$$

where  $\tau$  is the time mean path length

is the effective life span

As is the characteristic permeability of the core

the substitution of this equation for  $\rho$  in equation (1)

$$\frac{d\rho}{dt} = \rho \left( \frac{1}{\tau} - \rho \right)$$

The life span and initial flux density can often be assumed to be

that simplifying the equation to

$$\frac{d\rho}{dt} = \rho \left( \frac{1}{\tau} - \rho \right)$$

In the limit region of the transition, where the characteristic permeability

is a constant, the relationship between  $\rho$  and  $\tau$  is

proportional to the flux density. In the transition region where the

permeability decreases, the relationship between  $\rho$  and  $\tau$  is

where  $\rho$  is the flux density.

For a given maximum flux density there is a given maximum current. This is true even in the saturated region, since for a certain flux density there is a corresponding given incremental permeability. Curves of magnetizing current versus time are shown in Figure 6 as a function of pulse amplitude. Note that the upward curvature of current begins at the same value of current, shown by the dashed line, for all curves. By Equation (11) the flux density

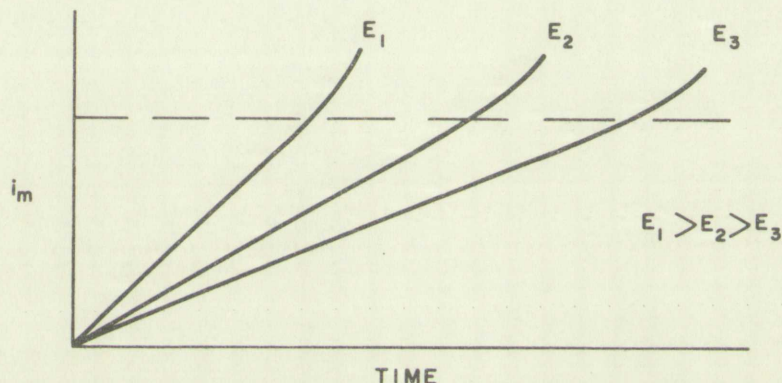


Figure 6. The Influence of Pulse Amplitude and Core Saturation on Magnetizing Current

should be the same at all intersections with this dashed line, It therefore is evident that the start of the upward curvature corresponds to entering the saturated region of the transformer, which occurs at a particular flux density. Also by Equation (11), the intersections with any other horizontal line will occur at identical flux densities.

It will be shown later that the maximum magnetizing current which a blocking oscillator can supply is usually determined by the characteristics of the tube or transistor and by the manner in which they are operated. The transformer design will control whether this maximum current occurs in the saturated or unsaturated region of the transformer by determining the maximum flux density.

This is a graph showing the influence of the parameter  $\alpha$  on the maximum error  $\epsilon_{max}$ . The x-axis represents  $\alpha$  and the y-axis represents  $\epsilon_{max}$ . Three curves are plotted, labeled 1, 2, and 3, showing that  $\epsilon_{max}$  decreases as  $\alpha$  increases.

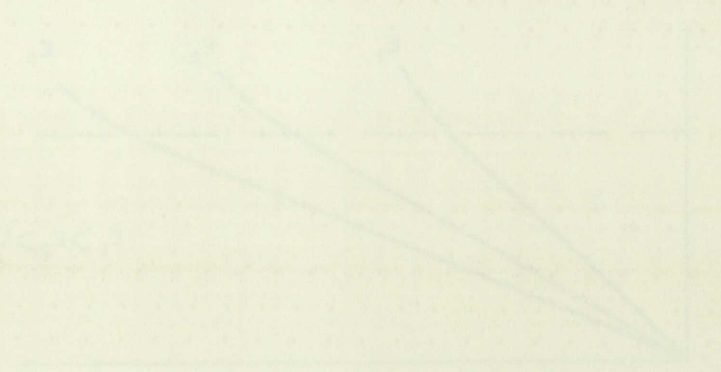


Figure 1. The influence of the parameter  $\alpha$  on the maximum error  $\epsilon_{max}$ .

It will be shown later that the maximum error  $\epsilon_{max}$  depends on the parameter  $\alpha$  and the parameter  $\beta$ . The parameter  $\beta$  is defined as the ratio of the length of the tube to the radius of the tube. The parameter  $\alpha$  is defined as the ratio of the length of the tube to the length of the tube.

The maximum error  $\epsilon_{max}$  is a function of the parameters  $\alpha$  and  $\beta$ . The maximum error  $\epsilon_{max}$  is a function of the parameters  $\alpha$  and  $\beta$ . The maximum error  $\epsilon_{max}$  is a function of the parameters  $\alpha$  and  $\beta$ .

The maximum error  $\epsilon_{max}$  is a function of the parameters  $\alpha$  and  $\beta$ . The maximum error  $\epsilon_{max}$  is a function of the parameters  $\alpha$  and  $\beta$ .



The average pulse amplitude, pulse width, and maximum magnetizing current may be considered fixed quantities for a given design. Hence, the volt-seconds given by Equation (8) and the current given by Equation (11) may be considered to be fixed quantities. Rewriting Equation (8) after assuming the initial flux density is zero, gives

$$ET = N B_m A = \text{constant} \quad (12)$$

Also from equation (11)

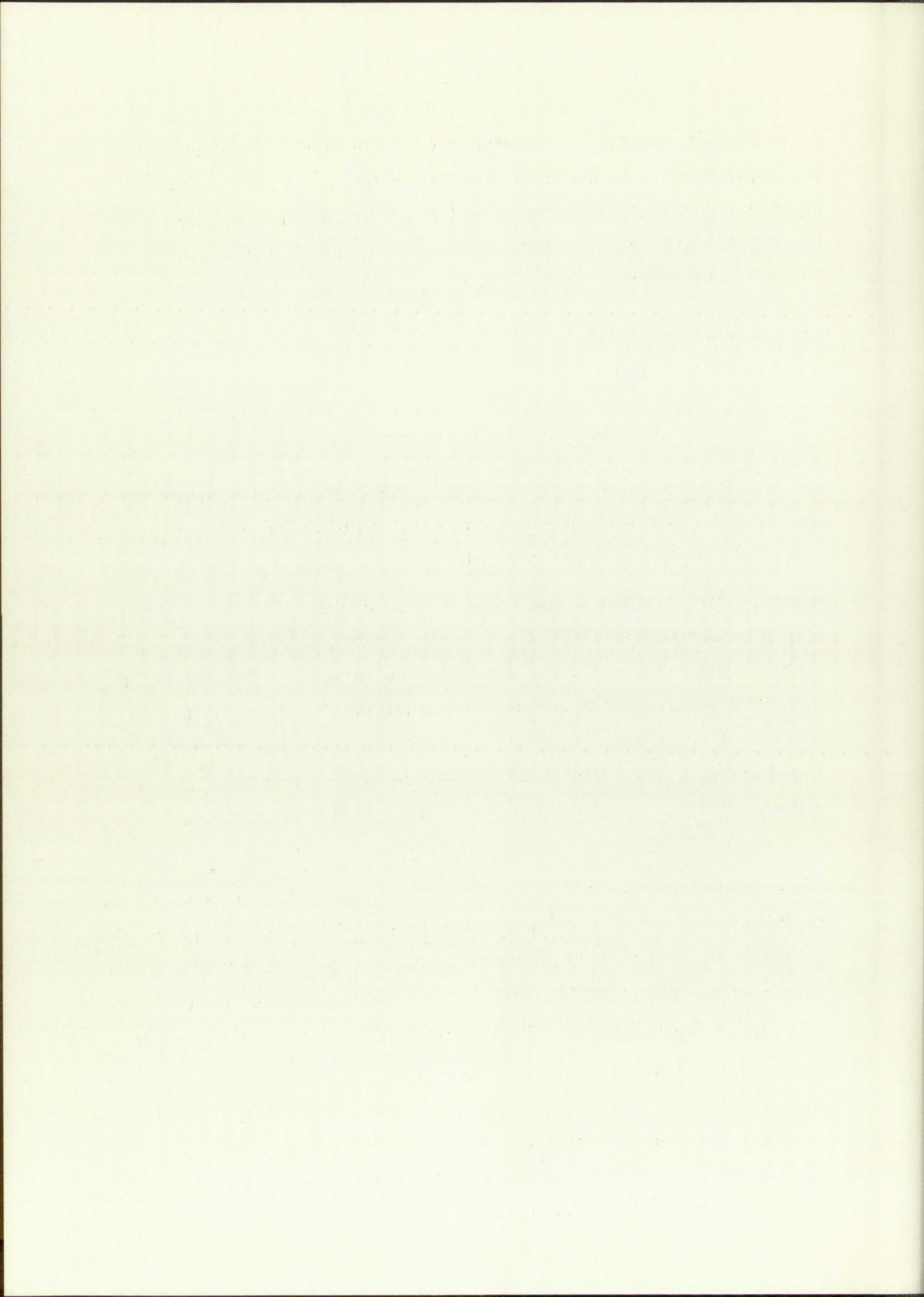
$$I_m \propto \frac{1_c B_m}{N \Delta \mu} = \text{constant} \quad (13)$$

The values of  $N$ ,  $B_m$ ,  $A$  and  $1_c$  must be such that Equations (12) and (13) are simultaneously satisfied; the result is that independent variation of these parameters is not possible.

These equations are primarily useful in optimizing a preliminary design. For example, assume that after a preliminary transformer design it is found desirable to increase the number of turns while still maintaining a linear transformer. By Equation (13) a fractional increase in turns will require the same fractional increase in flux density. By Equation (12) this will require the core area to be reduced by twice this fractional amount. It is evident that there is a maximum number of turns for a linear design, because of the saturation flux density.

Suppose a saturating transformer is being designed and it is found desirable to increase the number of turns. A fractional increase in the turns in Equation (13) may cause little increase in flux density due to the reduction in incremental permeability. Thus, by Equation (12) a reduction in area, approximately equal to the increase in turns, is required.

The actual transformer design calculations may use Equations (12) and (13) or, as is more common, Equations (8) and (9). In either case, the calculations are approximations since the pulse voltage may not be constant throughout the pulse, and the inductance, even in the so-called linear region, will be nonlinear because of the variation of incremental



permeability with flux density. The accurate calculations of turns and core area are quite complicated. The usual method is to use these equations for rough estimates, choosing the final values experimentally. The mechanics of estimating the characteristics of the core material, inserting them into these equations, and solving the equations, can be found in many sources, such as Lee [1].\*

### Choice of Core Material

The type of core material has a direct bearing on the number of turns and the core dimensions necessary for a given primary inductance, because of the influence of incremental permeability. In addition, it will govern how the primary inductance varies with operating conditions and environment. It may also determine the type of construction allowable.

The more important properties to be considered are the saturation flux density, the variation of permeability with flux density, the effects of temperature, and the sensitivity to strain and pressure. The effects of temperature, strain, and pressure appear as variations in the saturation flux density and the permeability. If square B-H loop materials are used, additional properties to consider are the residual flux density and the reset characteristics.

A large selection of core materials is commercially available, including metal alloys, powdered iron, and ferrites. The characteristics and applications of these various materials can be found in Lee [1] and Owens [2].

The materials are also available in a variety of forms. Examples are cup-cores, laminations, toroids, C-cores, and bulk tape. The choice of core shape should be determined individually for each blocking oscillator design, for optimum results.

---

\* Numbers in brackets refer to the List of References on page 87.

## Choice of Core Material

The type of core material has a great bearing on the number of turns for the core dimensions necessary for a given primary inductance because of the influence of the material permeability. In addition, it will provide for the primary inductance values with operating conditions and variations. It may also determine the type of construction allowable.

The core material properties to be considered are the permeability, the density, the saturation, and the consistency in stress and pressure. The effects of temperature, aging, and pressure appear as variations in the nature of permeability and the consistency. The density of the material is also an important property to consider as the residual flux density and the core losses are affected.

Large selection of core materials is now commercially available in many different sizes, powdered type, and laminated. The characteristics and applications of these various materials can be found in [1] and [2].

The materials are also available in a variety of forms. Examples of these are: laminated, powdered, ferrite, and glass. The choice of core material should be determined individually for each design case.

The most widely used core material for blocking oscillator transformers is ordinary silicon-iron<sup>4</sup> with tape thicknesses between one-half and twelve mils. This material has good temperature characteristics and is only slightly strain- or pressure-sensitive. It is available in such forms as laminations, toroids, C-cores, or bulk tape. With bulk tape, hand- or machine-wound cores may be fabricated for special applications.

There are occasions when the use of materials having a square B-H loop is desirable or necessary. Various nickel alloys and ferrites are available in toroidal cores. Toroidal shapes are necessary to reduce the effects of air gaps to a minimum. These materials generally have greater variations due to temperature, and are more expensive than silicon-iron.

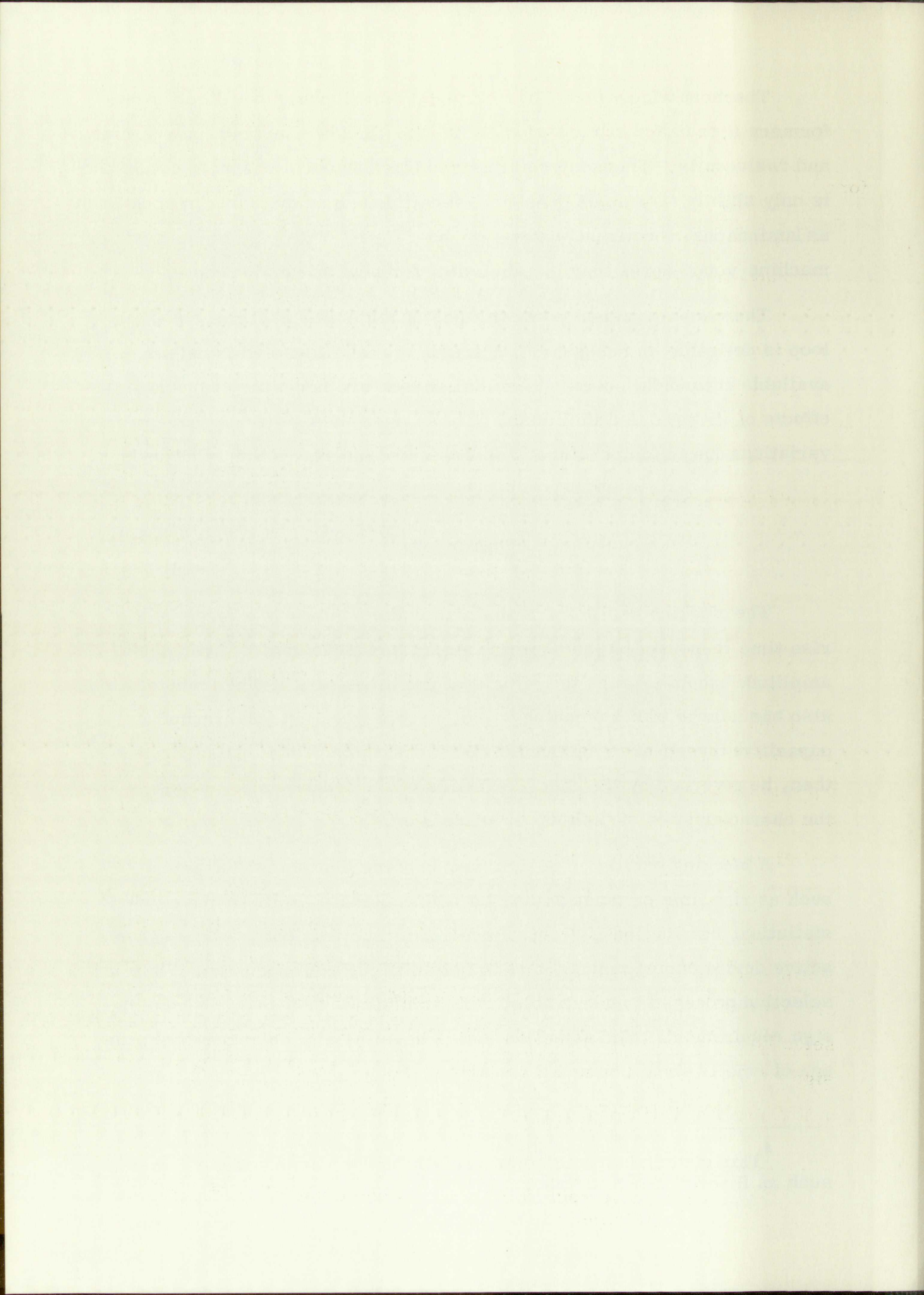
### Uniformity

The blocking oscillator transformer determines to a large degree the rise time response; but as shown later, it has little control over pulse amplitude except through the effects of the turns ratio. The transformer also has a large effect on pulse width, except when external turnoff or capacitive turnoff are employed. The blocking oscillator pulse shape will, then, be governed by the characteristics of the transformer as well as by the characteristics of the tube or transistor.

A blocking oscillator design may require that some characteristic, such as rise time or pulse width, be within certain limits or have given statistical distributions. Control over the important parameters of the active device during manufacture is both difficult and expensive. While a selection process is undesirable, it is sometimes necessary to meet design requirements; the selection tests should be simple and the percentage of rejects should be small for a good design.

---

<sup>4</sup>This material is sold commercially under various trade names, such as Hipersil and Silectron.



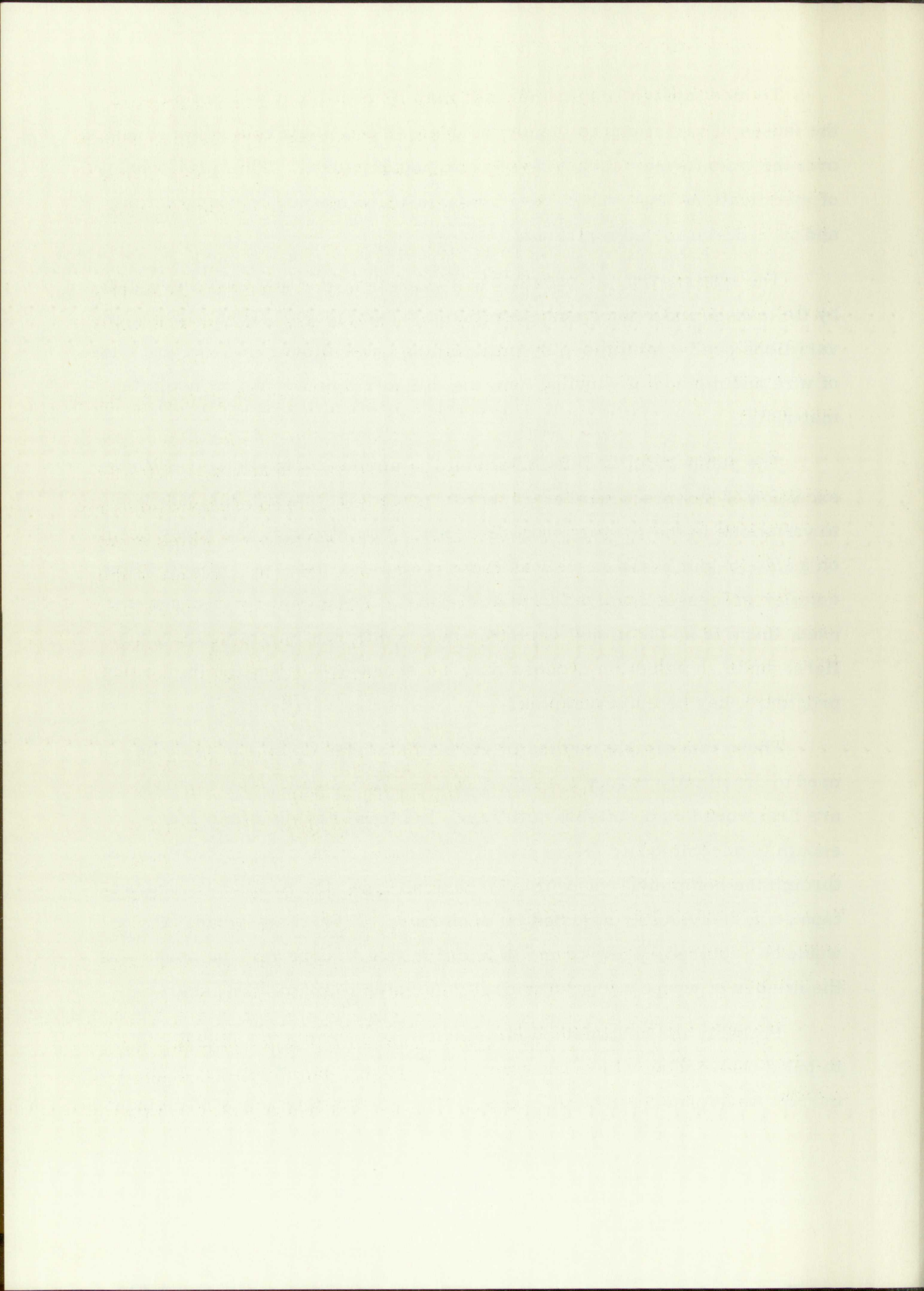
To meet design requirements it may be necessary to allot most of the causes of variations to the active device, and to exercise close control over the transformer during design and manufacture. This may consist of specifications and control over materials and method of construction, and procedures for adjusting and testing.

The rise period, as previously discussed, is determined primarily by the leakage inductance and distributed capacitances. Thus, rise time variations can be minimized by maintaining control over dimensions, size of wire and method of winding, and the dielectric constants of insulating materials.

The pulse width is determined by the primary inductance. With the exception of incorrect number of turns, pulse width variations will be due to variations in the properties of the core. Variations in the cores occur on a unit-to-unit basis as well as from production lots, as a result of the complex processes involved in manufacture. When cup- or C-cores are used, there is an additional variation due to different effective air gaps. Here, again, a selection process may be necessary, although the testing procedure may be quite complex.

There is a simple method of core adjustment which can often be used to drastically reduce the effect of core variations. The windings are first wound on a suitable coil form, the form having a hole large enough to accommodate the required core area. The core is then wound through the completed coil with silicon-iron tape, the number of wraps of tape being individually adjusted on each core. If too many wraps of tape would be required, a few wraps in addition to a C-core may be used, with the number of wraps being individually adjusted to match the cores.

Probably the best method of determining proper core adjustment is to pulse one winding with a fixed amplitude pulse, and monitor the exciting current waveform on an oscilloscope. The core is then adjusted to provide





a given exciting current at a specified time after the start of the pulse. For maximum accuracy this value of exciting current should be chosen to be within the range of the maximum magnetizing current obtained in actual circuit operation.

With unadjusted C-cores the distribution of pulse widths due to the transformers has been found to have standard deviations as high as 25 percent of the average pulse width. Using this adjustment procedure this figure can be reduced to less than 5 percent.

Pictures of various transformers, designed for adjustment by the above method, are shown in Figure 7. Note that the coil portion of the production type transformers has been potted before assembly of the cores, resulting in a very stable unit. While the cores of these units are not tightly anchored, they were made to go into assemblies which would also be potted.

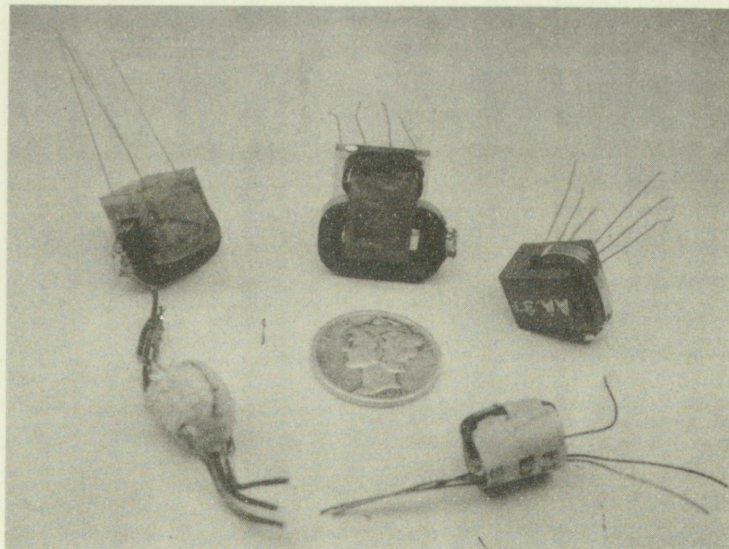
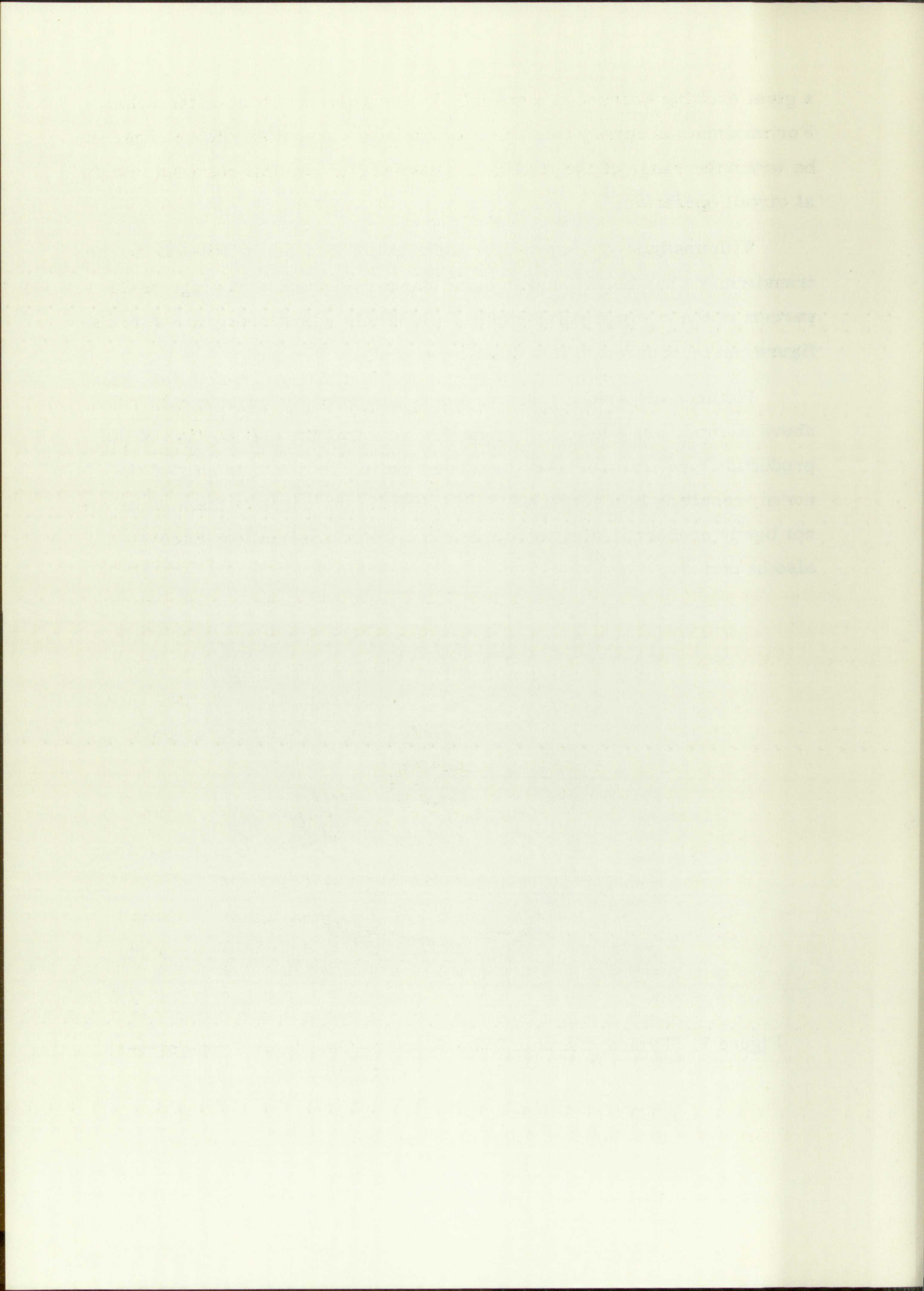


Figure 7. Typical Vacuum Tube Blocking Oscillator Transformers



## CHAPTER IV -- VACUUM TUBE INTRINSIC BLOCKING OSCILLATORS

### Graphical Analysis

#### Tube Characteristics

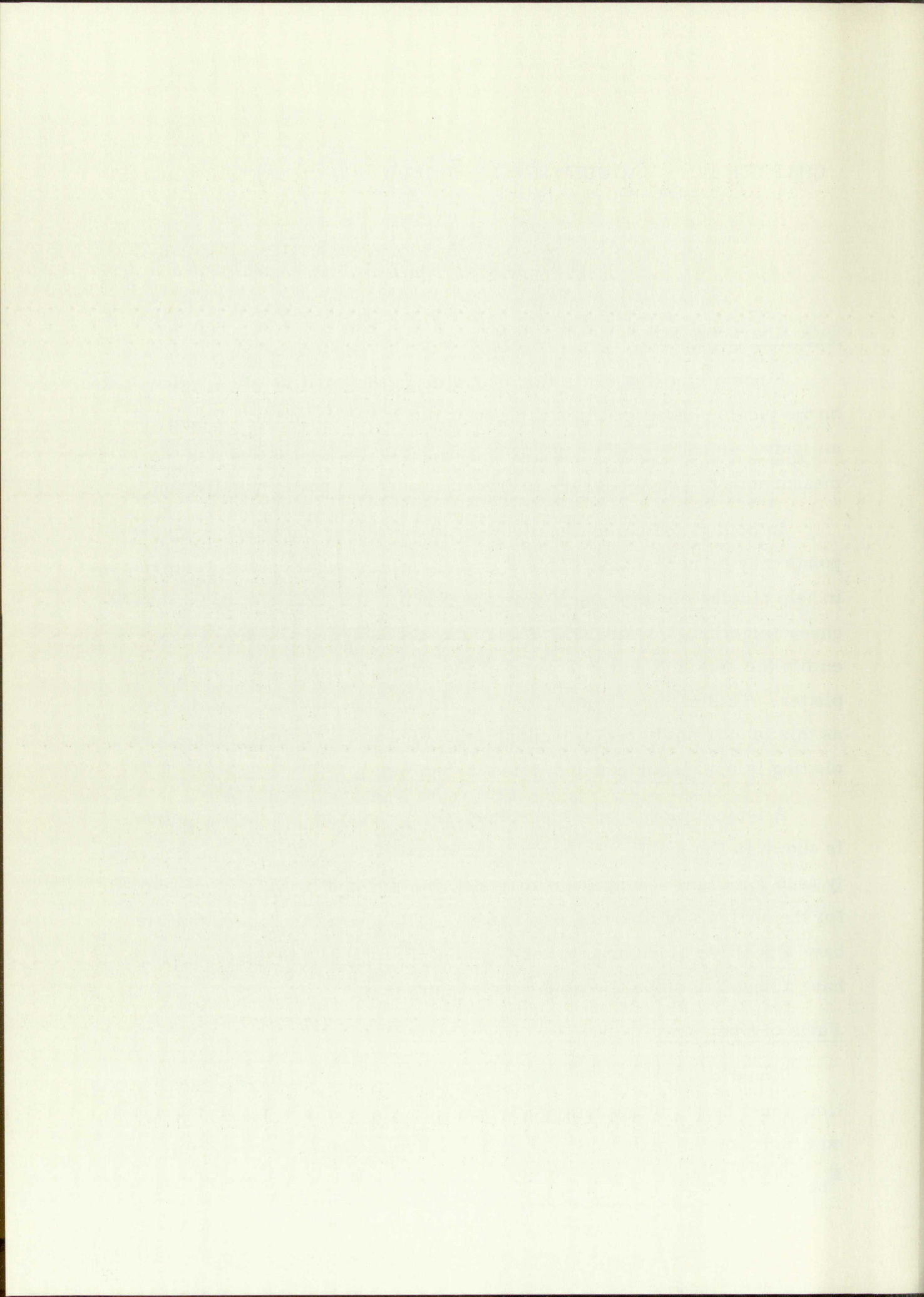
Since a blocking oscillator operates in the positive grid region, data on the tube's characteristics in this region is required for a graphical analysis. Because of the high peak power dissipation in this region, pulse measurements are necessary to limit the average power dissipation.

In both graphical and mathematical analyses, only data at discrete points may be necessary. To aid in determining what data is required and to help picture blocking oscillator operation, a general plot of the tube's characteristics is desirable. A circuit was designed and constructed to enable the semiautomatic plotting of the tube's characteristics on an X-Y plotter. This circuit is described briefly in Appendix A. A method such as this is extremely useful if many tubes are to be studied, since point plotting is both laborious and time-consuming.

A typical plot of tube characteristics, made by the above method, is shown in Figure 8. While constant current characteristics are normally used for Class C amplifier analysis, the present form is more suitable for the analysis of blocking oscillators. The curves in Figure 8 which have a positive slope are curves of plate current; and the curves which have a negative slope are grid current curves.

#### Paths of Operation

Equations (1) and (2) relate the plate and grid voltages; these equations must be simultaneously satisfied. Plots of values satisfying these equations for the plate and grid currents are shown in Figure 8 for  $E_{bb} = 150$ ,  $E_k = 18$ , and  $n = 1.2$ .



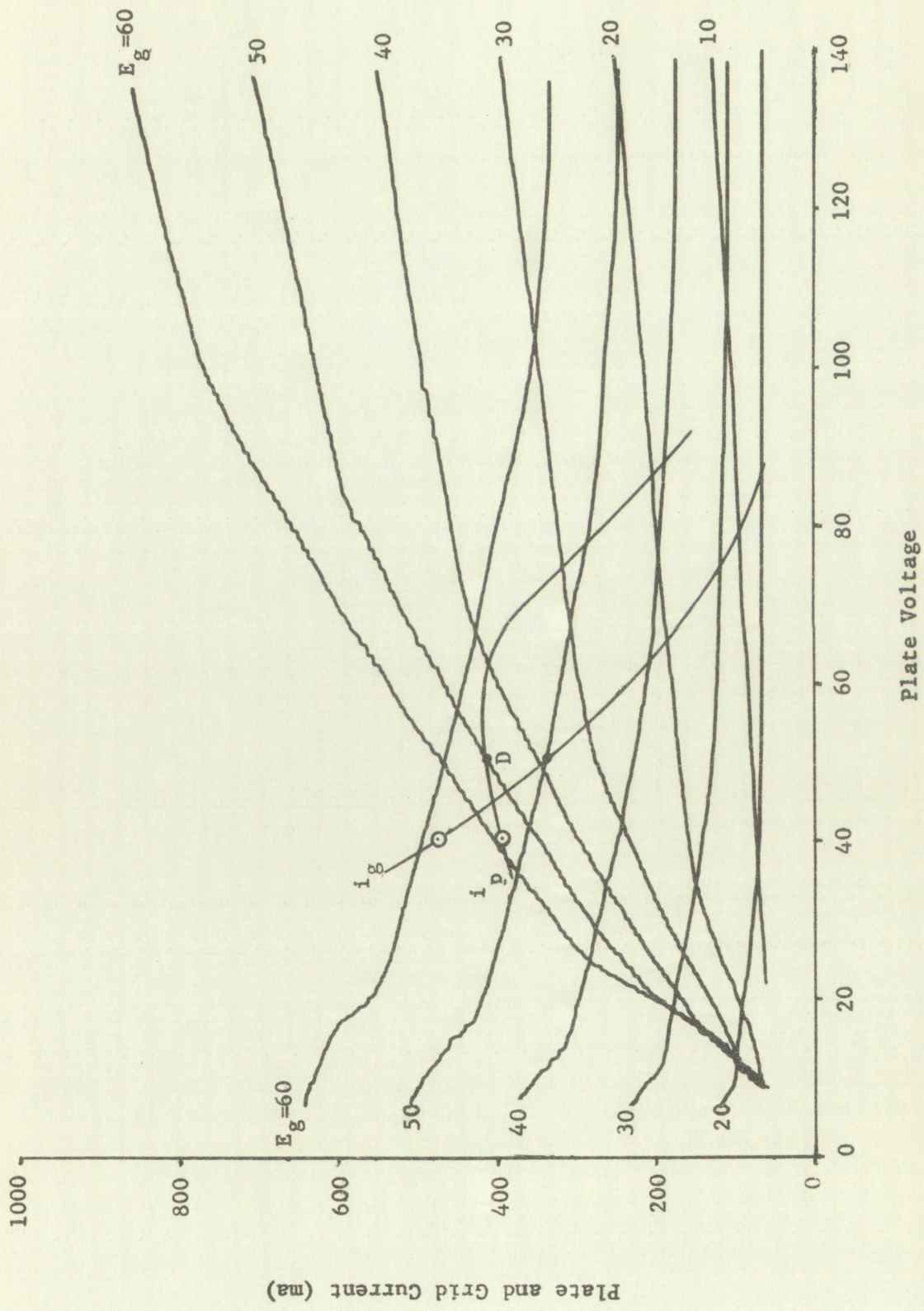
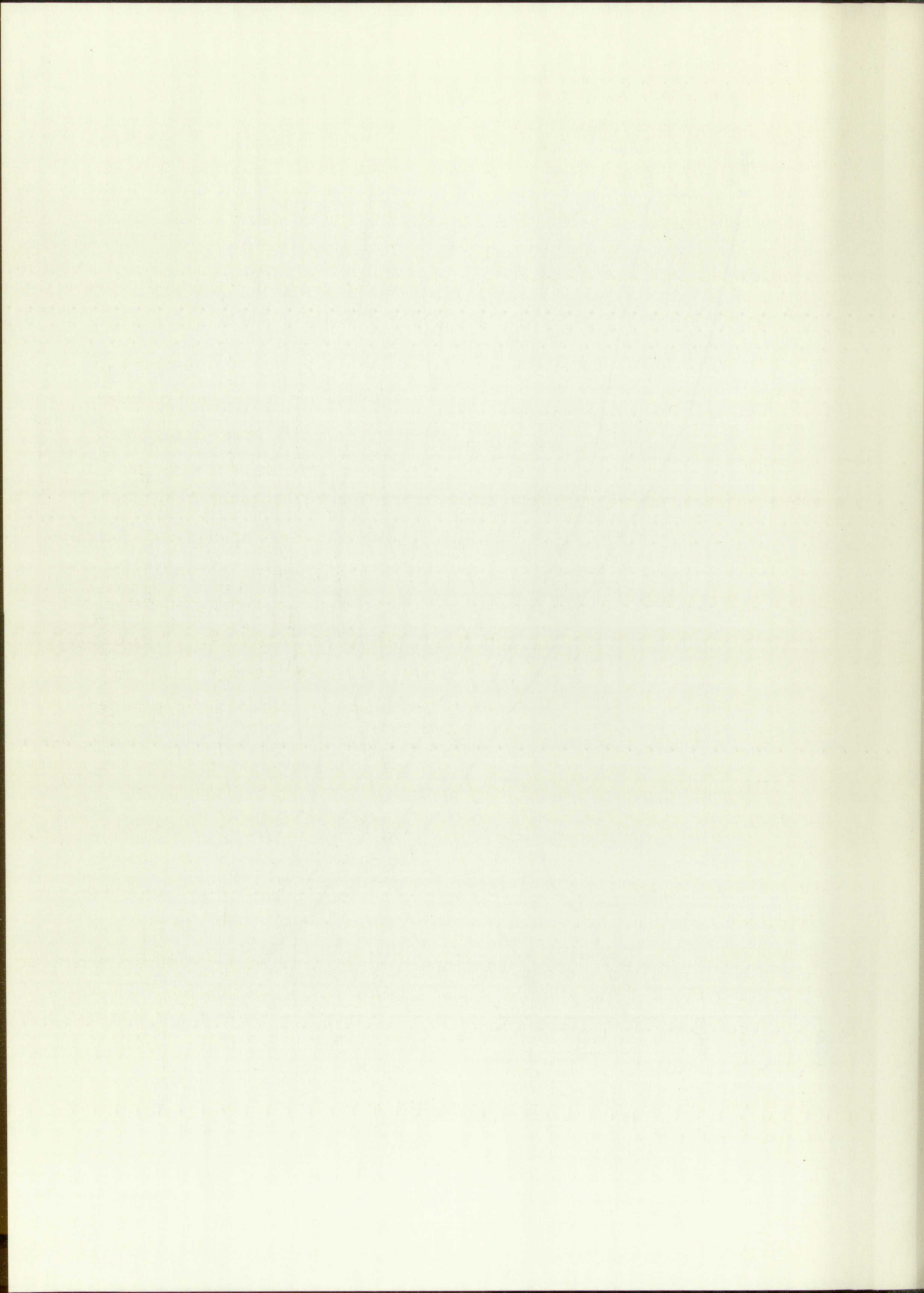


Figure 8. Typical Positive-Grid Characteristics and Paths of Operation



Assume that the magnetizing current is zero during the rise period, an assumption that should contribute very little error. The currents at the start of the main part of the pulse are found from Equation (3) to be

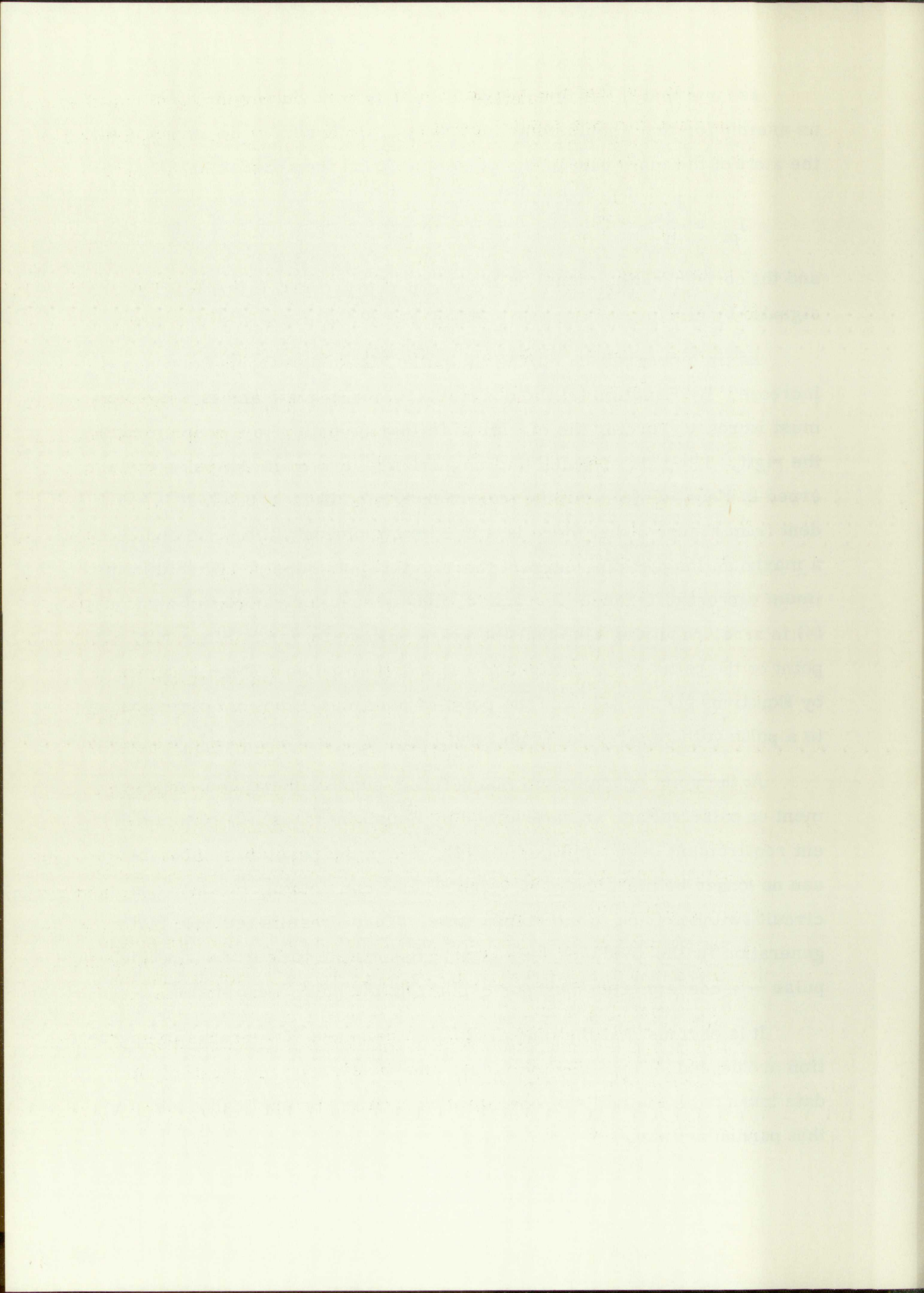
$$I_{pi} = \frac{I_{gi}}{n}$$

and the corresponding points on the paths of operation in Figure 8 are designated by circles.

As time progresses during the pulse, the magnetizing current will increase. By Equation (3) the difference between plate and grid currents must increase, forcing the circuit to follow the path of operation toward the right. The rate at which the magnetizing current increases is governed by Equation (4). As the path of operation is traversed, it is evident from Figure 8 that there is a maximum current difference and, hence, a maximum magnetizing current that the tube can supply. When this maximum current difference is reached, the current derivative in Equation (4) is zero, requiring also that the pulse voltage be zero. However, each point on the paths of operation corresponds to a pulse voltage as given by Equations (1) and (2), and the point of maximum current corresponds to a pulse voltage different from zero.

At the point of maximum magnetizing current there is a requirement on pulse voltage as determined by Equations (1) and (2), and a different requirement based on Equation (4). Since the physical requirements can no longer be met, the quasi-stable state can no longer exist, and the circuit switches back to the stable state. These results indicate that regeneration in the feedback loop is not responsible for terminating the pulse — a concept often used for explaining the pulse termination.

It is obvious that the magnitude and the shape of the paths of operation are dependent upon the individual tube's characteristics. Actual data taken from the paths of operation will, then, be applicable only for that particular tube.





## Theory of Analysis

The relationship between pulse voltage and magnetizing current can be obtained by rewriting Equation (4) as follows:

$$e_o = L_p \frac{di_m}{dt} = L_p \frac{di_m}{de_o} \frac{de_o}{dt} \quad (14)$$

where the values of the derivative of magnetizing current with respect to the pulse voltage can be obtained from the paths of operation.

The direct solution of Equation (14) for pulse voltage as a function of time is quite complicated because the pulse voltage is a double-valued function of time. As time is a single-valued function of the pulse voltage, this equation may be solved for time,  $t$ , giving

$$t = L_p \int_{E_i}^{e_o} \frac{di_m/de_o}{e_o} de_o \quad (15)$$

where  $E_i$  is the output pulse voltage at the start of the quasi-stable interval. A solution of this equation for time as a function of pulse voltage will, in the end, give the same information as a solution of Equation (14).

Although the current derivative is nonlinear, a graphical solution of Equation (15) can be obtained by performing the following steps:

1. From the path of operation, plot the magnetizing current versus the output pulse voltage.
2. Graphically differentiate the resulting curve at discrete points.
3. Divide the derivatives by the value of the pulse voltage at the corresponding points.
4. Plot the resultant points versus the pulse voltage and draw a smooth curve through them.

The first part of the report is devoted to a general survey of the situation in the country.

The second part contains a detailed account of the work done during the year.

The third part is a summary of the results of the work.

The fourth part is a list of the names of the persons who have taken part in the work.

The fifth part is a list of the names of the persons who have been appointed to the various offices.

The sixth part is a list of the names of the persons who have been elected to the various offices.

The seventh part is a list of the names of the persons who have been appointed to the various offices.

The eighth part is a list of the names of the persons who have been elected to the various offices.

The ninth part is a list of the names of the persons who have been appointed to the various offices.

The tenth part is a list of the names of the persons who have been elected to the various offices.

The eleventh part is a list of the names of the persons who have been appointed to the various offices.

The twelfth part is a list of the names of the persons who have been elected to the various offices.

The thirteenth part is a list of the names of the persons who have been appointed to the various offices.

The fourteenth part is a list of the names of the persons who have been elected to the various offices.

The fifteenth part is a list of the names of the persons who have been appointed to the various offices.

5. Graphically integrate this curve.
6. Multiply the result by the value of primary inductance.
7. Plot the result as output pulse voltage versus time.

An illustration of these steps is given in Figure 9.

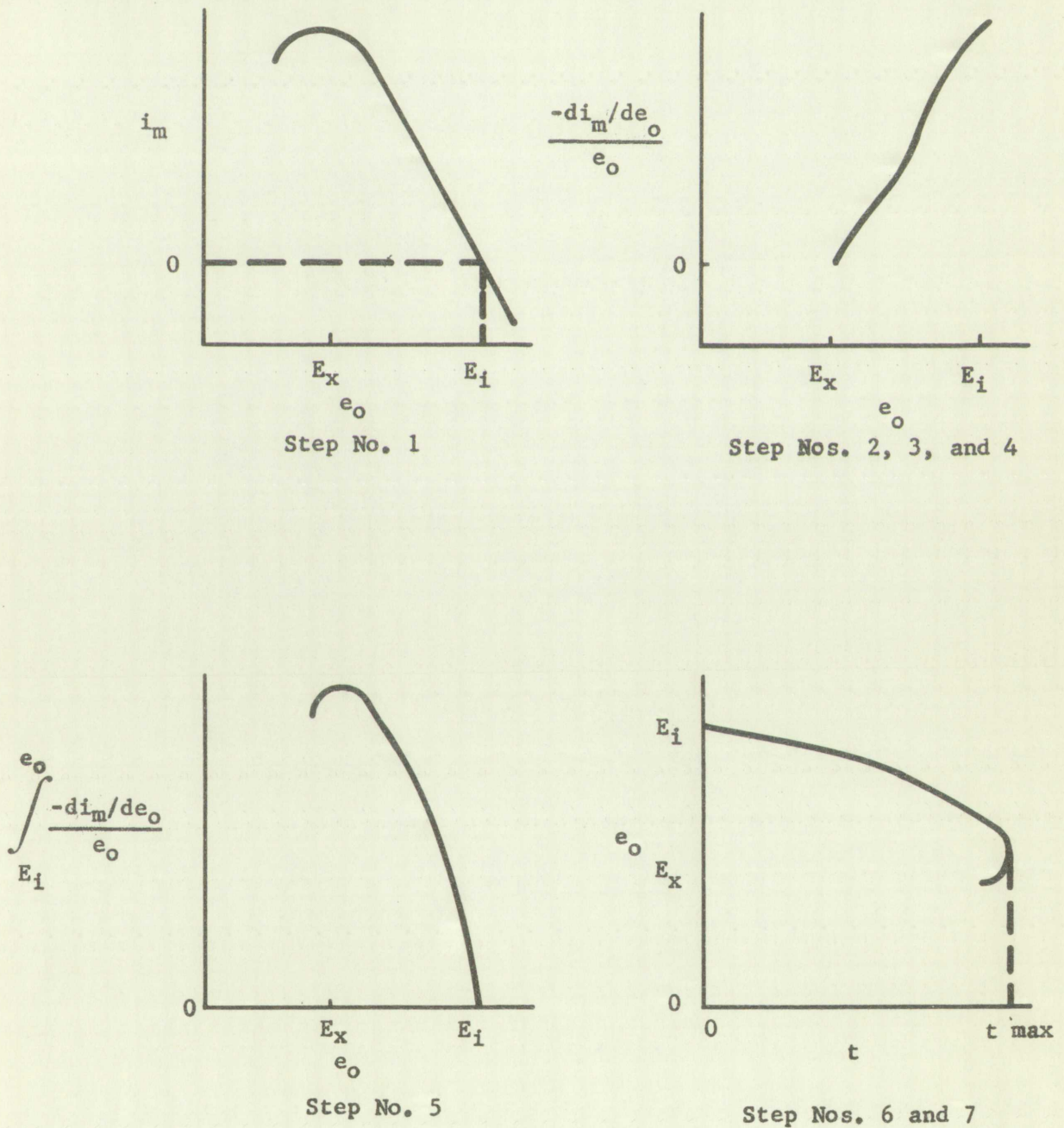


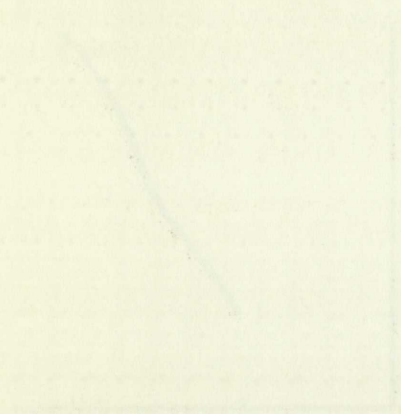
Figure 9. Illustrations of Steps Involved in Graphical Analysis

1. The function  $f(x)$  is given by

2. The function  $f(x)$  is given by

3. The function  $f(x)$  is given by

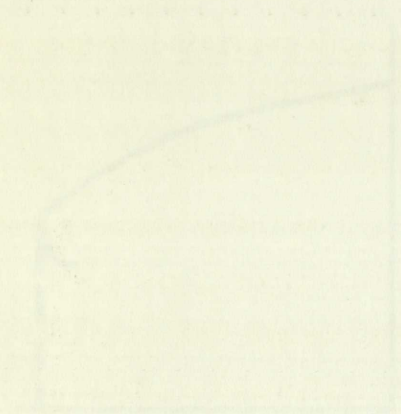
4. The function  $f(x)$  is given by



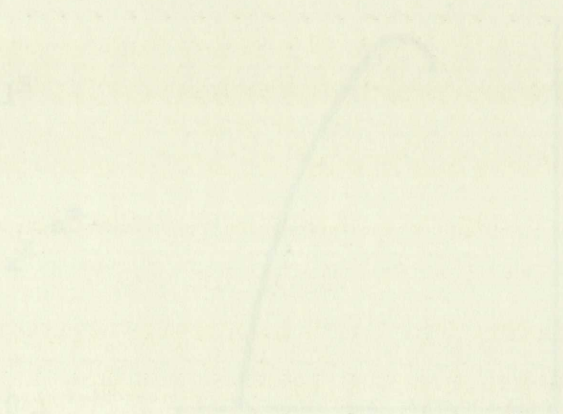
Graph 1



Graph 2



Graph 3



Graph 4

No approximations for the tube's characteristics are required by this graphical method. The accuracy of the final results are dependent only upon the accuracy of the tube data and the graphical techniques and upon the effect of the transformer approximations.

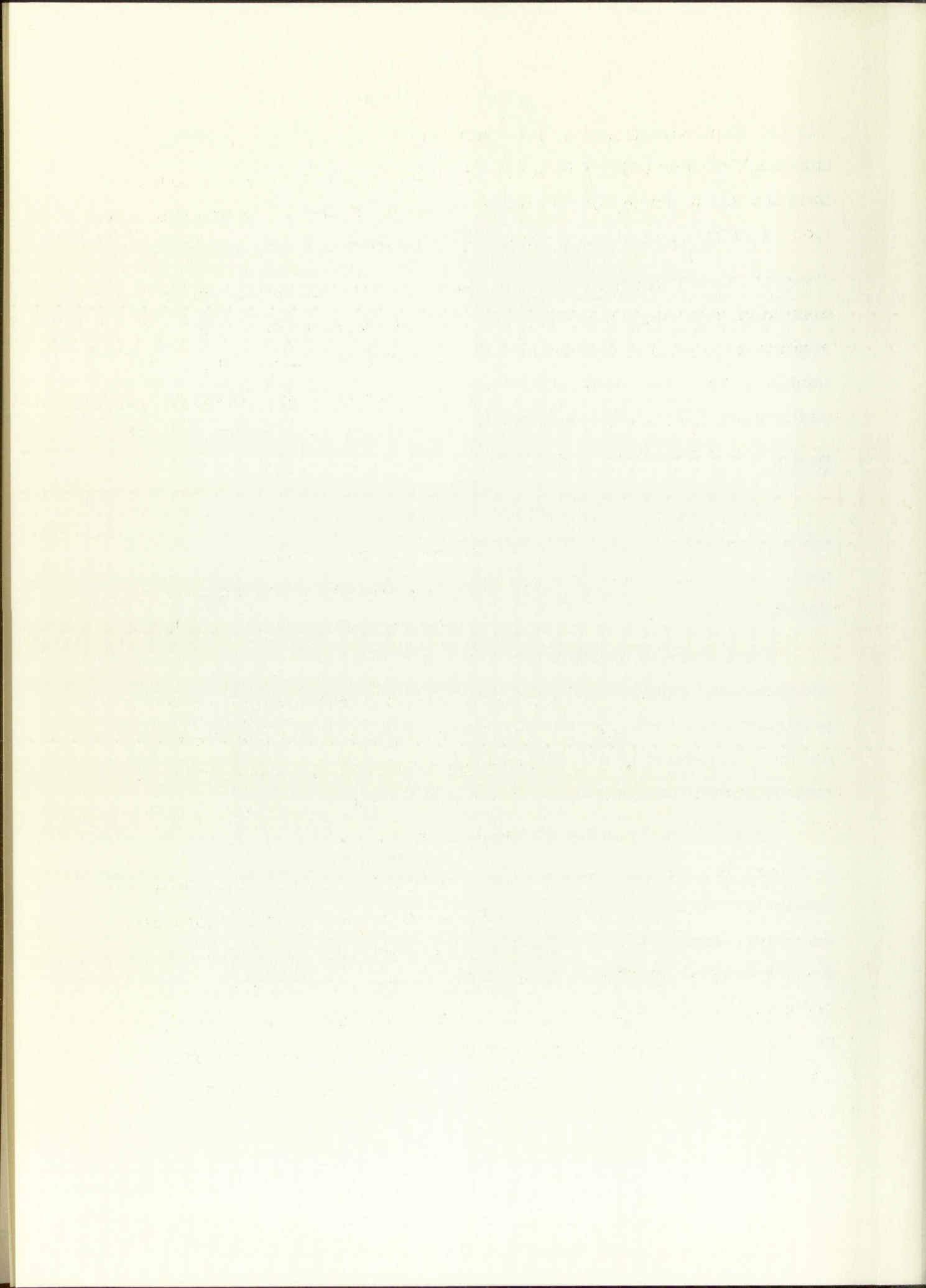
When the magnetizing current reaches a maximum, the current derivative goes through zero and the integral in Equation (15) reaches a maximum. Solutions beyond the point of maximum magnetizing current require that the time decrease, a physical impossibility. Thus, the pulse terminates when the current reaches a maximum, in agreement with the explanation in the previous section.

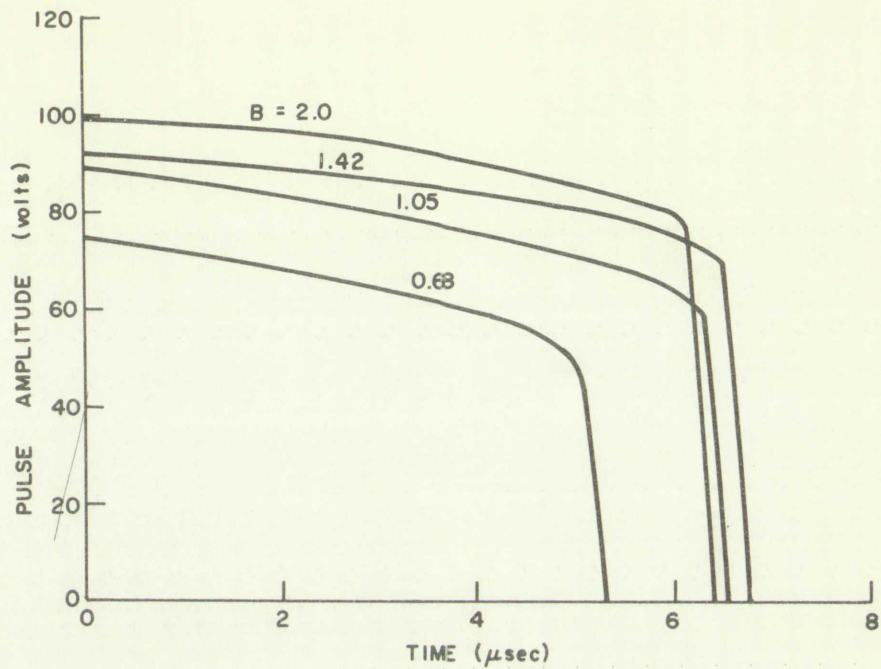
### Results

The result of performing the above graphical procedures on four tubes is shown in Figure 10. For comparison, the results obtained in the actual blocking oscillator circuit shown in Figure 11 are included in this figure.

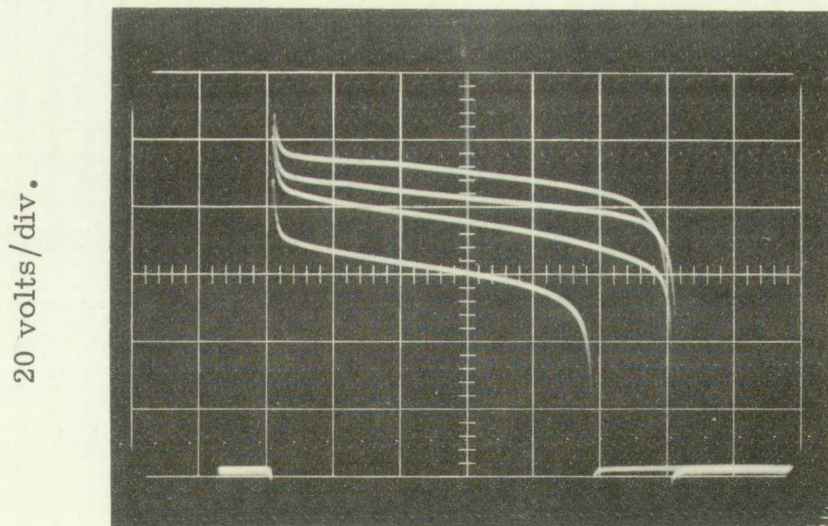
Since there is a relatively close agreement between the calculated and measured pulse shapes, the transformer approximations (for this particular transformer) are shown to be valid. This, as it turns out, is the most important result obtainable from a graphical analysis, as the method is too time-consuming to be used on a large scale.

The blocking oscillator circuit used to obtain these results is shown in Figure 11, along with data on the transformer. The transformer used single-layer windings and its design was based on considerations discussed in Chapter III. The transformer equivalent circuit values used in the graphical analysis were  $n = 1.2$  and  $L_p = 2$  millihenrys. The relationship between these equivalent circuit values and the actual transformer characteristics can be obtained from the information in Figures 11 and 12.





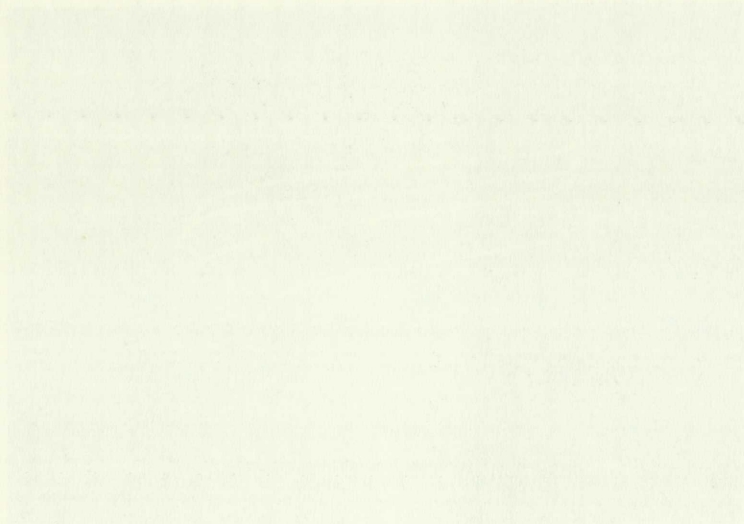
10(a). Pulse Shape Calculated From Tube Characteristic Curves



1 sec/div

10(b). Measured Pulse Shape

Figure 10. Comparison of Graphical and Measured Pulse Shapes





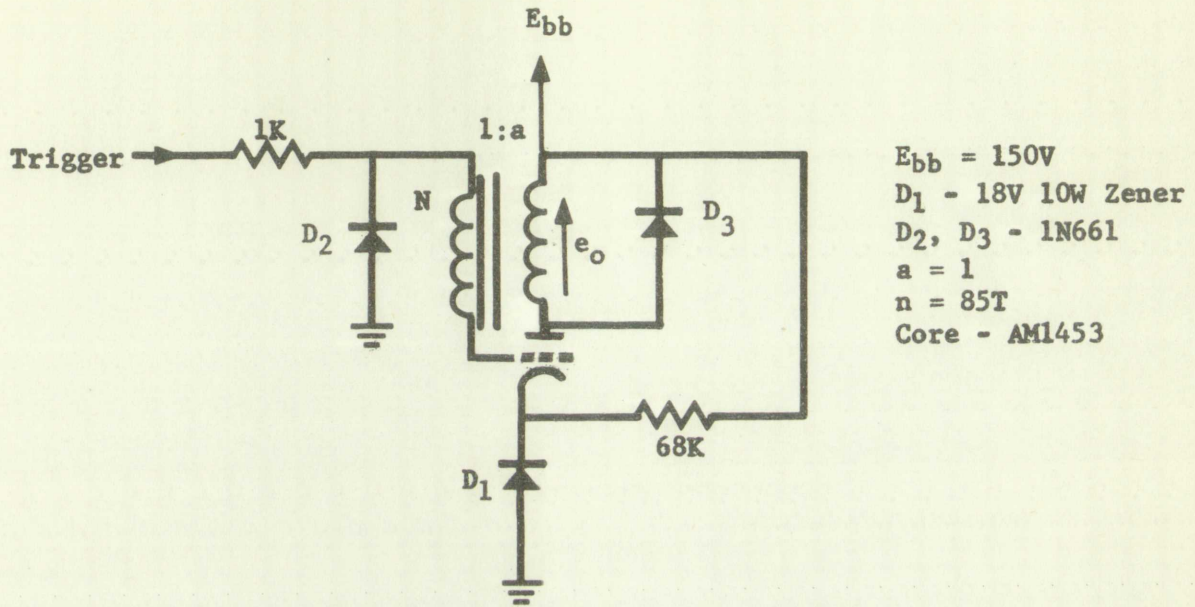


Figure 11. Intrinsic Blocking Oscillator

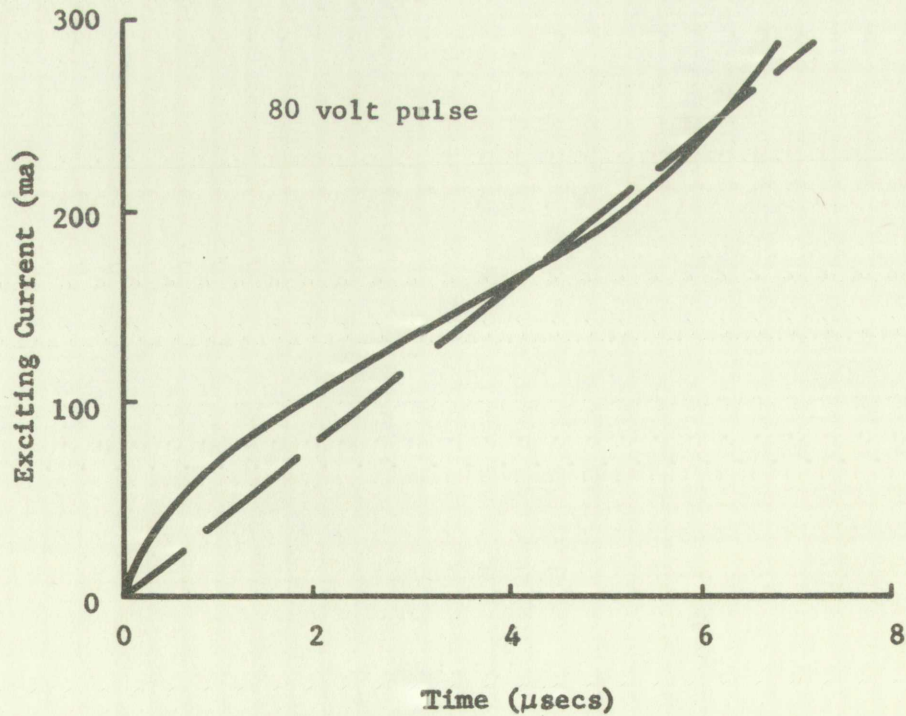


Figure 12. Exciting Current Waveform and Linear Approximation

$V_{CC} = 12V$   
 $R_1 = 10k\Omega$   
 $R_2 = 10k\Omega$   
 $R_E = 1k\Omega$   
 $R_C = 1k\Omega$   
 $\beta = 100$

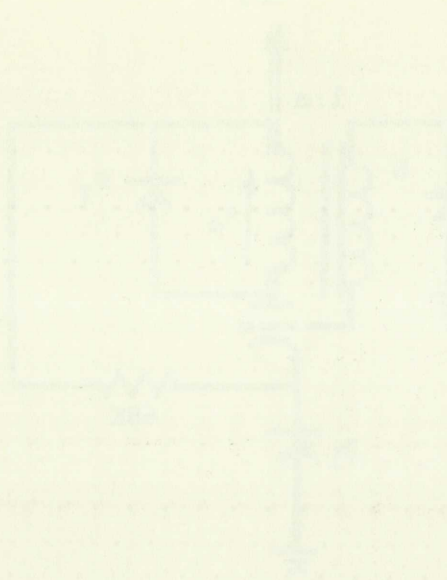


Figure 1: The basic BJT amplifier circuit.



Figure 2: Relationship between  $I_C$  and  $I_B$ .

The actual turns ratio of unity and the effective turns ratio of 1.2 implies by Equation (6) that the power efficiency is approximately 70 percent, a reasonable value for the high currents involved. Instead of estimating efficiency, a more accurate method of determining the effective turns ratio is to measure the primary and secondary pulse voltages under actual blocking oscillator operation.

The plot of exciting current versus time in Figure 12 was obtained by pulsing the primary winding with a constant voltage pulse. The maximum magnetizing current for the four tubes in Figure 10 was found during the graphical analysis to lie between 170 and 300 milliamperes. Assuming that the exciting current is predominantly magnetizing current, and choosing 250 milliamperes as a typical maximum value, a straight line is drawn through the origin and this current value on the exciting current waveform in Figure 12. The value of inductance corresponding to this straight line is found by Equation (4) to be 2 millihenrys. While the position of this straight line is somewhat arbitrary, it appears to be a good method of approximating the primary inductance. Although it is evident from the exciting current waveform that there is soft saturation at the higher currents for some tubes, this approximation is sufficient. If hard saturation were obtained, the method of approximation would have to be modified.

There is a relatively large difference between a portion of the exciting current waveform and the straight line approximation. There is some compensation, however, since both plate and grid currents decrease during the pulse. As these currents decrease, there is less drop in the series elements of the transformer, causing a relative increase in the voltage across the mutual inductance. While the exciting current waveform in Figure 12 was obtained with a constant voltage pulse and no load current, the actual waveform will be more nearly a straight line.

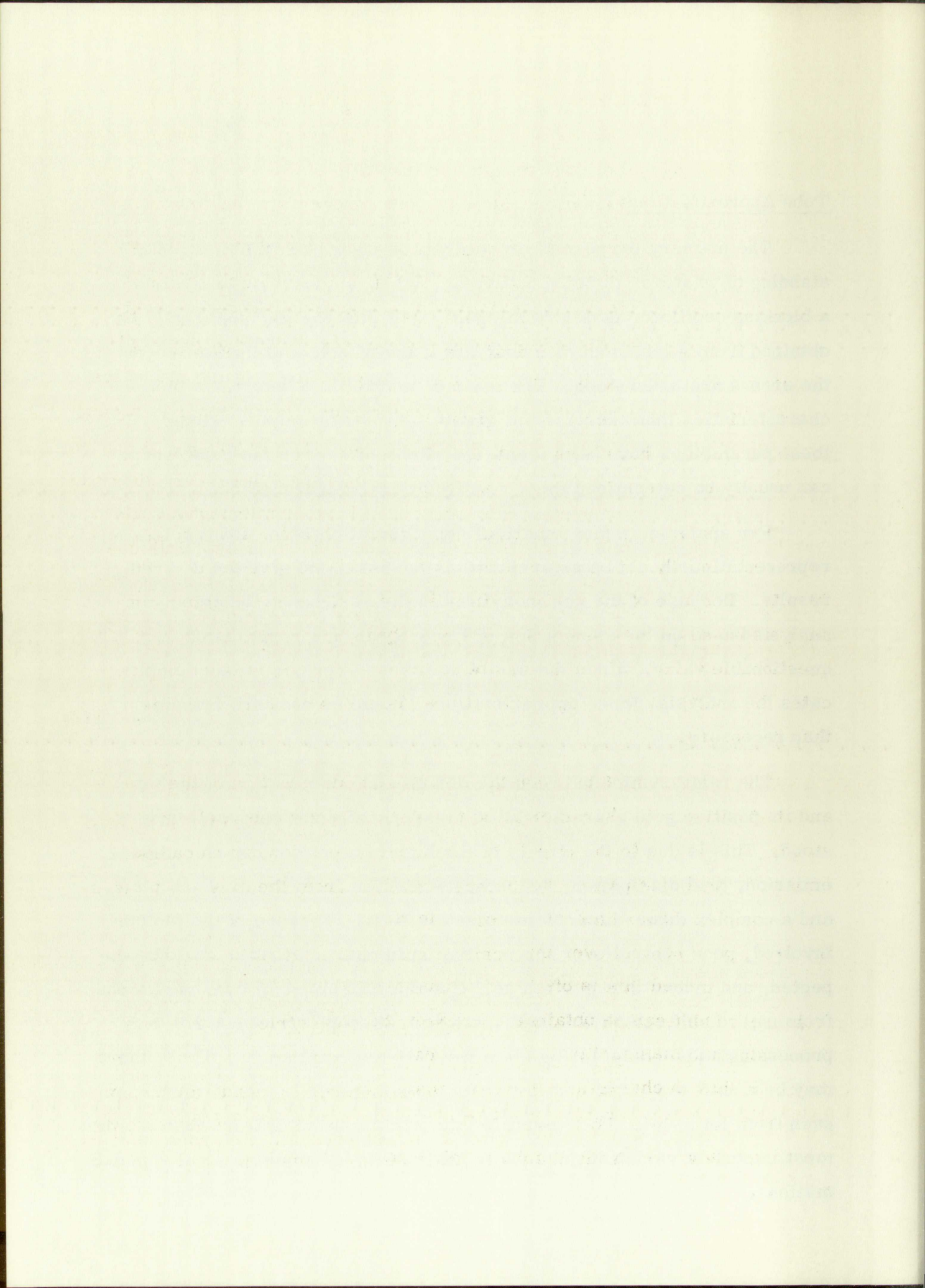


### Tube Approximations

The primary purpose of an analysis is to provide a better understanding of whatever is being analyzed. While an accurate analysis of a blocking oscillator is desirable, sufficient information can usually be obtained from a less accurate analysis if the effects and limitations of the errors are understood. The main objective is to determine the tube characteristics that exercise the greatest influence on pulse shape. Once these parameters have been identified, their effects on the pulse shape can usually be determined most readily by statistical methods.

For analysis, a mathematical representation is necessary; this representation should be as accurate as necessary to give the desired results. Because of the nonlinearities in the positive-grid region, an analysis based on the assumption of linearity in this region is of very questionable value. Since the use of nonlinear approximations complicates the analysis, these approximations should be no more complex than necessary.

The relationships between the design and construction of the tube and its positive grid characteristics are generally not very well understood. This is due to the effects of the high current density on cathode emission, grid dissipation, secondary emission from the grid and plate, and a complex three-dimensional electric field. Because of the factors involved, poor control over the positive grid characteristics could be expected, and indeed this is often so. Considerable control over variations from unit to unit can be obtained, however, through strict control over processing and manufacturing from the raw-material stage. Thus, there may be a shift in characteristics from manufacturer to manufacturer, or even from lot to lot. To account for the variations in characteristics, the most important variations should be inherent to the mathematical approximations.



Characterization of the tube can be accomplished by relating the plate and grid currents to the plate and grid voltages;<sup>5</sup> or, as indicated by Equation (3), by use of one current and the ratio of the currents. Lange [3] has shown that the ratio of plate to grid current is a function of the ratio of plate to grid voltage. This is to be expected, since, for a given voltage ratio, a change in the magnitude of the voltages will not appreciably alter the electric field configuration. Equations for the current ratio in terms of the tube dimensions have been developed by Spangenberg [4, p. 232] and by Jonker and Tellegen [5]. An equation relating the ratios is not strictly accurate, because of second-order effects, such as secondary emission and a change in the position of the virtual cathode. A sketch of the current ratio versus the voltage ratio on a log-log scale is shown in Figure 13 for several tubes. The tubes used here and throughout this article are a high pulse current version of the Type 6111 subminiature twin triode. Because primary interest will be in voltage ratios between one-half and four, the curves of Figure 13 show the possibility of using the following expression:

$$\frac{I_p}{I_g} = B \frac{E_p}{E_g} \quad (16)$$

where B is the ratio of plate to grid current when the plate and grid voltages are equal and is commonly called the current division factor. This equation approximates the curves with a straight line having a slope of unity.<sup>6</sup> There is a considerable error in this approximation with tubes

<sup>5</sup> Attempts to use Childs' Law have not been successful. This is apparently because the amplification factor in the positive grid region is not nearly as constant as in the negative grid region.

<sup>6</sup> The slope of the curves of the current ratio versus the voltage ratio will depend upon the tube type. Spangenberg [4, p. 225] shows curves with segmented slopes of two and of one-half, where the segment having a slope of unity, as shown in Figure 13, is not present. An approximation of these curves by Equation (16) is still feasible, although less accuracy can be expected.

The characteristics of the tube are as summarized by relating the  
flow rate  $Q$  to the pressure  $P$  and grid voltage  $V_g$  on an arbitrary  
coordinate system of grid voltage and the ratio of the current  $I$  to  
the grid voltage  $V_g$  to that of grid current  $I_g$  as a function of the  
ratio of grid voltage to grid current. This is to be expected, since for a  
given tube a change in the magnitude of the voltage will not produce  
any effect on the ratio  $I/I_g$  and the ratio  $I/I_g$  will be the same for  
all tubes of the same diameter. This has been demonstrated by comparing  
the data of Jones and Telford (1) with the data of the present  
investigation. The use of second-order effects, which is typical  
of the present and a change in the position of the virtual cathode. A  
plot of the virtual cathode position  $z$  versus the ratio  $I/I_g$  is shown in  
Figure 1. The present data are shown as open circles and the data of  
Jones and Telford (1) as solid circles. The Type 211 is a diode tube  
and the data of Jones and Telford (1) are for a diode tube. The  
present data are for a diode tube and the data of Jones and Telford  
are for a diode tube. The data of Jones and Telford (1) are for a  
diode tube and the data of the present investigation are for a  
diode tube.

(10)

$$\frac{I}{I_g} = \frac{V_g}{V_g - V_c} \left( \frac{V_g - V_c}{V_g} \right)^{3/2}$$

where  $V_c$  is the virtual cathode voltage and  $V_g$  is the grid voltage.  
The present data are in complete agreement with the data of Jones  
and Telford (1) for the diode tube with a virtual cathode voltage  
of zero. There is a significant error in the present data with  
non-zero virtual cathode voltage.

Attention is called to the fact that the present data are in  
complete agreement with the data of Jones and Telford (1) for the  
diode tube with a virtual cathode voltage of zero.

The data of the present investigation are for a diode tube with  
a virtual cathode voltage of zero. The data of Jones and Telford (1)  
are for a diode tube with a virtual cathode voltage of zero. The  
present data are in complete agreement with the data of Jones and  
Telford (1) for the diode tube with a virtual cathode voltage of  
zero.



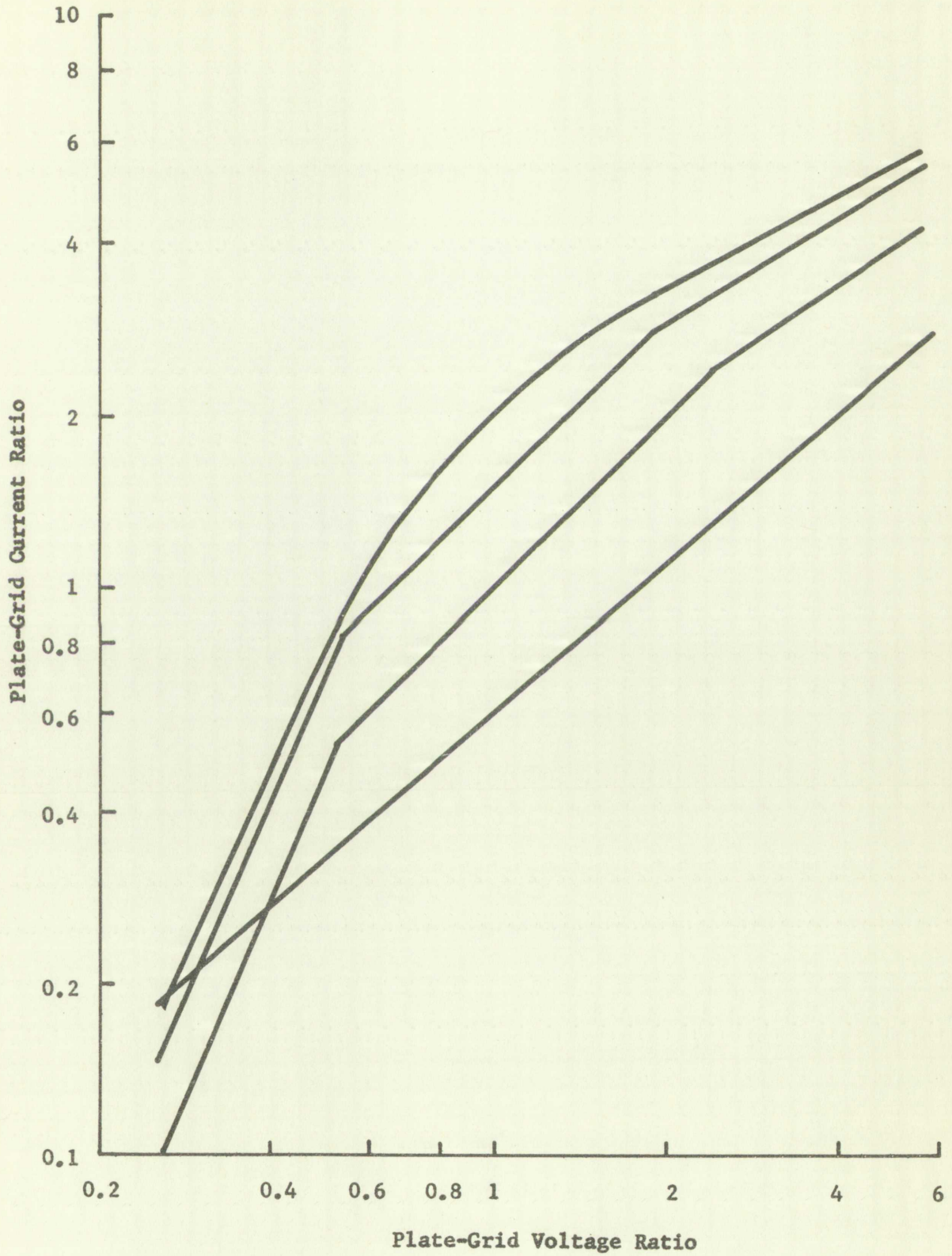
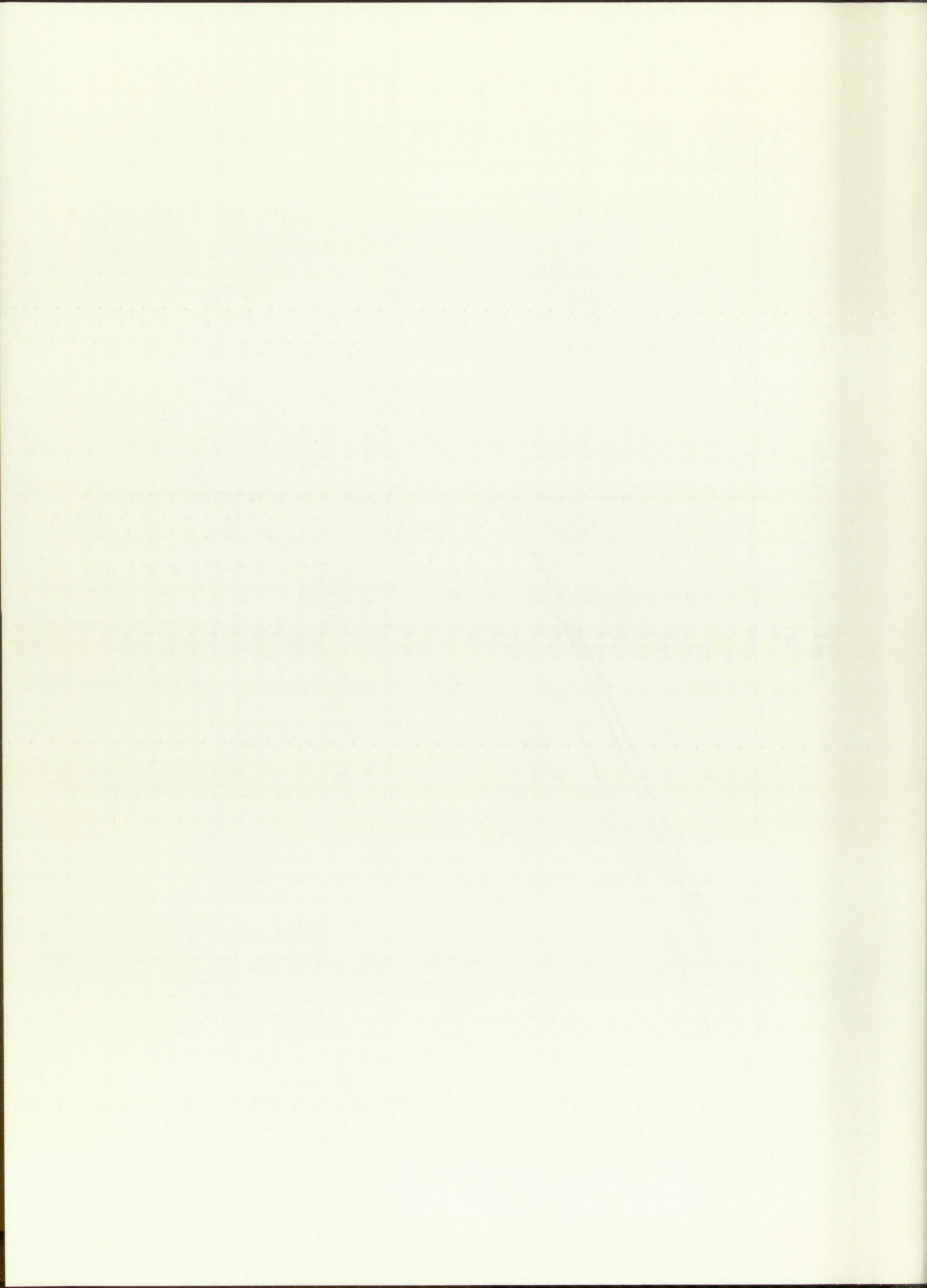


Figure 13. Typical Current Ratios as a Function of the Voltage Ratios



having a high current division factor. Better approximations could be made for these tubes; but the use of slopes other than unity would greatly complicate the mathematical analysis which follows.

Use of the current division factor appears to be warranted since it is worthy of consideration as a fourth tube constant by Spangenberg [4, p. 227]. The current division factor is not a true constant, primarily because of the effects of secondary emission. While various points on the tube's characteristics at which the plate and grid voltages are equal will give different values of B, these differences are usually small.

With use of Equation (16) as an approximation for the current ratio, there is need for an expression relating either the plate or grid current to the plate and grid voltages. Sketches on a log-log scale of grid current versus grid voltage over a path of operation are shown in Figure 14, for several tubes. A study of many similar curves reveals that the grid current can be approximated by

$$I_g = \frac{nKE_g^2}{B} \quad (17)$$

where the factor K accounts for the vertical displacement of the grid current characteristic curves. This parameter is, therefore, called the current emission factor. The approximations of Equations (16) and (17) result in the plate current being approximated by

$$I_p = nKE_p E_g$$

Since Equation (17) was obtained from paths of operation of intrinsic blocking oscillators of the type illustrated in Figures 1 and 11, this expression is not a general tube characteristic, but a nonlinear relationship which is valid only for this particular path of operation. While a general approximation for the plate or grid characteristic is desirable, the present approach has been chosen on the basis of the previous discussion on simplicity.

Using a first-order approximation... the results for these tubes... the mathematical analysis which follows...

Use of the current division factor appears to be warranted since... it is worthy of consideration as a function independent of geometry... The current division factor is not a true constant... While various points on... the tube's characteristic at which the initial grid voltage is equal... all give different values of  $\beta$ , these differences are usually small.

With use of Equation (10) as an approximation for the current... there is need for an approximation regarding either the plate or grid current... at the plate and grid voltages... sketches on a logarithmic scale of grid current... versus grid voltage over a part of operation are shown in Figure 11 for... several plates. A study of many similar curves reveals that the grid cur-

rent can be approximated by

$$I_g = I_{g0} \left( \frac{V_g}{V_{g0}} \right)^n \quad (17)$$

where the factor  $n$  accounts for the vertical displacement of the grid... characteristic curves. The parameter  $n$ , however, is called the... current emission factor. The approximations of Equations (16) and (17)... result in the plate current being approximated by

$$I_p = I_{p0} \left( \frac{V_p}{V_{p0}} \right)^m \left( \frac{V_g}{V_{g0}} \right)^n \quad (18)$$

Since Equation (17) was obtained from a first-order relation of uniform... plotting relations of the type illustrated in Figures 1 and 11. This ex-... relation is not a general tube characteristic, but a nonlinear relation... and which is valid only for the particular tube in question. While a... general approximation for the plate or grid characteristic is desirable... the present approach has been chosen on the basis of the previous... equation as applicable.

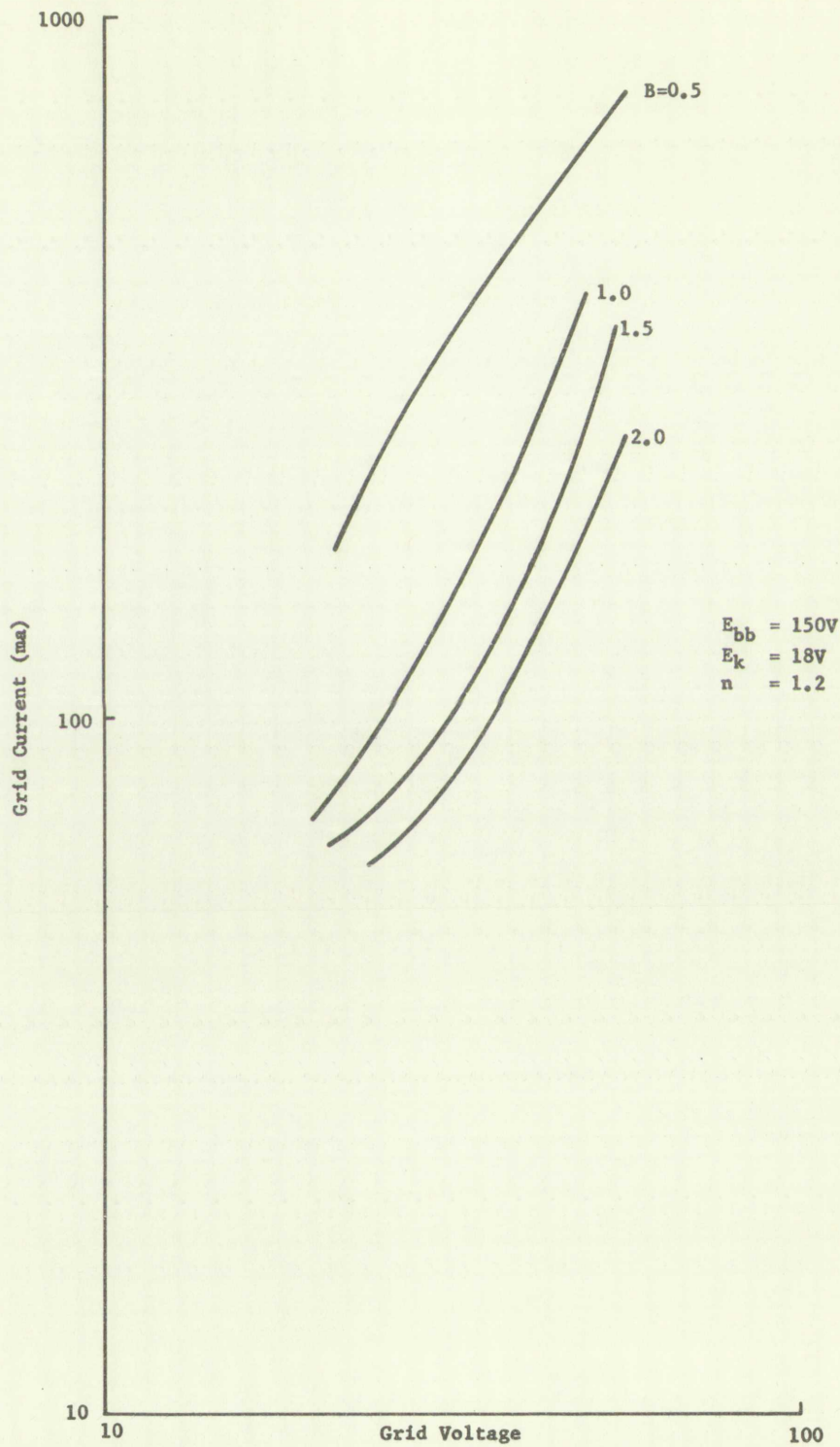
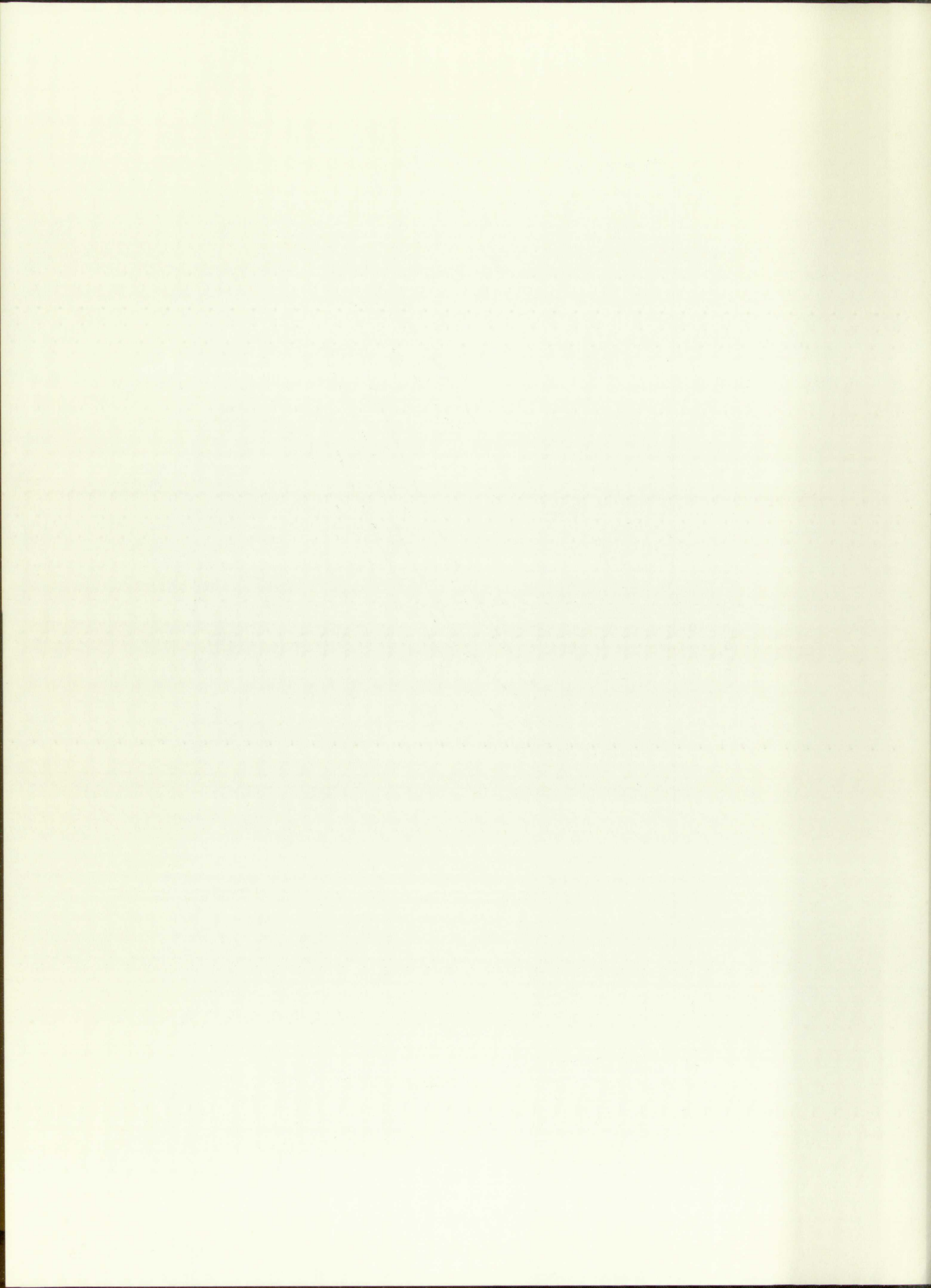


Figure 14. Typical Grid Currents on the Path of Operation



While the current emission factor<sup>7</sup> is a function of the supply and bias voltages, this relationship is not shown in Equation (17); it can be obtained if desired. The chief interest will be in the variations of K from tube to tube, rather than its magnitude.

The representation of the tube characteristics in an intrinsic blocking oscillator circuit by Equations (16) and (17) involves only two easily measurable parameters. While different tube types may require a change in the slopes of the approximating curves, the approximating equations will still involve these two parameters. The relative effects of these parameters will be dependent upon the tube type, however, because of the new equations.

### Calculation of Pulse Shapes

Any desired voltage or current for the intrinsic blocking oscillator circuits of Figures 1 and 11 can now be calculated for the main part of the pulse. Calculations will be restricted here to those necessary for obtaining the output pulse and magnetizing current, since these are usually of primary interest.

Substituting Equations (16) and (17) into Equation (3) gives

$$i_m = nKe_g \left( e_p - \frac{e_g}{nB} \right) \quad (18)$$

The magnetizing current as a function of the output pulse can be obtained by expressing the plate and grid voltages in terms of the output pulse voltage with Equations (1) and (2), resulting in

---

<sup>7</sup>It should be noted that K is not a dimensionless constant. It has units of amperes per squared volt, and its magnitude depends upon the particular point of measurement.

The current-voltage factor is a function of the voltage and the voltage, the relationship is not shown in Equation (17) it can be obtained it is noted that the current will be in the direction of  $K$  from the tube, rather than the opposite.

The representation of the tube characteristics as an intrinsic property and relation to the characteristics of the tube is shown in Figure 1. The characteristic parameters, which are not shown, are the logarithmic gain, in the sense of the logarithmic curve, the logarithmic gain, will still involve these two parameters. The relative effects of these parameters will be dependent upon the tube type, however, because of the new definition.

### Calculation of Tube Factors

Ay desired value or current for the intrinsic blocking coefficient of Figure 1 and (1) can now be calculated for the main part of the tube. Calculations will be performed here in those necessary for obtaining the output for the logarithmic current, since these are the only of primary interest.

Substituting Equations (16) and (17) into Equation (8) gives

$$I = \frac{K}{2} \left( \frac{V}{V_0} \right)^2 \quad (18)$$

The logarithmic current as a function of the output bias can be obtained by expressing the bias and grid voltages in terms of the output bias voltage with Equations (1) and (2), resulting in

It should be noted that  $K$  is not a dimensionless constant, it has units of amperes per square volt, and its magnitude depends upon the particular kind of vacuum tube.



$$I_m = nK \left[ \left( \frac{E_{bb}}{n} + \frac{2+nB(n-1)}{n^2 B} E_k \right) e_o - \frac{n^2 B + 1}{n^3 B} e_o^2 + \frac{nB-1}{nB} E_k^2 - E_k E_{bb} \right] \quad (19)$$

To simplify the form of the following equations it is convenient to express Equation (19) in the form

$$i_m = nK \left[ G e_o - H e_o^2 - J \right] \quad (19)$$

where  $G = \frac{E_{bb}}{n} + \frac{2+nB(n-1)}{n^2 B} E_k$

$$H = \frac{n^2 B + 1}{n^3 B}$$

$$J = E_k E_{bb} - \frac{nB-1}{nB} E_k^2$$

and G, H, and J involve only  $E_{bb}$ ,  $E_k$ , n, and B.

The derivative of Equation (19) with respect to the output pulse voltage is

$$\frac{di_m}{de_o} = nK (G - 2H e_o)$$

Thus, from Equation (15), the time as a function of pulse amplitude is

$$t = nKL_p \left[ 2H (E_i - e_o) - G \ln \frac{E_i}{e_o} \right] \quad (20)$$

While the pulse amplitude as a function of time can be obtained by a graphical solution of Equation (15), an approximate analytical solution is given directly by Equation (20).

(1111)

Often, sufficient information is gained by determining only the pulse amplitude and pulse width, instead of the whole pulse shape. The pulse amplitude at the start of the main part of the pulse can be calculated from the fact that the magnetizing current is approximately zero; thus, by Equation (18)

$$GE_i - HE_i^2 - J = 0$$

where  $E_i$  is the initial pulse voltage at the start of the main part of the pulse. A solution of this quadratic equation gives

$$E_i = \frac{G}{2H} + \left[ \left( \frac{G}{2H} \right)^2 - \frac{J}{H} \right]^{1/2} \quad (21)$$

Since the pulse is terminated when the derivative of magnetizing current is zero, the pulse voltage at termination is found to be

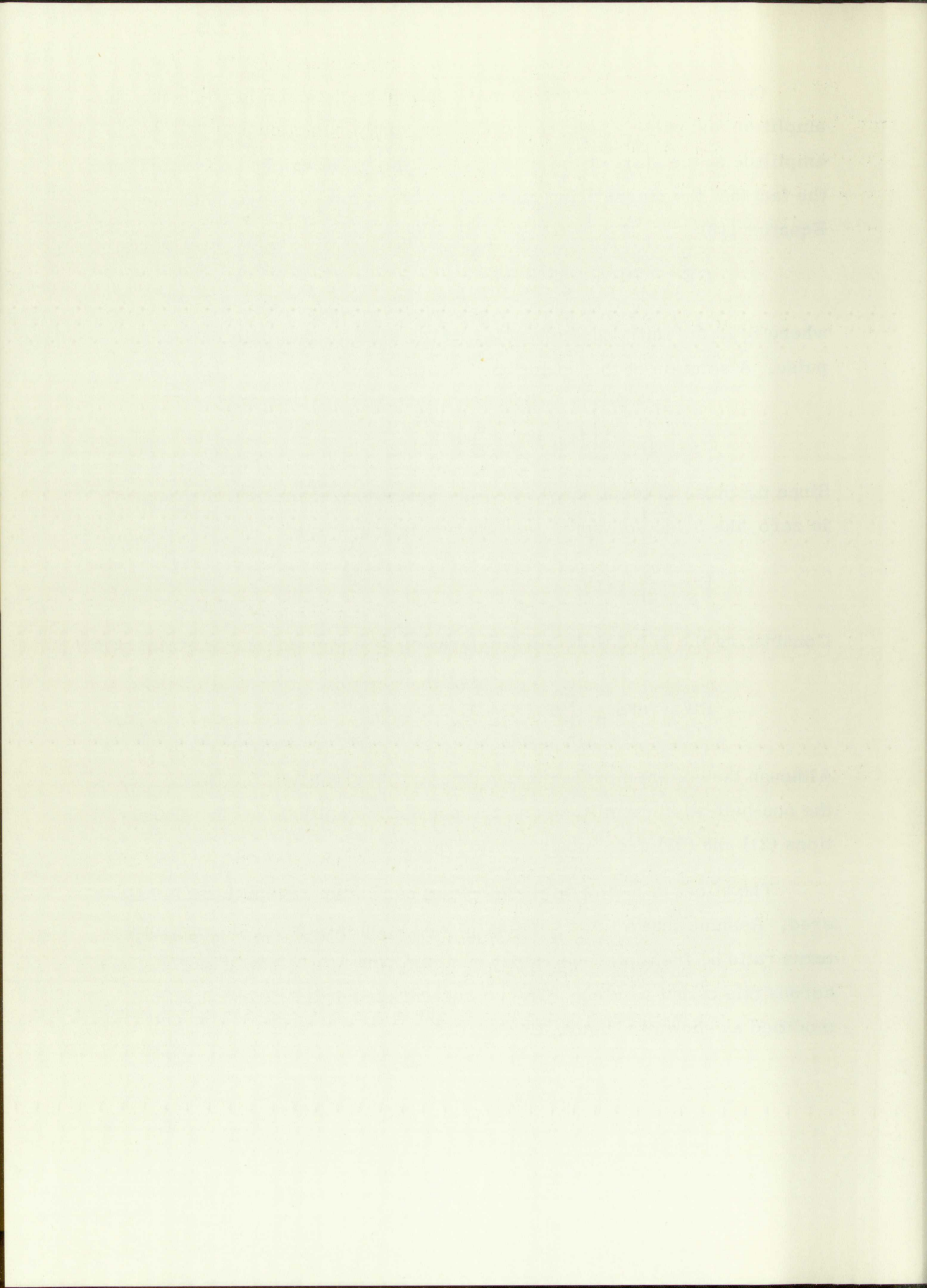
$$E_x = \frac{G}{2H} \quad (22)$$

Considering the pulse width as the duration of the quasi-stable state, then

$$PW = nKL_p \left[ 2H (E_i - E_x) - G\eta \frac{E_i}{E_x} \right] \quad (23)$$

Although the common pulse measurements for amplitude and width are the one-half-width amplitude and the one-half-amplitude width, Equations (21) and (23) are closely related quantities.

The effect of a load on the blocking oscillator has not been considered. Assume that a third winding is wound on the transformer with a turns ratio  $b$ , from plate to output winding, and a load resistance  $R_L$  across this output winding. The equivalent circuit in Figure 2 is then modified as shown in Figure 15.



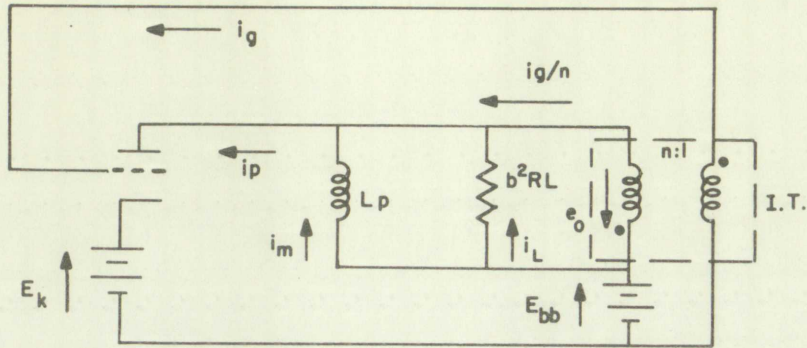


Figure 15. Equivalent Circuit for the Loaded Intrinsic Blocking Oscillator

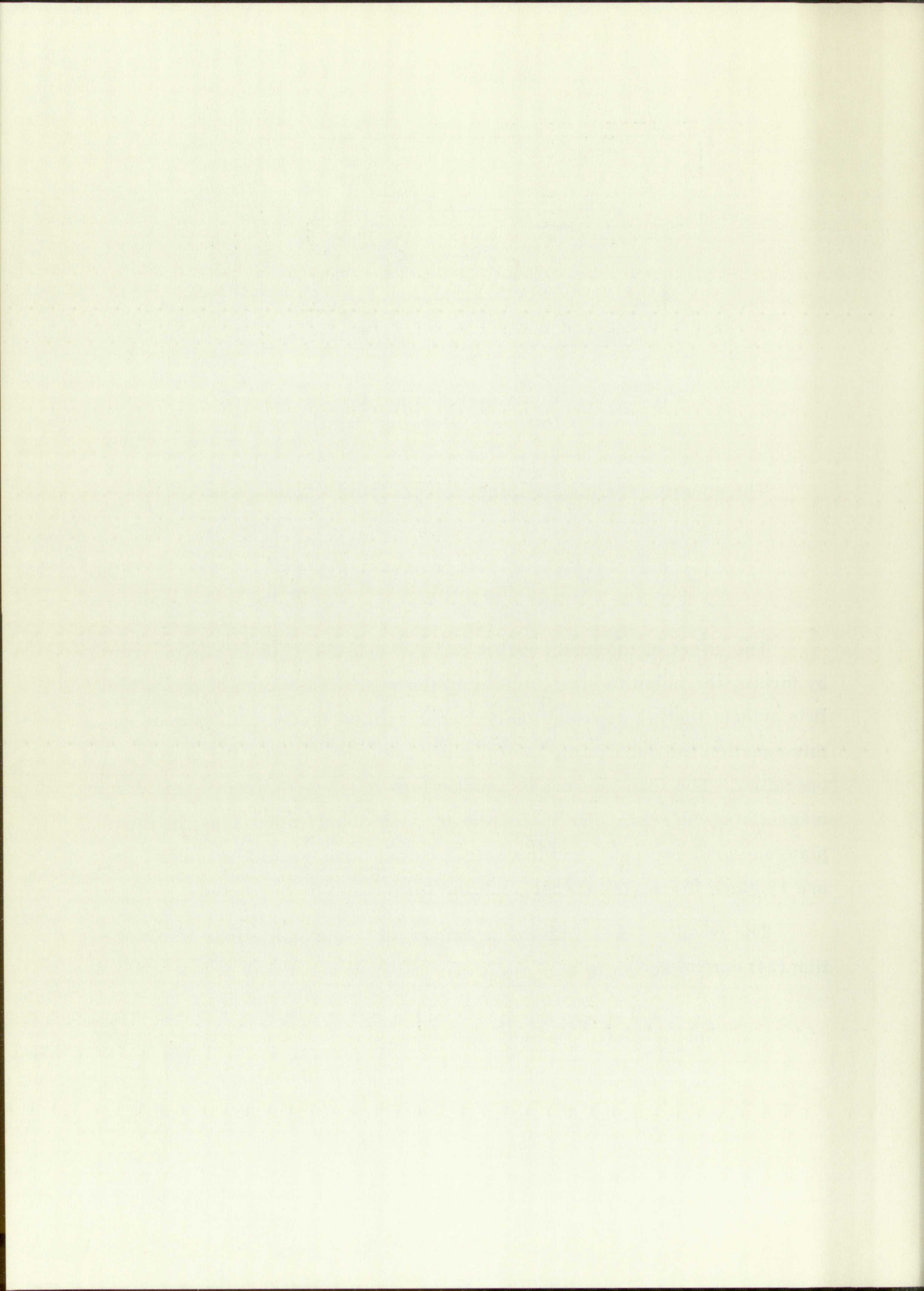
The equation for magnetizing current from Figure 15 is

$$i_m = i_p - i_g/n - i_L = i_g \left( \frac{i_p}{i_g} - \frac{1}{n} \right) - \frac{e_o}{b^2 R_L} \quad (24)$$

The effect of the load current is to reduce the magnetizing current by forcing the pulse to start farther to the right on the path of operation. It is evident that a graphical analysis can still be made simply by using this equation for calculating the magnetizing current from the path of operation. The load current is usually less than one-fourth the maximum magnetizing current. The load current is obviously much less than the plate and grid currents; and the actual output turns ratio is used in Figure 15 since the series output coupling losses can be neglected.

The result of inserting the previous tube approximations into Equation (24) can be shown to be

$$i_m = nK \left[ G'e_o - H e_o^2 - J \right] \quad (25)$$



where

$$G' = G - \frac{1}{nb^2 KR_L} \quad (26)$$

Thus, Equation (19) is the same as Equation (25) if  $G'$  is substituted for  $G$ . It follows, then, that the effects of the load can be included in Equations (19) through (23) simply by substituting  $G'$  for  $G$ .

It is evident from Equation (26) that if the load is to have little effect, then

$$\frac{1}{R_L} \ll nb^2 KG \quad (27)$$

### Results

A plot of Equation (20) for several values of  $B$  is shown in Figure 16. While a comparison of these curves with Figure 10 reveals good agreement with pulse amplitude, there is a considerable discrepancy with pulse width. Although Figure 10 was obtained with only four particular tubes, which could be "oddballs," a study of many tubes reveals that Figure 10 gives typical results. Thus, pulse width is expected to be a maximum with tubes having a current division factor in the vicinity of 1.5 instead of continuing to increase with an increase in  $B$  as indicated by Figure 16. It has been determined that this error is due mainly to the approximation for the current ratio by Equation (16), and much better agreement can be obtained with an effective current division factor as given by

$$B_{\text{eff}} = 0.2 + 0.8B \text{ for } B \geq 1$$

No new significant information is gained by a better approximation, however, since the primary objective is to determine the important tube parameters and this new approximation is still a function of  $B$ .

The first part of the report deals with the general situation of the country and the progress of the work during the year. It is followed by a detailed account of the various projects and the results achieved. The report concludes with a summary of the work done and the plans for the future.

The second part of the report deals with the financial statement of the organization. It shows the income and expenditure for the year and the balance sheet at the end of the year. It also shows the details of the various items of income and expenditure.

The third part of the report deals with the administrative and general matters. It includes a list of the members of the organization and the names of the various committees and sub-committees. It also includes a list of the various reports and documents submitted during the year.

The fourth part of the report deals with the various projects and the results achieved. It includes a list of the various projects and the names of the persons who were responsible for them. It also includes a list of the various results achieved and the progress made during the year.



$E_{bb} = 150V$   
 $E_k = 18V$   
 $n = 1.2$   
 $L_p = 2 \text{ mh}$   
 $K = 1.3 \times 10^{-4}$

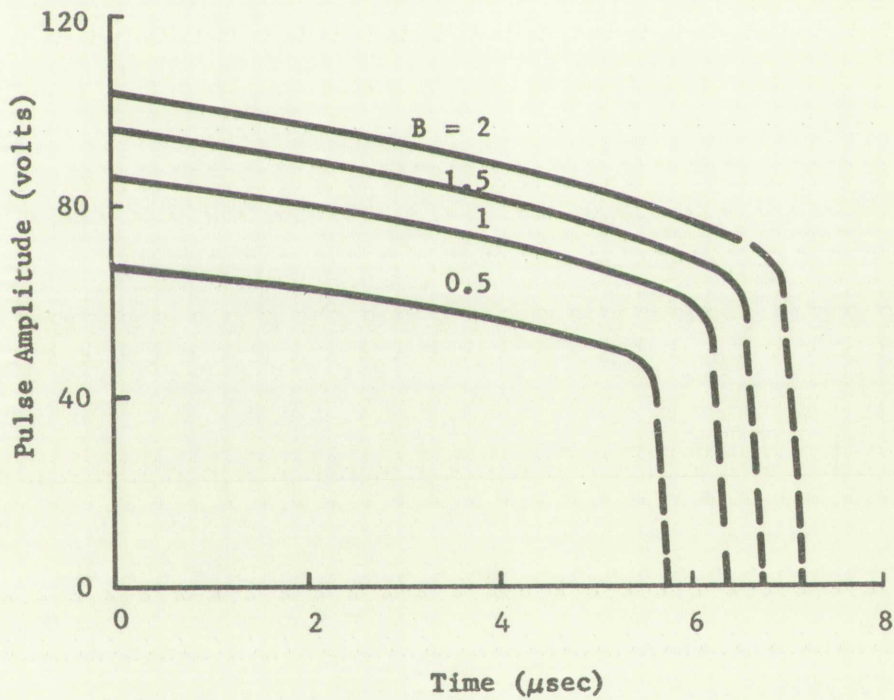


Figure 16. Output Pulse Calculated from the Nonlinear Mathematical Analysis

*[Faint, illegible handwritten text, possibly bleed-through from the reverse side of the page.]*

By Equations (21) and (22), pulse amplitude is independent of  $K$ , and the only transformer parameter having any effect is  $n$ . Addition of a load resistor will make the pulse amplitude dependent upon  $K$ , because of the presence of the parameter  $K$  in the equation for  $G'$ . The manner in which the load affects the pulse shape will be determined by the particular values of both  $K$  and  $B$  as well as the values of  $E_{bb}$ ,  $E_k$ , and  $n$ .

### Saturating Transformers

No consideration has yet been given in this chapter to a transformer which saturates hard enough to invalidate the linear transformer approximations which have been used. Assume that the primary inductance of a saturating transformer can be approximated by

$$L_p = L_o \text{ for } i_m \leq I'_m \quad (28A)$$

$$L_p = \frac{C}{i_m^j} \text{ for } i_m \geq I'_m \quad (28B)$$

Where  $L_o$  and  $C$  are constants and  $I'_m$  is the value of the magnetizing current at which saturation begins;  $I'_m$  is directly related to the flux density at which saturation starts, by Equation (10) or (11). For silicon iron a value of unity for the exponent has been found to be a good approximation in many cases. For a square-loop core material the value of  $j$  will be much larger. Using this approximation, it is clear that the previous analytical solution is valid until the magnetizing current reaches the value  $I'_m$ . For higher current values the equation for pulse shape can be obtained by combining Equations (19), (20), and (28B). Thus

$$t = nKL_o \int_{E_i}^{e_o} \left( \frac{G}{e_o} - 2H \right) de_o \text{ for } i_m \leq I'_m \quad (29A)$$

The first part of the paper is devoted to the study of the asymptotic behavior of the solutions of the system (1) as  $t \rightarrow \infty$ . It is shown that the solutions of the system (1) are bounded and tend to zero as  $t \rightarrow \infty$ . The second part of the paper is devoted to the study of the asymptotic behavior of the solutions of the system (1) as  $t \rightarrow \infty$ . It is shown that the solutions of the system (1) are bounded and tend to zero as  $t \rightarrow \infty$ .

The third part of the paper is devoted to the study of the asymptotic behavior of the solutions of the system (1) as  $t \rightarrow \infty$ . It is shown that the solutions of the system (1) are bounded and tend to zero as  $t \rightarrow \infty$ . The fourth part of the paper is devoted to the study of the asymptotic behavior of the solutions of the system (1) as  $t \rightarrow \infty$ . It is shown that the solutions of the system (1) are bounded and tend to zero as  $t \rightarrow \infty$ .

The fifth part of the paper is devoted to the study of the asymptotic behavior of the solutions of the system (1) as  $t \rightarrow \infty$ . It is shown that the solutions of the system (1) are bounded and tend to zero as  $t \rightarrow \infty$ . The sixth part of the paper is devoted to the study of the asymptotic behavior of the solutions of the system (1) as  $t \rightarrow \infty$ . It is shown that the solutions of the system (1) are bounded and tend to zero as  $t \rightarrow \infty$ .

The seventh part of the paper is devoted to the study of the asymptotic behavior of the solutions of the system (1) as  $t \rightarrow \infty$ . It is shown that the solutions of the system (1) are bounded and tend to zero as  $t \rightarrow \infty$ . The eighth part of the paper is devoted to the study of the asymptotic behavior of the solutions of the system (1) as  $t \rightarrow \infty$ . It is shown that the solutions of the system (1) are bounded and tend to zero as  $t \rightarrow \infty$ .

$$t = \int_{E'}^{e_o} \frac{C(G-2He_o)}{e_o (Ge_o - He_o^2 - J)^j} de_o \text{ for } i_m \geq I'_m \quad (29B)$$

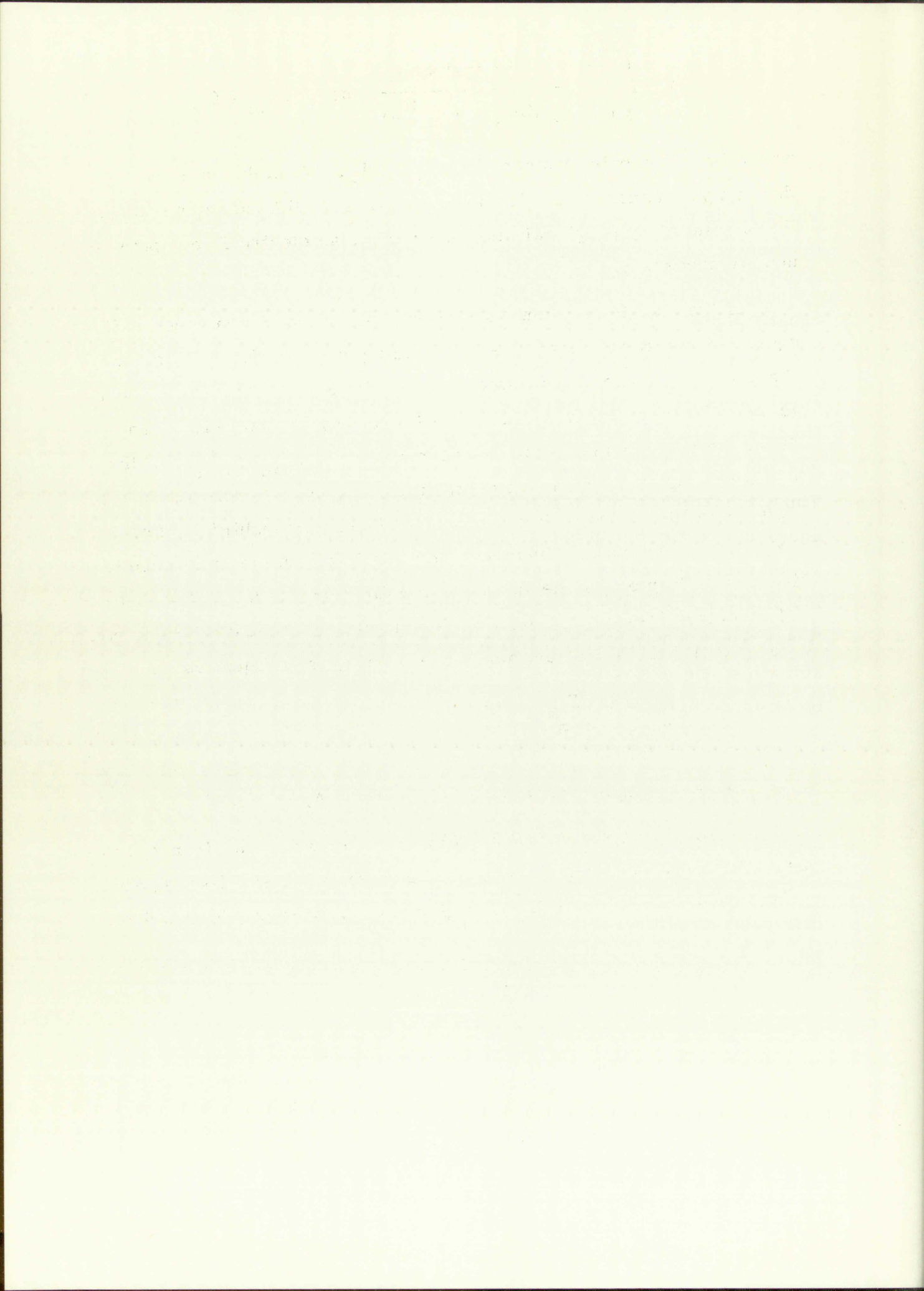
where  $E'$  is the pulse voltage when  $i_m = I'_m$ . When the value of  $j$  is other than unity, an analytical solution of Equation (29B) becomes so complex that a solution by graphical integration or on an electronic computer is usually necessary.

If the transformer undergoes hard saturation, as can occur with a square-loop core material, the magnetizing current will increase very sharply at saturation. The time required for the magnetizing current to go from this value to the maximum allowable by the tube will be small. Thus, the pulse can be assumed to terminate when  $i_m = I'_m$ , and the additional portion of the pulse contributed by Equation (29B) can be neglected with little error. Because of the higher permeability of this core material, the primary inductance can be higher than the inductance of a linear transformer for the same pulse width. The higher inductance results in much less voltage variation during the pulse, and the pulse can be assumed to have constant amplitude. Thus, from Equation (8)

$$PW = \frac{NA (B_m - B_i)}{E_i} \quad (30)$$

a considerable simplification over Equations (29A) and (29B).

It is evident from Equation (30) that hard saturation will not eliminate pulse amplitude and width variations in the intrinsic blocking oscillator, since the pulse amplitude as given by Equation (21) is a variable.



## Statistical Verification

The graphical and mathematical procedures give considerable insight into the operation of the circuit. A determination of the over-all effects of the tube parameters by only these methods would require a large amount of computation, and the accuracy of the results would be difficult to ascertain. A statistical study has the advantage of showing the effects on pulse shape without the necessity of making any approximations for the tube or transformer characteristics. It is very useful, therefore, for checking a preliminary design and for indicating that circuit modifications may be necessary to meet design requirements.

The distributions of rise time, pulse amplitude, and pulse width can be obtained simply by substituting a statistical distribution of tubes into an actual circuit. Because of tube variations from production lots as well as from tube to tube, the statistical distribution should include several lots unless the actual tubes which will be used in the circuits are available. While the thousands of tubes from which to select a true statistical distribution are not always available, a satisfactory sample can usually be selected from a much smaller quantity. Thus, a study of the effects of the tube parameters, which have been isolated in the section on mathematical analysis, can be extended with statistical methods; the results should not only be more accurate and representative, but also easier to obtain.

### Typical Results

To illustrate the usefulness of statistical methods, some typical results will be shown. A 50-tube sample, which includes four lots, was used to obtain the data. The tubes were Type SA-310, a high current version of the commercial Type 6111.

The British Patent... The object of the present invention is to provide a method of... The invention consists in the following... The object of the present invention is to provide a method of... The invention consists in the following...

The object of the present invention is to provide a method of... The invention consists in the following... The object of the present invention is to provide a method of... The invention consists in the following...

The object of the present invention is to provide a method of... The invention consists in the following...

The object of the present invention is to provide a method of... The invention consists in the following...

The object of the present invention is to provide a method of... The invention consists in the following...



Pulse amplitude, pulse width, and cathode current were measured in the circuit of Figure 11 with this tube sample and three different transformers. The distributions of these quantities were found to be approximately Gaussian. The results are given in Table I in terms of the means and the sample standard deviations,

where 
$$\bar{X} = \frac{\sum X_i}{N}$$

$$S^2 = \frac{N \sum X_i^2 - (\sum X_i)^2}{N(N-1)}$$

and N is the sample size.

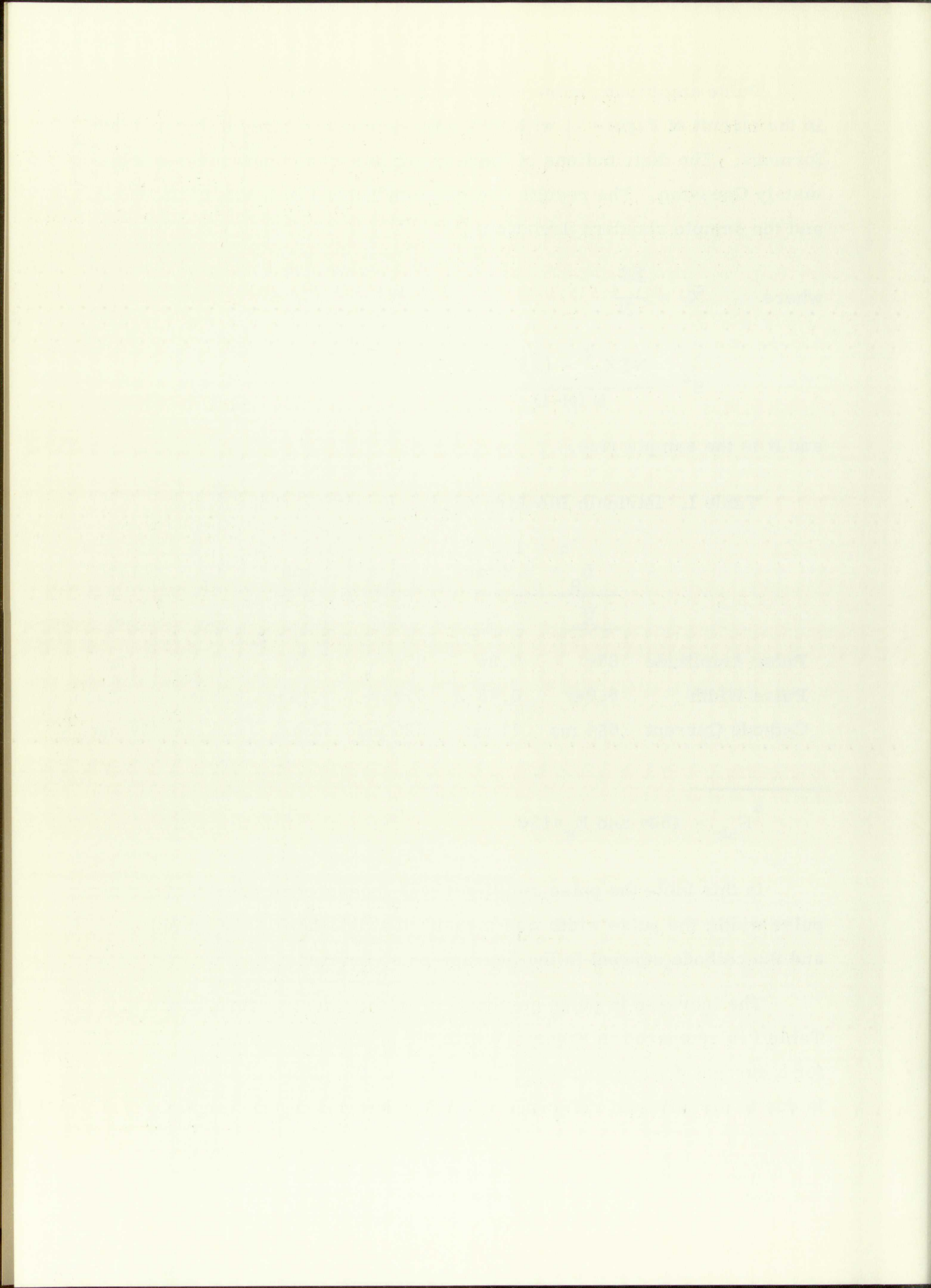
Table I. Intrinsic Blocking Oscillator with 50-Tube Sample\*

	n = 1.2 $L_p = 2.2$ mh		n = 1.5 $L_p = 2.7$ mh		n = 2.0 $L_p = 3.2$ mh	
	$\bar{X}$	S	$\bar{X}$	S	$\bar{X}$	S
Pulse Amplitude	86v	6.8v	95v	5.8v	103v	4.7v
Pulse Width	6.0 $\pi$ s	0.43 $\pi$ s	6.95 $\pi$ s	0.44 $\pi$ s	6.35 $\pi$ s	0.50 $\pi$ s
Cathode Current	684 ma	71 ma	620 ma	58 ma	459 ma	39 ma

\*  $E_{bb} = 150$ v and  $E_k = 18$ v

In this table the pulse amplitude was measured at one-third of the pulse width; the pulse width was measured at one-half of the amplitude; and the cathode current is the average pulse current.

The increase in pulse amplitude with the effective turns ratio in Table I is compared in Figure 17 with the mean of Equations (21) and (22) for a current division factor of 1.5. Part of the difference in these curves is due to the different reference width for determining the amplitude.



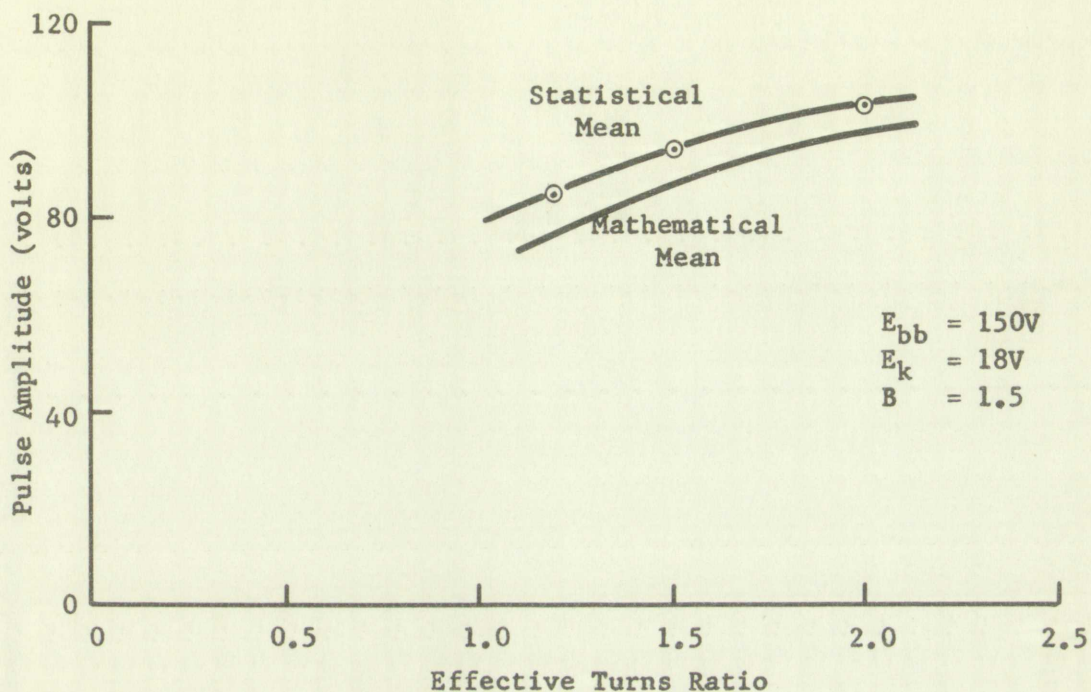


Figure 17. Influence of Turns Ratio on Pulse Amplitude

The variation of pulse width with the effective turns ratio as determined from Table I is compared with that calculated by Equation (23) in Figure 18. The values of primary inductance given in Table I were obtained by the method illustrated by Figure 12. Since pulse width is influenced by these inductance values, the statistical curve is also an approximation.

Since the statistical curves are based on a relatively large number of tubes and few approximations, these results should be considered more accurate than the mathematical results. The good agreement between the pairs of curves in Figure 17 and 18 indicates that the analytical equations are also representative.<sup>8</sup>

The tube approximations made in the section on mathematical analysis indicated the importance of two tube parameters — a current division factor  $B$  and a current emission factor  $K$ . Pulse measurements of these

<sup>8</sup>If a piecewise linear analysis had been employed, the calculated pulse widths could have easily differed from the experimental values by a factor of two.

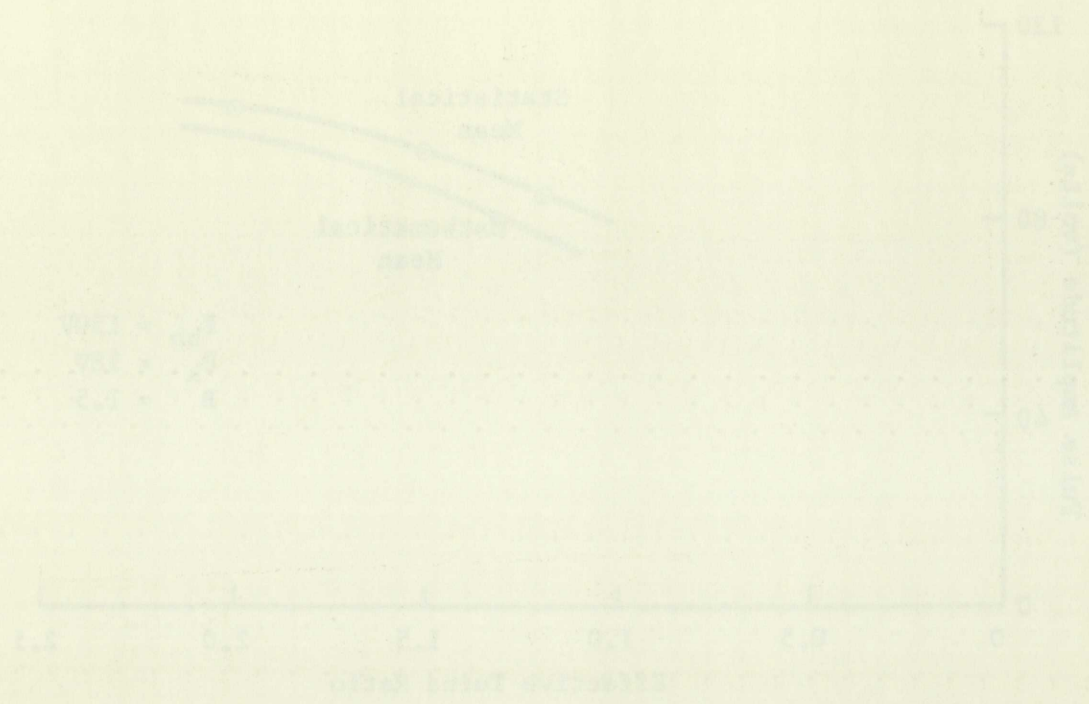


Figure 11. Influence of Pulse Ratio on Pulse Amplitude

The variation of pulse width with the effective pulse ratio is shown in Figure 12. The comparison with the calculated by Equation (12) for Figure 12. The values of primary resistance given in Table 1 were obtained by the method illustrated by Figure 12. Since pulse width is influenced by these resistance values, the statistical curve is also an approximation.

Since the statistical curves are based on a relatively large number of tubes and low approximations, these results should be considered more accurate than the mathematical results. The good agreement between the pulse of curves in Figure 11 and 12 indicates that the statistical equations are also representative.

The same approximations made in the section on mathematical analysis indicated the importance of two time parameters - a current division factor through current induction time,  $K$ . Pulse measurements of these

It is considered that analysis has been completed, the calculated pulse widths could have easily differed from the experimental values by a factor of two.

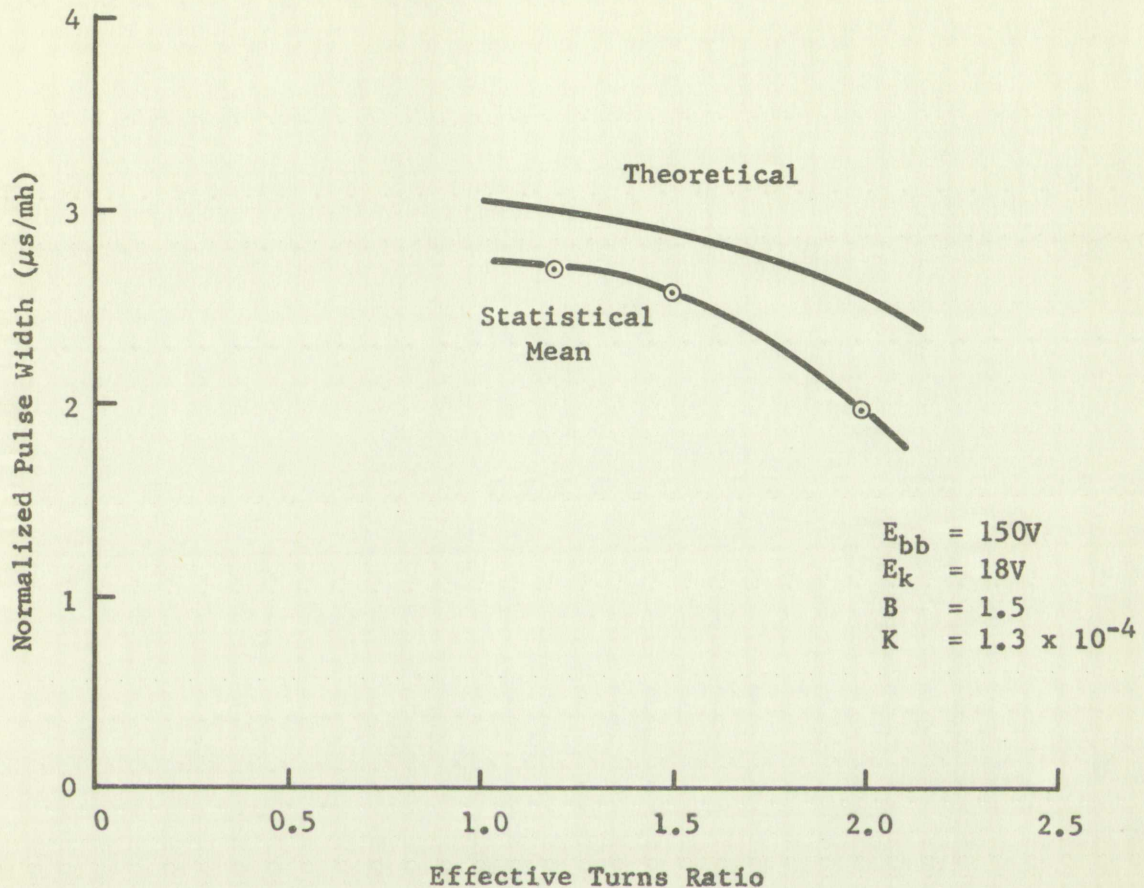


Figure 18. Influence of Turns Ratio on Pulse Width

parameters were made on the sample of 50 tubes. Histograms of these parameters are shown in Figures 19 and 20. The method of making the measurements is covered briefly in Appendix B.

The influence of the current division factor on pulse amplitude is shown in Figure 21. The relatively good correlation agrees with the mathematical predictions.

While the pulse width as given by Equation (23) is a function of both  $K$  and  $B$ , it is proportional to  $K$  and is a complex function of  $B$ . The effect of  $B$  on pulse width can, therefore, be determined from the scatter plot of  $\frac{PW}{K}$  vs  $B$  as shown in Figure 22. The limiting of the pulse width as  $B$  increases does not agree with the results obtained previously with Equation (23). However, the relatively good correlation evident in Figure 22 further indicates that the current division factor is a primary



The following table shows the data points estimated from the graph above:

Time (x)	Distance (y)
0	0
1	2.5
2	4.5
3	5.5
4	6.0
5	6.5
6	6.8
7	7.0
8	7.1
9	7.2
10	7.2

The graph illustrates the relationship between time and distance, showing a non-linear increase in distance over time, characteristic of constant acceleration.

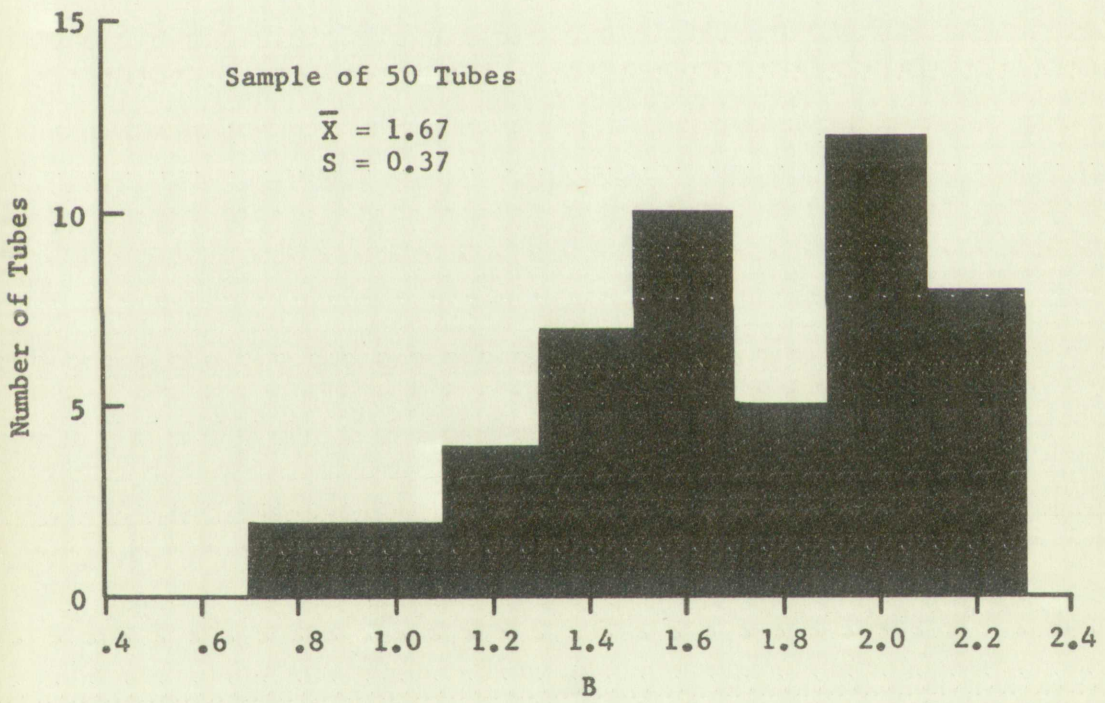
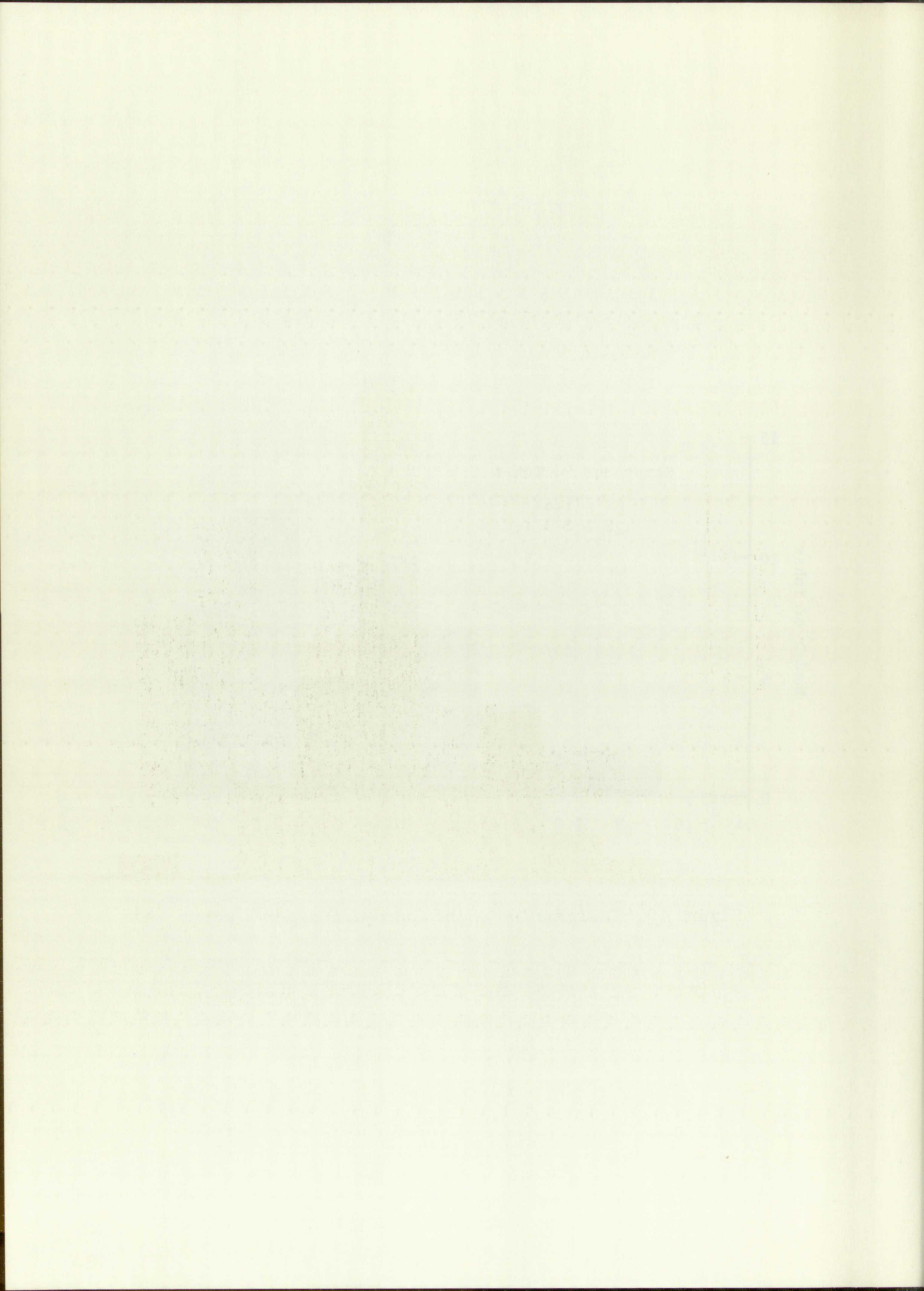


Figure 19. Distribution of the Current Division Factor





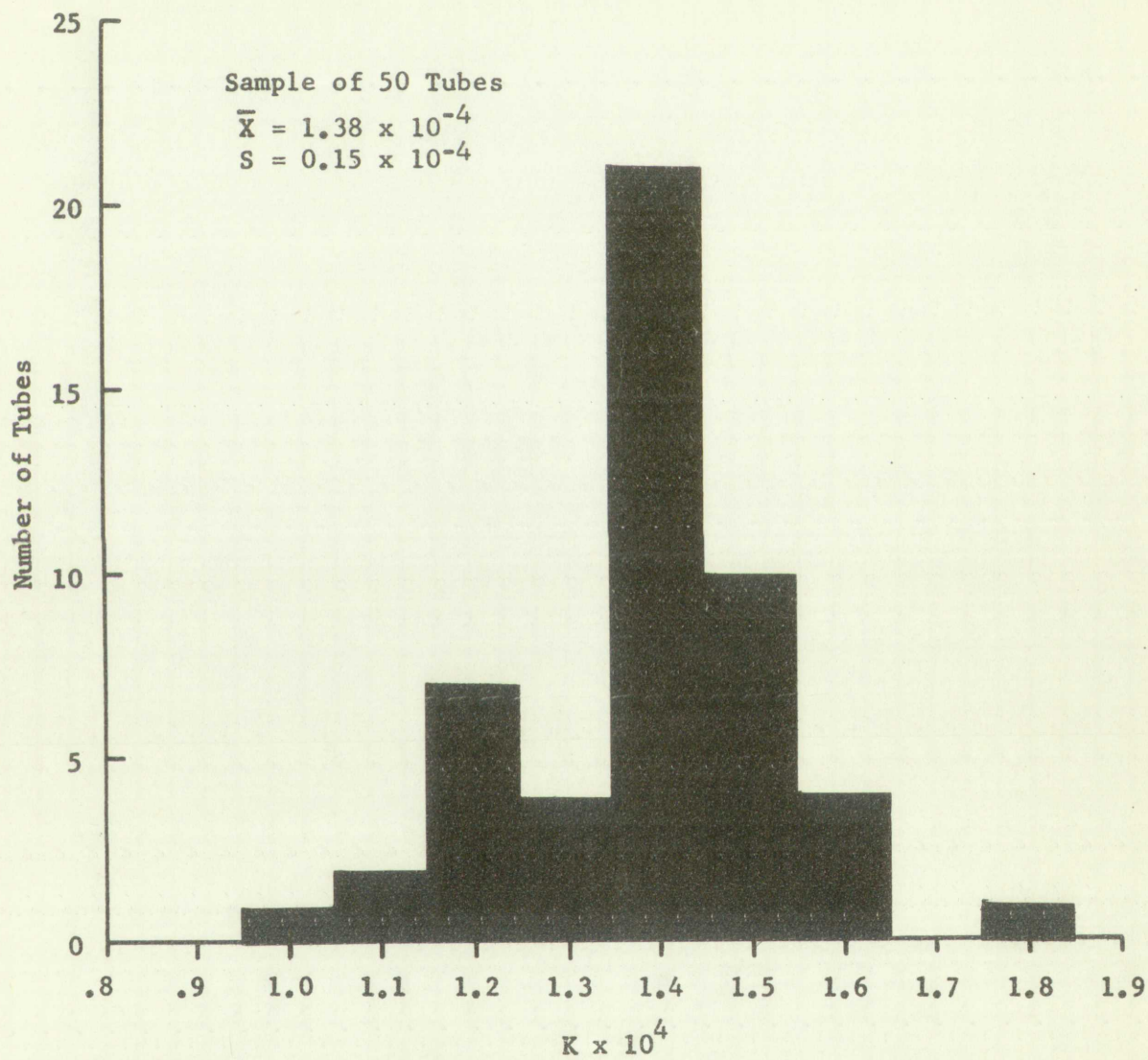


Figure 20. Distribution of the Current Emission Factor



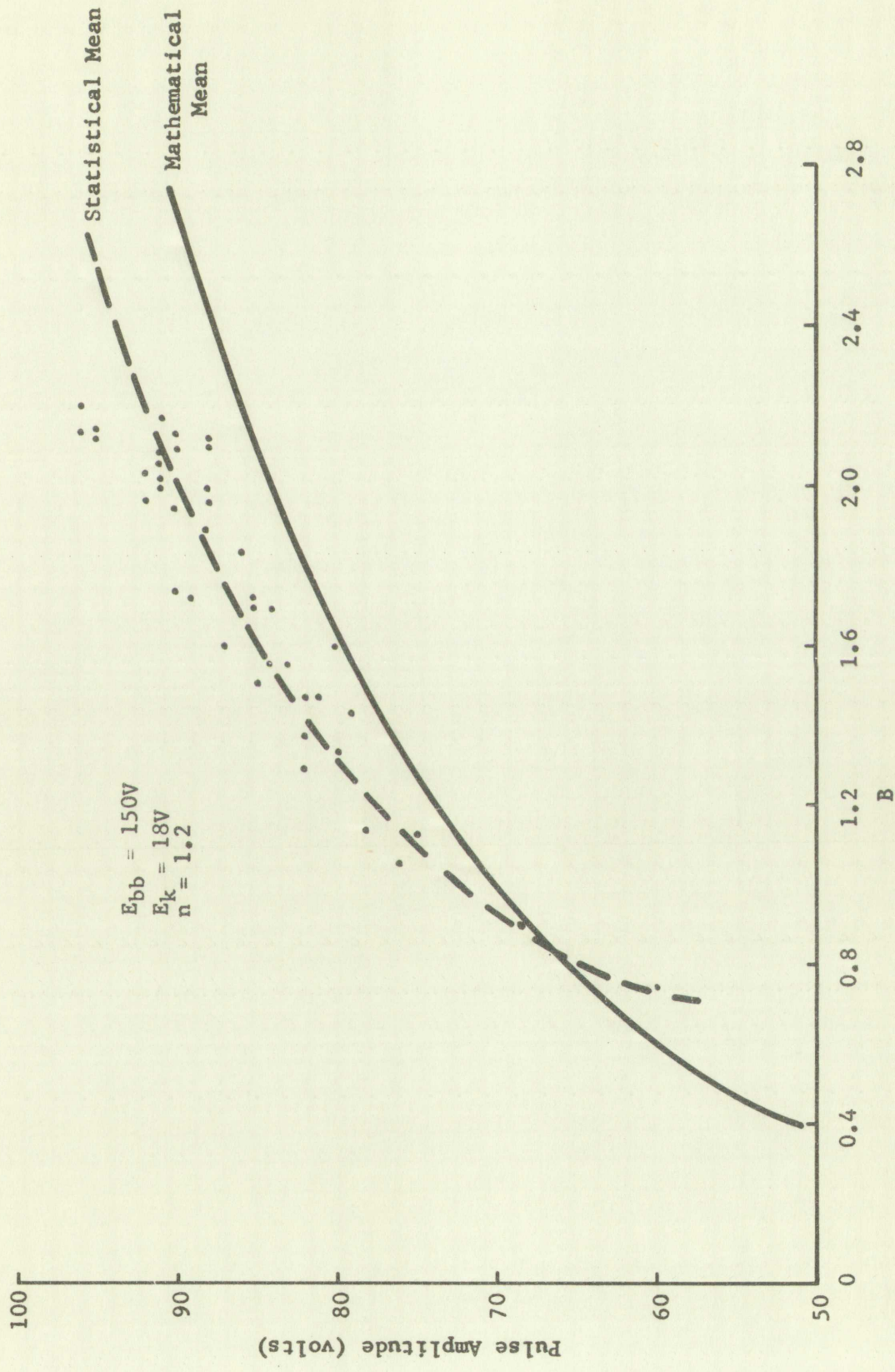
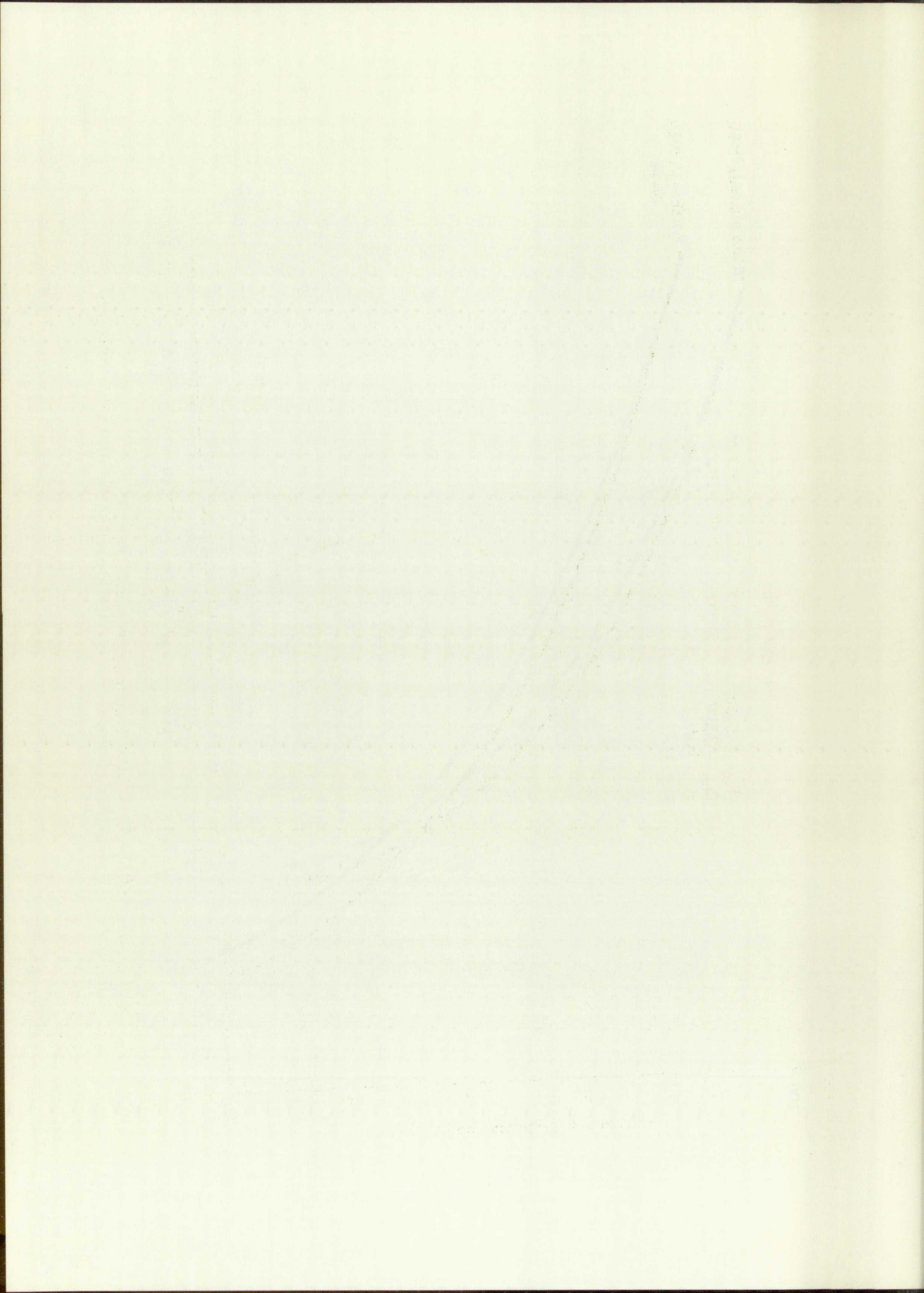


Figure 21. The Effect of the Current Division Factor on Pulse Amplitude



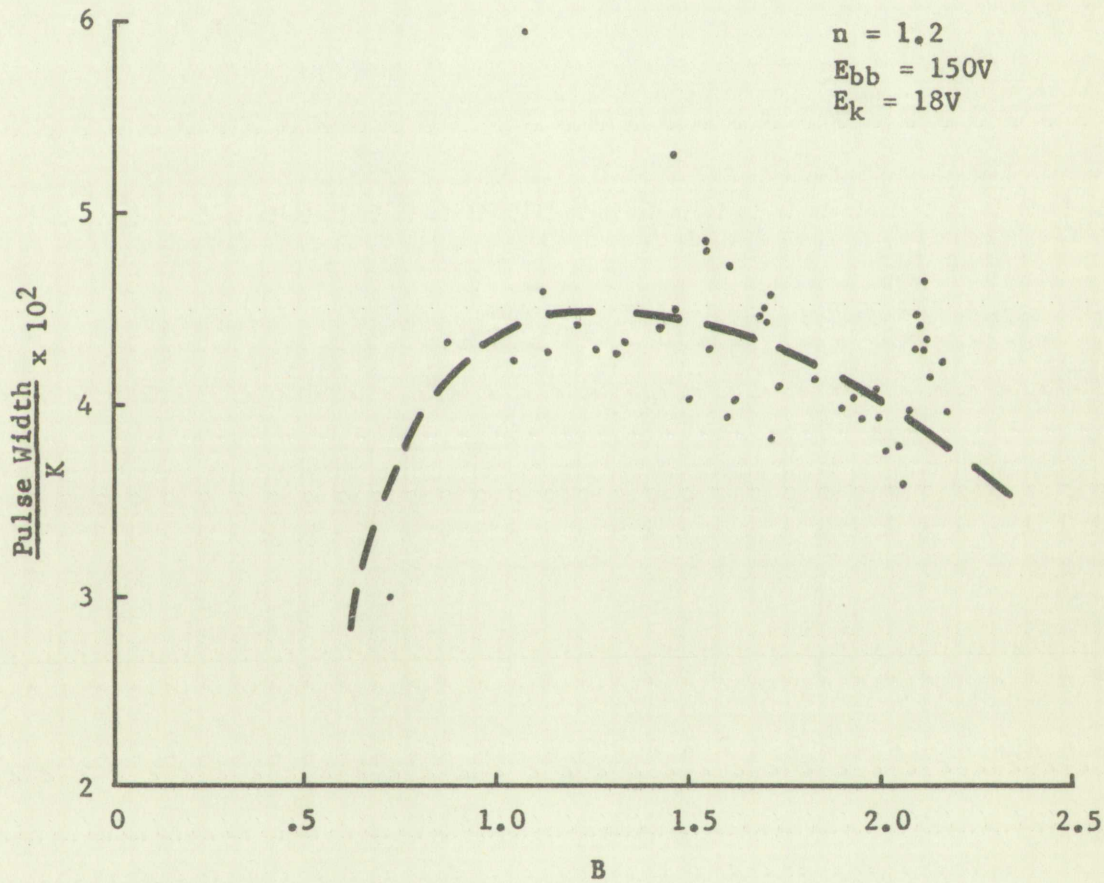
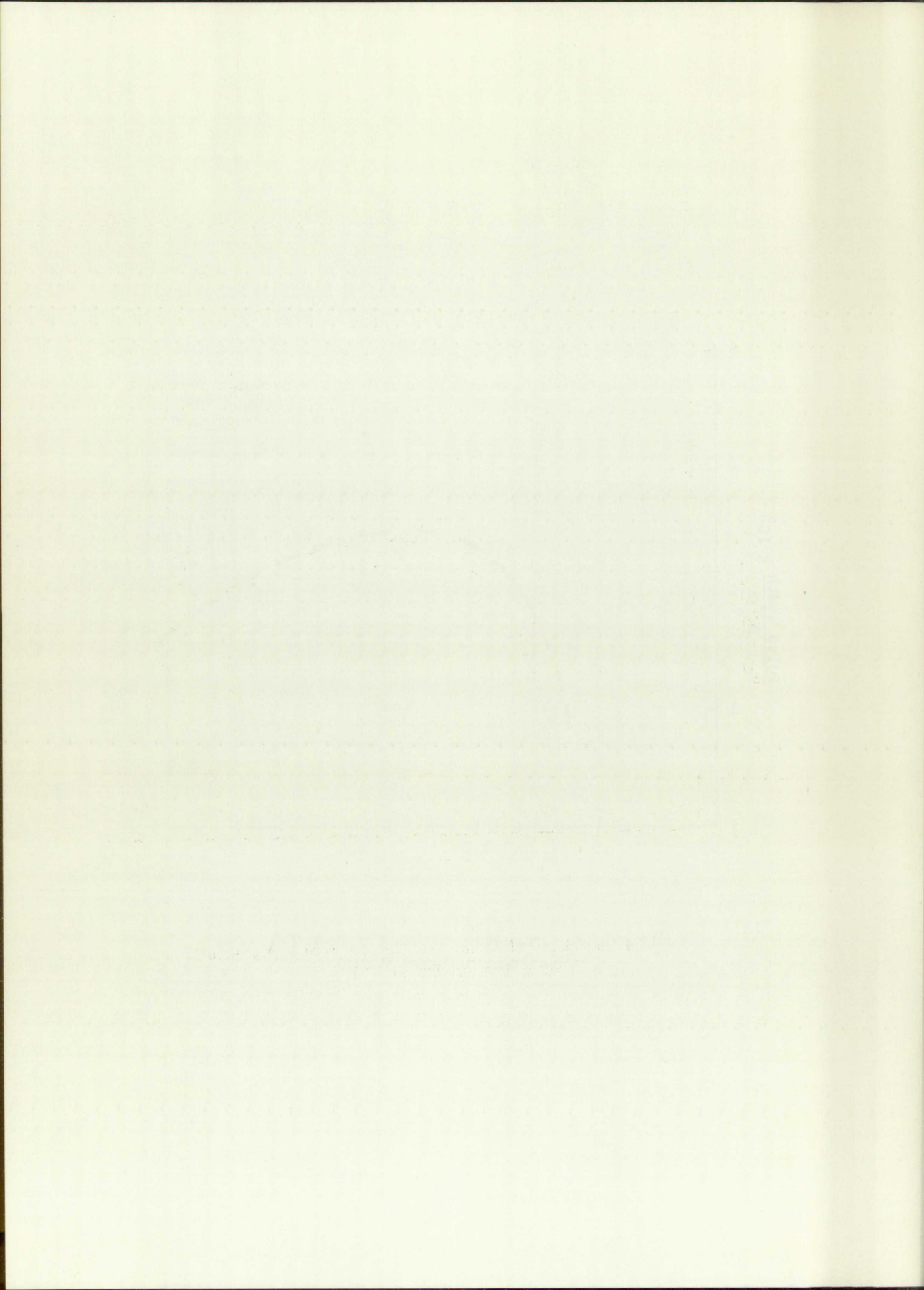


Figure 22. Influence of the Current Division Factor on Pulse Width



tube parameter; this fact is more important than the accuracy of the analytical equations. The scatter plot of pulse width versus K in Figure 23 also agrees with the prediction of Equation (23).

The importance of statistical data is made evident by the histograms for B and K. Because of the distribution of tube parameters, this type of data is needed even in a mathematical analysis to determine the values and weight to be allotted to these parameters. To meet the design requirements, the effects of the distributions will determine the particular circuit that is suitable, since the circuit must be designed to function properly with these distributions unless a selection process is to be employed.

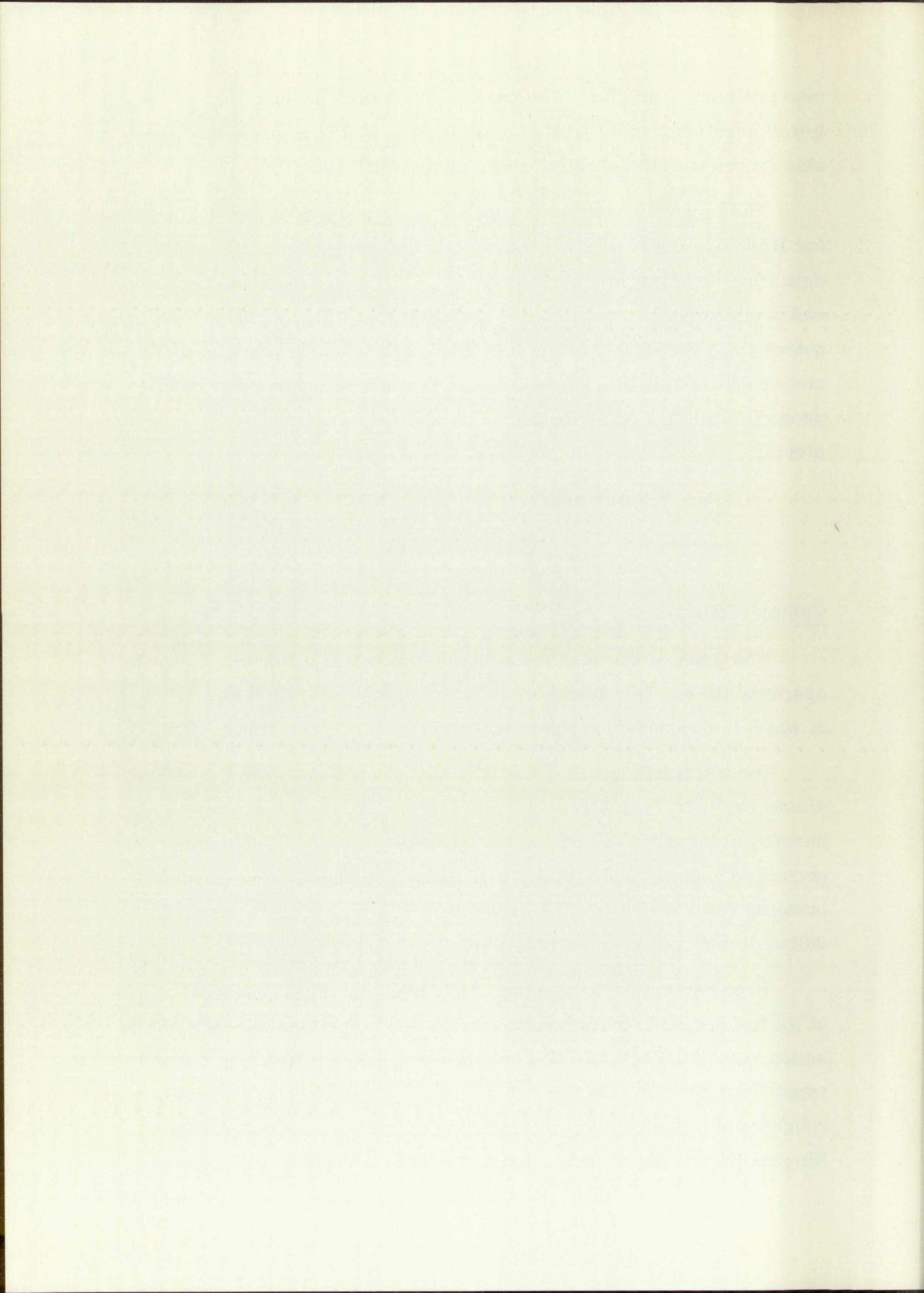
## Operating Life

### Cathode Emission

The pulse shape of a blocking oscillator will gradually change with operating time. This is due to a change in tube characteristics, most of which is due to variations in the properties of the cathode.

Oxide-coated cathodes are of primary interest since they are used almost exclusively in blocking oscillators. The oxide coatings consist of barium, strontium, and perhaps a small percentage of other oxides deposited on a base metal such as nickel. The oxides are formed by breaking down the respective carbonates at a high temperature. The resultant is a mixed grain of  $(Ba, Sr)O$ .

Free barium is formed primarily by a chemical reduction of part of the barium oxide by impurities in the base metal and by electrolytic action associated with the flow of current through the coating. The barium vapor flows through the pores of and is absorbed by the  $(Ba, Sr)O$  grains, resulting in oxygen ion vacancies being formed. It is believed by Nergaard [6] that the absorbed barium acts as a donor and results in





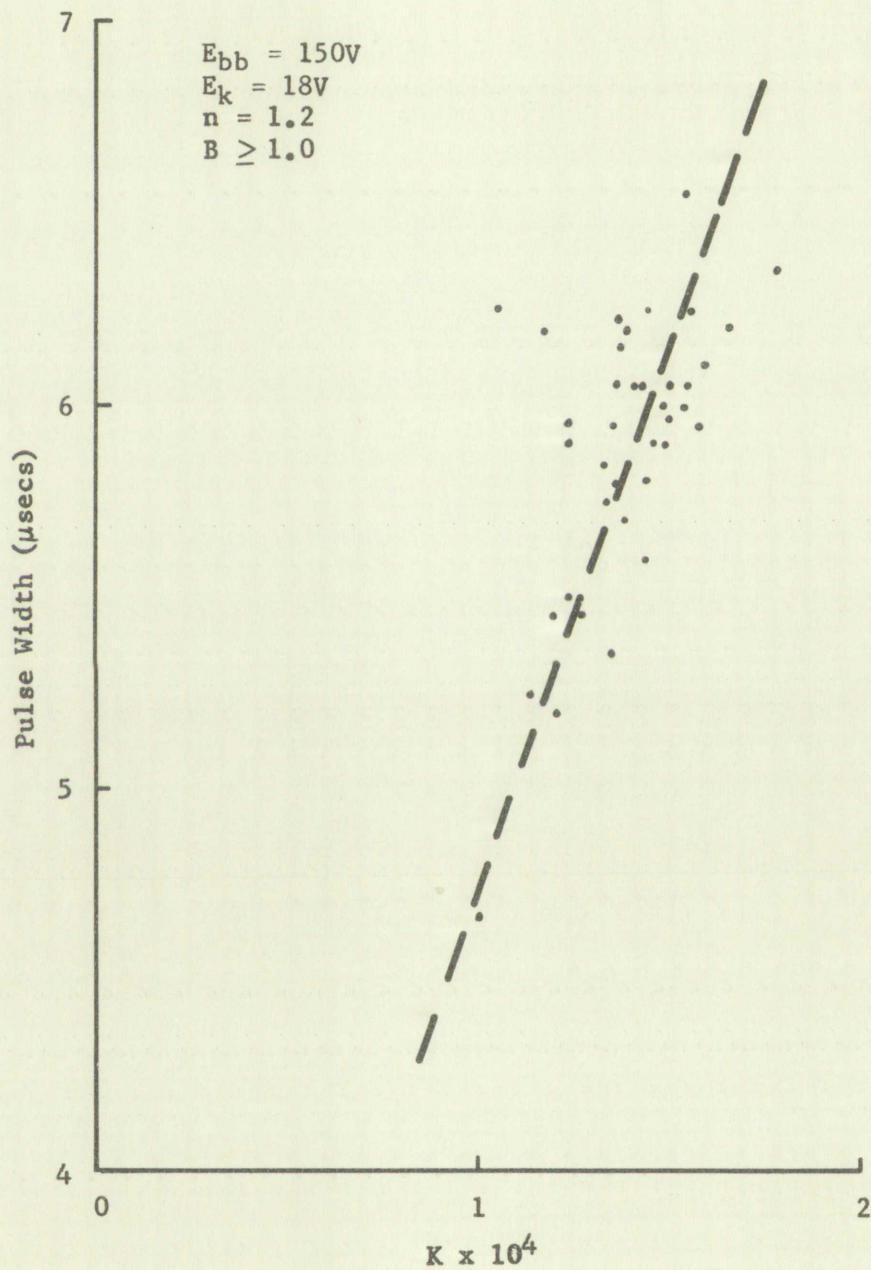
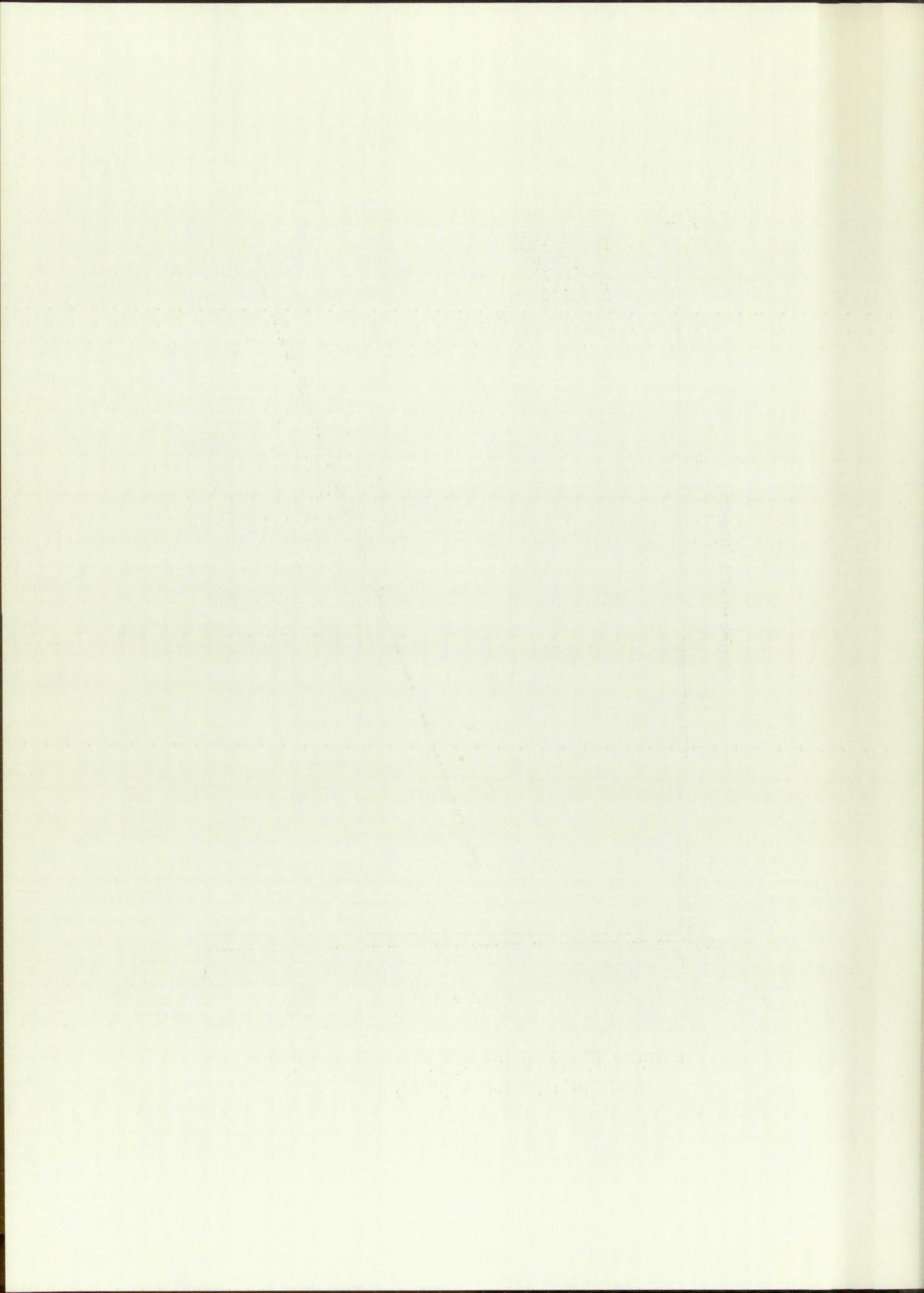


Figure 23. Dependence of the Pulse Width Upon the Current Emission Factor



an N-type semiconductor with small internal and external work functions; and that the current emission is due to the barium donors on the surface of the oxide coating.

In operation, barium metal is evaporated from the surface and is collected on the bulb and perhaps the grid and plate also. This means that an equilibrium must be established between the rate of formation and the rate of evaporation of the free metal. Eventually, the efficiency of formation starts decreasing, and the cathode emission slowly decays.

Under pulsed conditions the surface layer of barium has tremendous emission capabilities. The emission may be as much as three orders of magnitude greater than is obtainable under direct current emission. Under wide pulse conditions, the pulse emission<sup>9</sup> current decreases exponentially and approaches its DC value with a time constant on the order of milliseconds. After the pulse there is an exponential recovery interval during which the emission capability approaches its initial value. Thus, the emitted current consists of a conduction component and a capacitive displacement component.

### Design Considerations

Variation in pulse emission will directly affect the value of the current emission factor  $K$ . If a different method of approximating the tube characteristics had been employed, some other parameter dependent upon the magnitude of the currents would still be required to characterize the tube.

Since Equation (21) is independent of  $K$ , pulse emission should have no effect on pulse amplitude. There is, however, some variation in the current division factor (usually an increase) during tube life, apparently

---

<sup>9</sup>The term, pulse emission, is a misnomer in the sense that it is not all the current that can be drawn from the cathode. An increase in the pulse voltage will result in an increase in the emitted current.

...with the ... and ...  
...the ... of ...  
...the ... of ...

...the ... of ...  
...the ... of ...  
...the ... of ...

...the ... of ...  
...the ... of ...  
...the ... of ...

...the ... of ...  
...the ... of ...  
...the ... of ...

... ..

...the ... of ...  
...the ... of ...  
...the ... of ...

...the ... of ...  
...the ... of ...  
...the ... of ...

...the ... of ...  
...the ... of ...  
...the ... of ...

due to secondary emission from the grid. This is probably a result of grid contamination from materials boiled off the cathode. The change in B is usually small, and the pulse amplitude is relatively constant during the life of the tube.

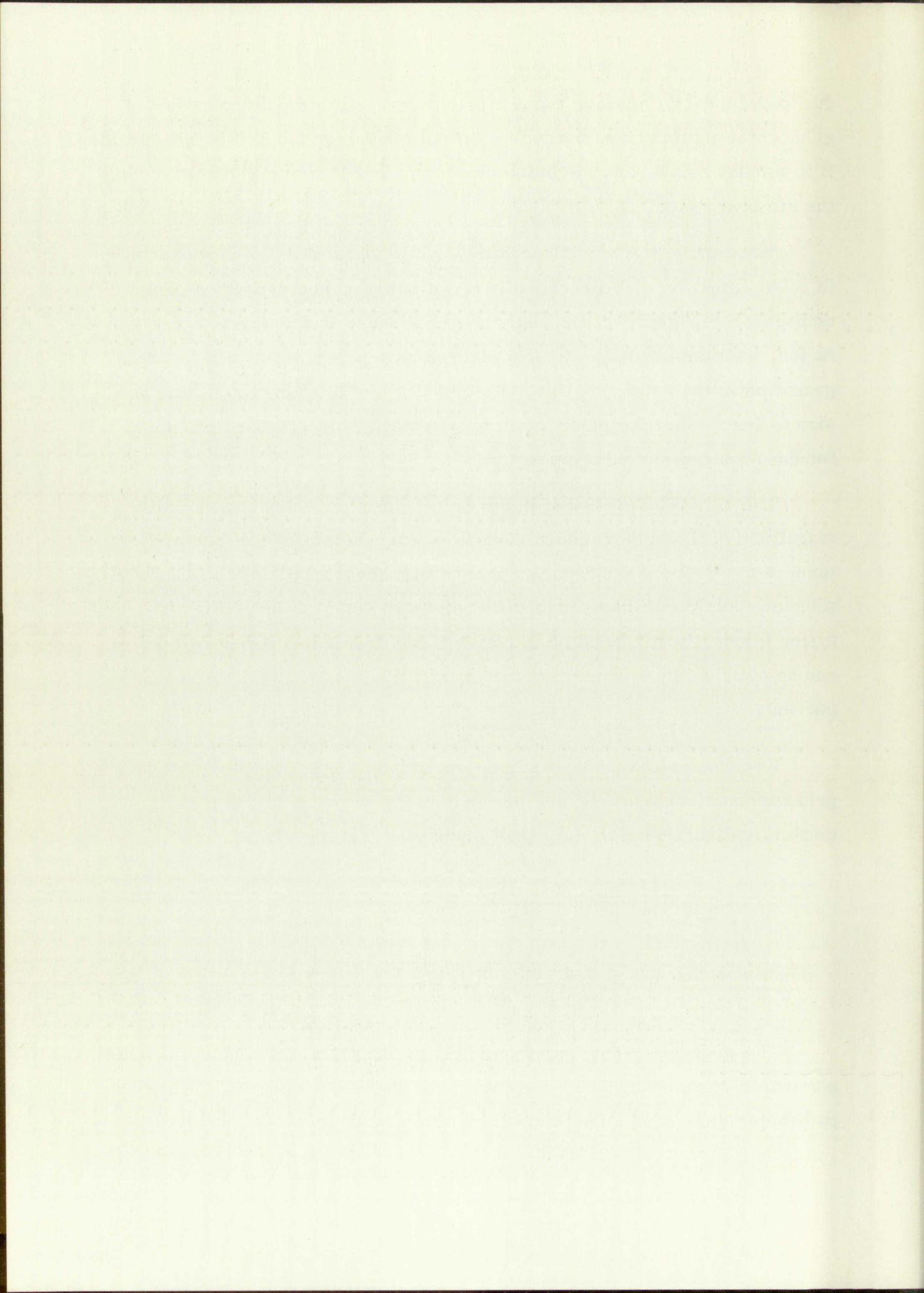
Since pulse width by Equation (23) is proportional to K, variations in pulse emission will directly affect the pulse width. There is some compensation, however, because of the increase in the current division factor, as mentioned above. The decrease in pulse width with the degradation in emission must be considered in the blocking oscillator design to insure that the pulse width will remain within the design limits for the required period of operation.

The rate of decrease of pulse emission is dependent upon both the magnitude of the cathode current and the duty factor. While the mechanism is not well understood, it appears that the operating life is a complicated function of these quantities raised to some power. Since the duty factor is usually governed by the design requirements, adequate tube life can be obtained by a proper choice of the tube and the maximum cathode current.

From the fact that the cathode current is the sum of the plate and grid currents, an equation can be derived for the cathode current by combining Equations (1), (2), (16), and (17). The result is

$$i_k = nK \left[ \left( \frac{E_{bb}}{n} + \frac{B(n-1)-2}{nB} E_k \right) e_o - \frac{nB-1}{n^2 B} e_o^2 + \frac{B+1}{B} E_k^2 - E_k E_{bb} \right] \quad (31)$$

The presence of the supply and bias voltages in this equation is not particularly important since they are usually predetermined. The one parameter subject to adjustment for control of the cathode current of a



given tube type is the effective turns ratio.<sup>10</sup> An examination of the paths of operation with different turns ratios readily reveals that the higher the turns ratio, the lower the cathode current; this is verified by the results that were given in Table I.

It is noteworthy in Equation (31) that the cathode current is proportional to  $K$ . Thus, a high pulse emission tube may require a higher turns ratio to limit the cathode current.

An additional possibility for extending tube life exists as a result of the influence of the cathode temperature on emission. A typical sketch of pulse emission as a function of heater voltage is shown in Figure 24 for a tube having a nominal rating of 6.3 volts. Note that the pulse emission flattens in the vicinity of 7 volts. There is some evidence to indicate that with operation at elevated voltages, the pulse emission does not decrease as fast during the first 100 hours or so of operation as it does with nominal heater ratings. The effects of heater voltage variations are also reduced. It is obvious that operation at elevated heater voltages is not permissible if extended tube life is required.

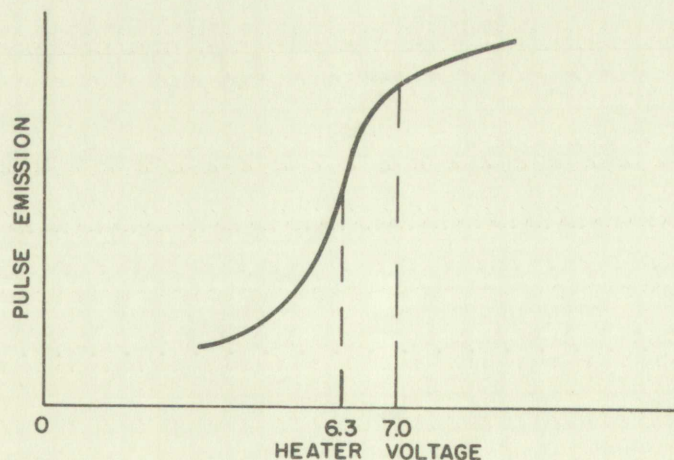
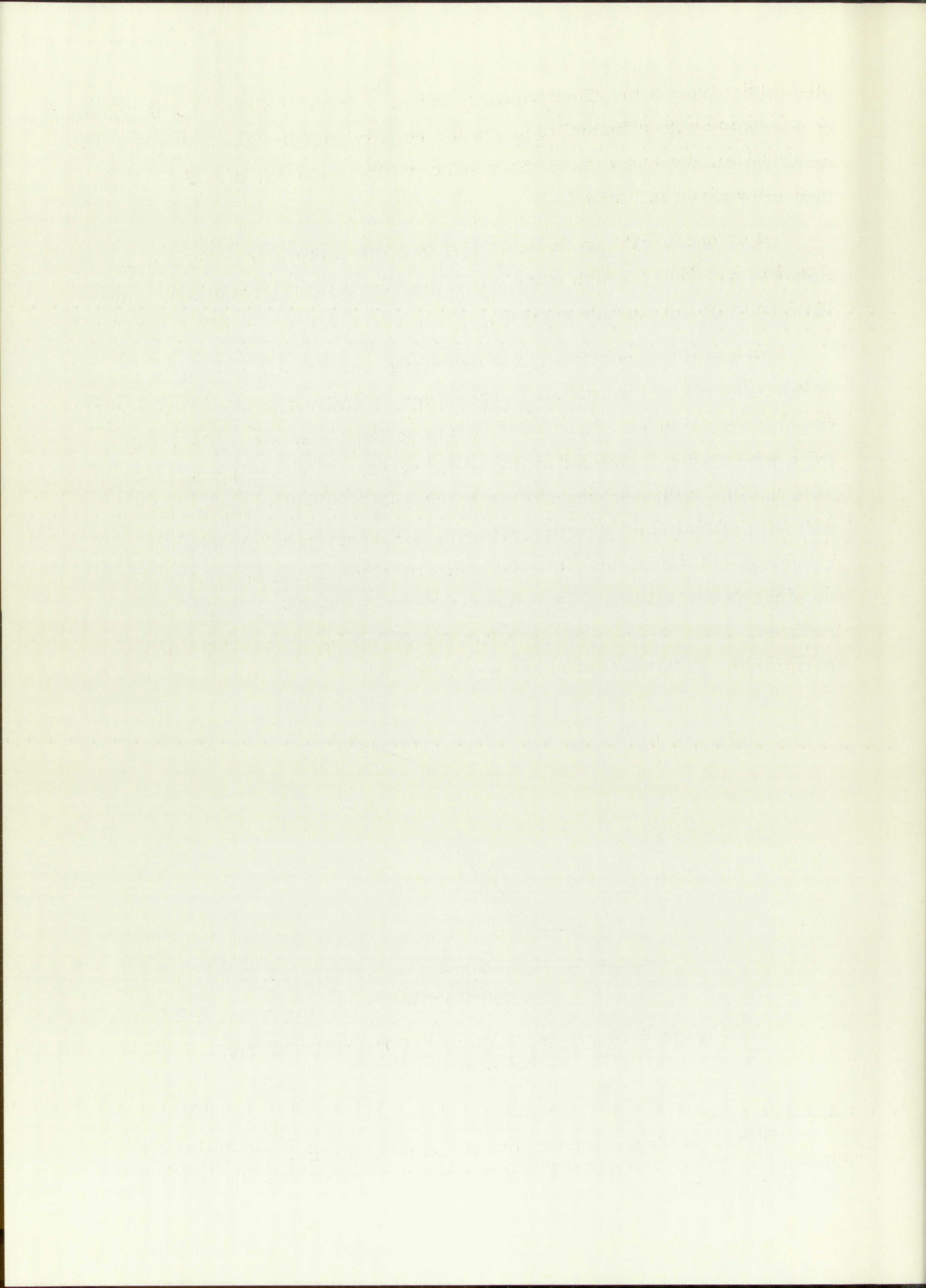


Figure 24. Typical Variation of Pulse Emission with Heater Voltage

---

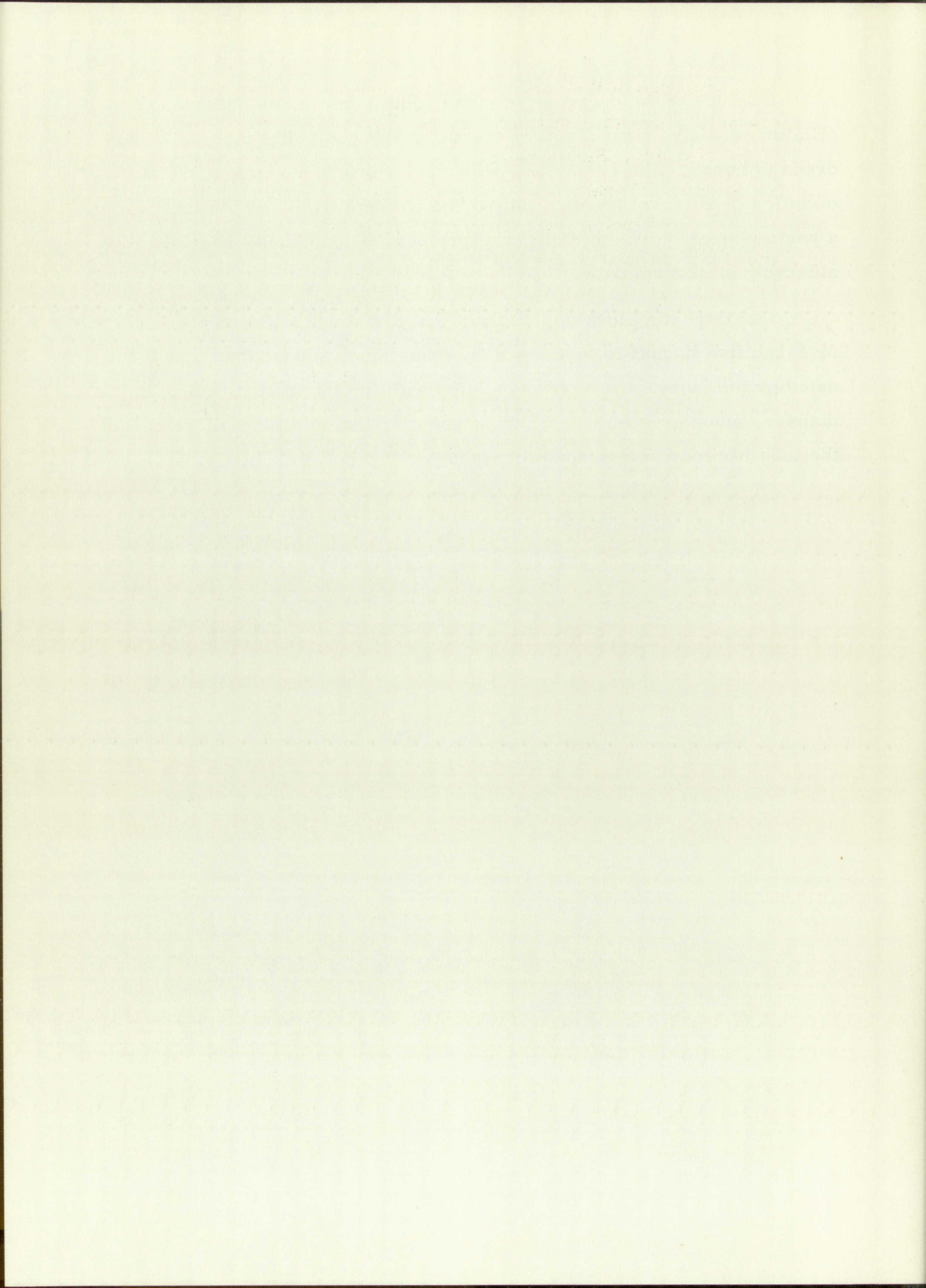
<sup>10</sup>This is for the intrinsic circuit. It is shown in the following chapter that the cathode current can also be controlled with the addition of a grid resistor.





Because of the decrease in pulse width, the intrinsic blocking oscillator may have a satisfactory operating life limited to the tens or hundreds of hours. Since there are wide variations in the emission characteristics of different types of tubes, the determination of the tube life in a particular circuit is an individual problem which usually requires considerable statistical data.

The intrinsic blocking oscillator may be modified to employ external or capacitive turnoff to terminate the pulse much sooner than it is terminated by the inherent turnoff associated with the intrinsic circuit. In this manner, much greater variations in pulse emission can be tolerated, and the tube life may be extended into thousands of hours.



## CHAPTER V -- MODIFICATIONS TO THE INTRINSIC BLOCKING OSCILLATOR

The intrinsic blocking oscillator may be modified in an almost unlimited number of ways. The previous material on this basic circuit holds in large part with many of these changes. Using the characteristics of the intrinsic circuit, the general effects of most modifications can then be deduced.

While a mathematical analysis of an intrinsic blocking oscillator is quite complicated because of the large number of variables and the nonlinearities, the analysis of a modified circuit is usually even more so. Since the primary tube parameters,  $K$  and  $B$ , have already been determined, and since a statistical approach is more practical and readily reveals the importance of all the circuit parameters, the greatest value of analytics tends to be academic rather than heuristic. Hence, the predominant use of statistical methods is advocated.

Three typical modifications, which require an extension of the previous analyses, will be considered. These circuit modifications and combinations of them allow a large variety of design requirements to be met.

### Capacitive Turnoff

The more conventional blocking oscillators use a capacitor in the grid circuit as shown in Figure 25. Examples of piecewise linear analyses are found in Strauss [7] and Smith [8]. The resistor  $R$  allows the capacitor to discharge during the recovery interval. The circuit may be operated in either a free-running or a monostable manner.

## CHAPTER 7 - ROTATIONS TO THE X-Y PLANE SINUSOIDAL OSCILLATION

The first step in the analysis of a sinusoidal oscillation is to determine its amplitude and phase. This is done by comparing the oscillation to a reference sinusoid of the same frequency. The reference sinusoid is usually chosen to be a cosine wave with an amplitude of 1 and a phase of 0. The amplitude of the oscillation is then determined by measuring the maximum value of the oscillation relative to the reference sinusoid. The phase of the oscillation is determined by measuring the time delay between the reference sinusoid and the oscillation.

Once the amplitude and phase of the oscillation have been determined, it can be expressed as a sinusoid of the form  $A \cos(\omega t + \phi)$ , where  $A$  is the amplitude,  $\omega$  is the angular frequency,  $t$  is time, and  $\phi$  is the phase. This representation is useful for many applications, such as determining the average value of the oscillation and the power it carries. The average value of a sinusoid is zero, and the power is proportional to the square of the amplitude.

Another important property of sinusoids is that they are closed under addition and subtraction. This means that the sum or difference of two sinusoids of the same frequency is also a sinusoid of the same frequency. This property is useful for analyzing complex waveforms that can be decomposed into a sum of sinusoids.

### Complex Plane

The complex plane is a mathematical tool used to analyze sinusoids. It consists of a horizontal real axis and a vertical imaginary axis. A sinusoid can be represented as a point in the complex plane, where the horizontal coordinate is the real part and the vertical coordinate is the imaginary part. The complex plane is useful for analyzing the addition and subtraction of sinusoids, as well as for determining the average value and power of a sinusoid.

The complex plane is also useful for analyzing the response of a system to a sinusoidal input. The response of a system to a sinusoidal input is also a sinusoid of the same frequency, and its amplitude and phase can be determined by analyzing the system's response in the complex plane.

The voltage equations for this circuit are:

$$e_p = E_{bb} - E_k - e_o \quad (1)$$

$$e_g = \frac{e_o}{n} - E_k - v_c \quad (32)$$

$$v_c = \frac{1}{C} \int i_g dt \quad (33)$$

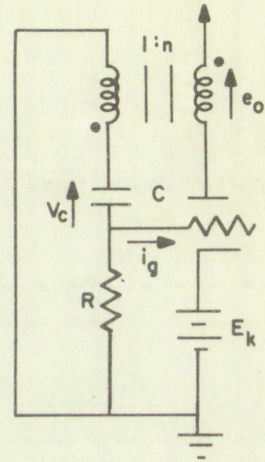


Figure 25. Blocking Oscillator with a Grid Capacitor

The only difference between Equations 2 and 32 is the presence of  $v_c$ . Assuming that the current through resistor R is negligible compared with the grid current, the current equations are the same as for the intrinsic circuit.

Because of the increasing voltage drop across the capacitor during the pulse, the pulse will be terminated earlier as a result of the reduced grid drive, and the paths of operation will be different than the paths for the intrinsic blocking oscillator. It has been found that Equation (17) still gives a fair approximation for the grid current even though it was obtained from the path of operation of the intrinsic circuit.

Making use of the approximations given by Equations (16) and (17) and combining them with Equations (1), (3), (14), (32), and (33), the output pulse can be obtained from a simultaneous solution of the following equations:

$$e_p = E_{bb} - E_k - e_o \quad (1)$$

$$e_g + \frac{nK}{BC} \int e_g^2 dt = \frac{e_o}{n} - E_k \quad (34)$$



$$i_m = nKe_g \left( e_p - \frac{e_{lg}}{nB} \right) \quad (18)$$

$$e_o = L_p \frac{di_m}{de_o} \frac{de_o}{dt} \quad (14)$$

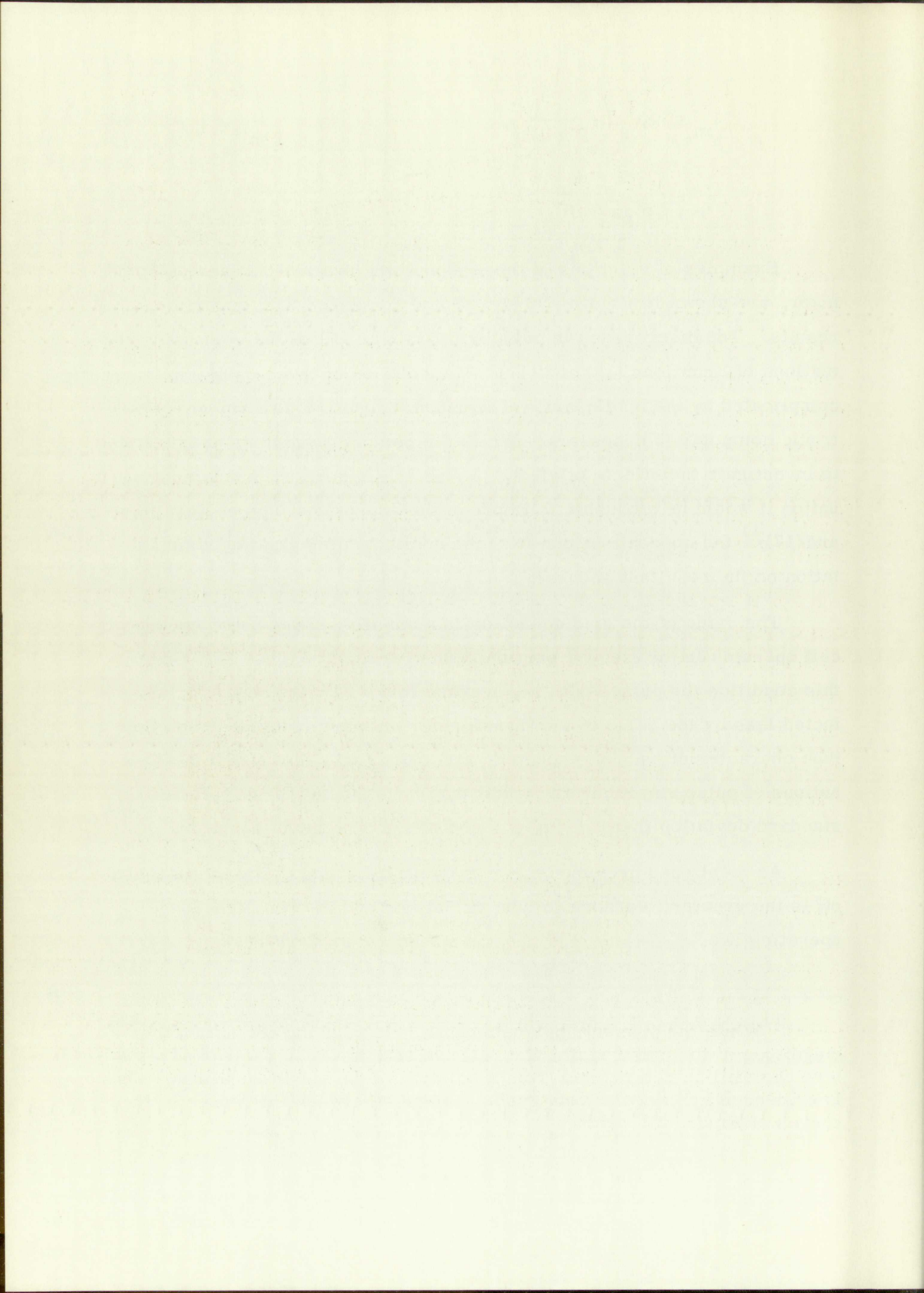
Examples of solutions of these equations, made on an analog computer, are shown in Figures 26 and 27 and compared with experimental results. The discrepancy in pulse width is a result of the poor approximations of Equations (16) and (17). The solution of these equations is greatly complicated by the nonlinearity of Equation (34), and a solution on an electronic computer is necessary. While the computer could be programmed to investigate the effects of all the variables, in such an extensive evaluation it would be advisable to improve the approximations of Equations (16) and (17);<sup>11</sup> the approximations for tube nonlinearities are the basic limitation on the resultant accuracy.

The value of the grid capacitor is normally chosen such that the circuit operates in the steeper portion of the curves in Figure 27. Under this condition the pulse width is governed largely by the capacitor and affected less by the value of the transformer primary inductance and the tube characteristics. As expected, statistical data shows that the distributions of pulse amplitude and width may have a considerably smaller standard deviation than can be obtained without the grid capacitor.

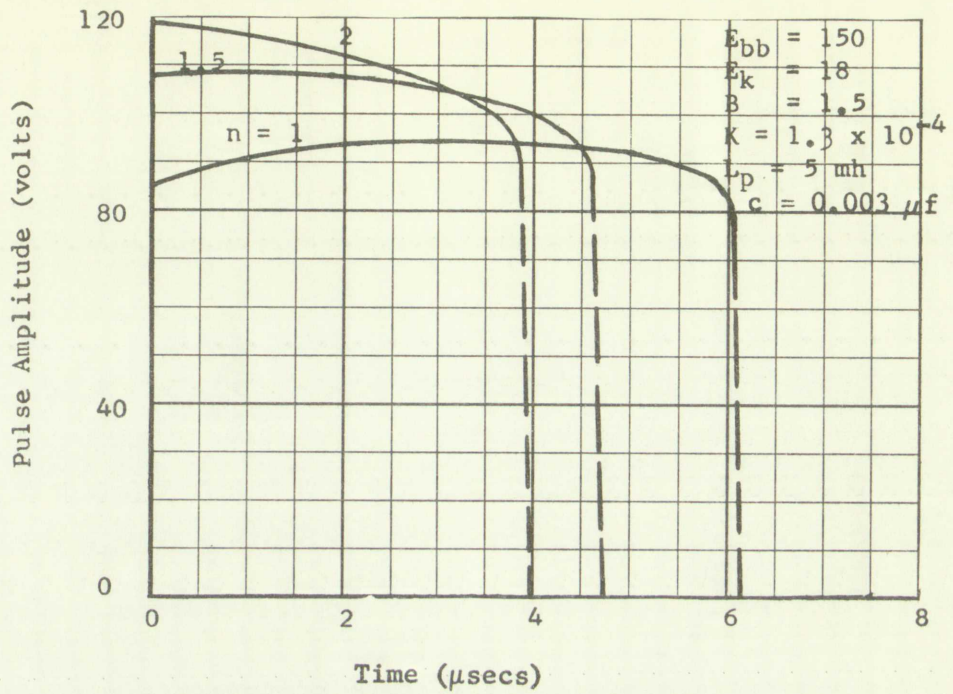
As mentioned previously, the greatest advantage of capacitive turn-off is the greater tolerance to tube variations and the resultant longer operating life.

---

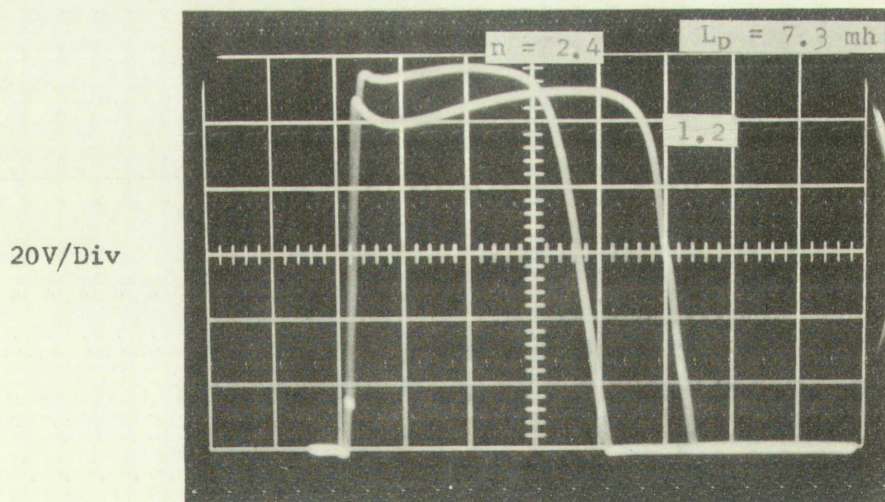
<sup>11</sup> While the present approximations give poor agreement on the magnitude of the pulse width, the relative effects of the various parameters can still be determined from a solution of the above equations. This is evidenced by the relatively good agreement between the slopes of the curves of Figure 27.







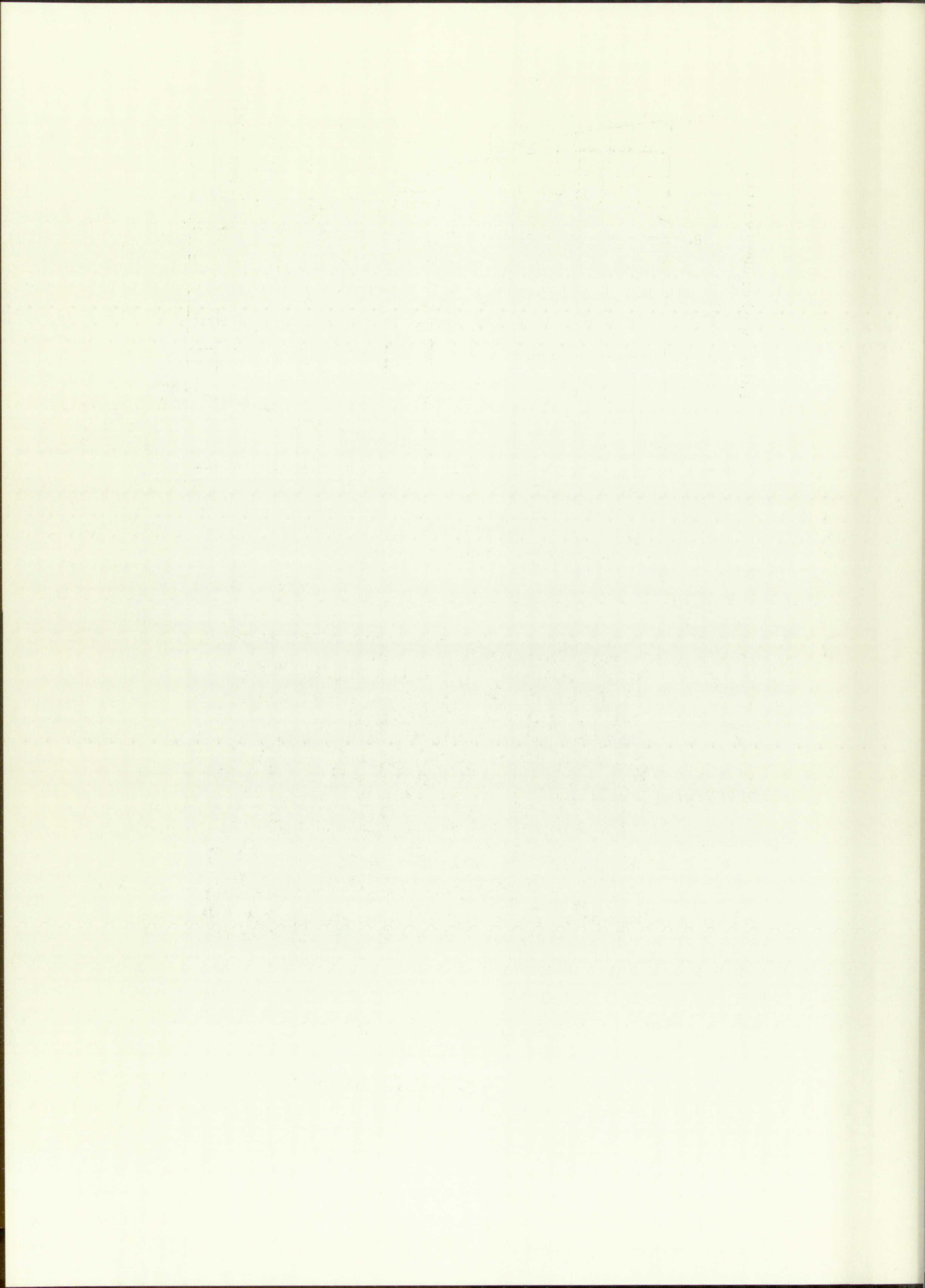
Results of Computer Solution



.5  $\mu\text{sec}/\text{Div}$

Measured Pulse Shape

Figure 26. Capacitive Turnoff



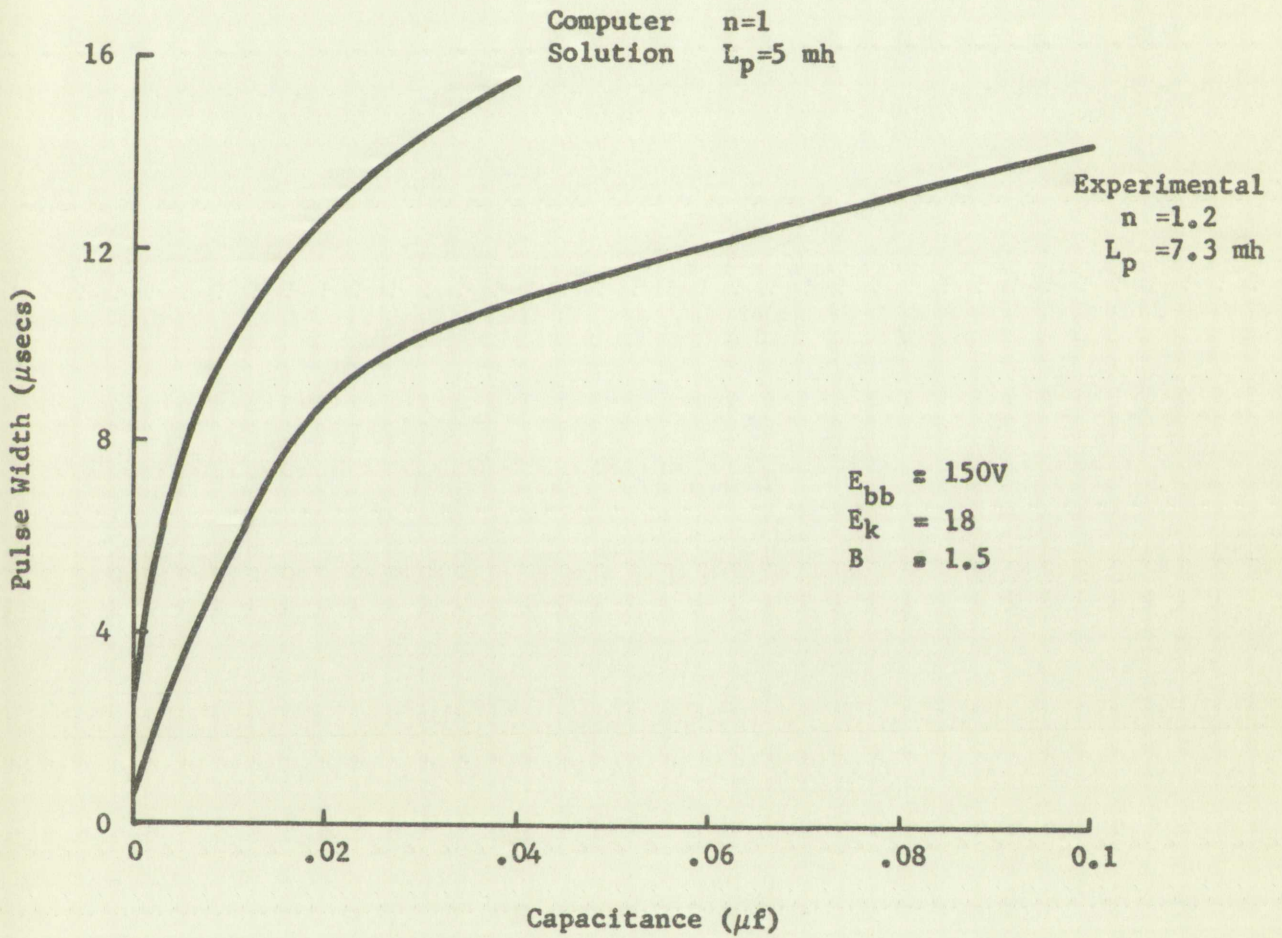


Figure 27. The Effect of the Grid Capacitor on Pulse Width

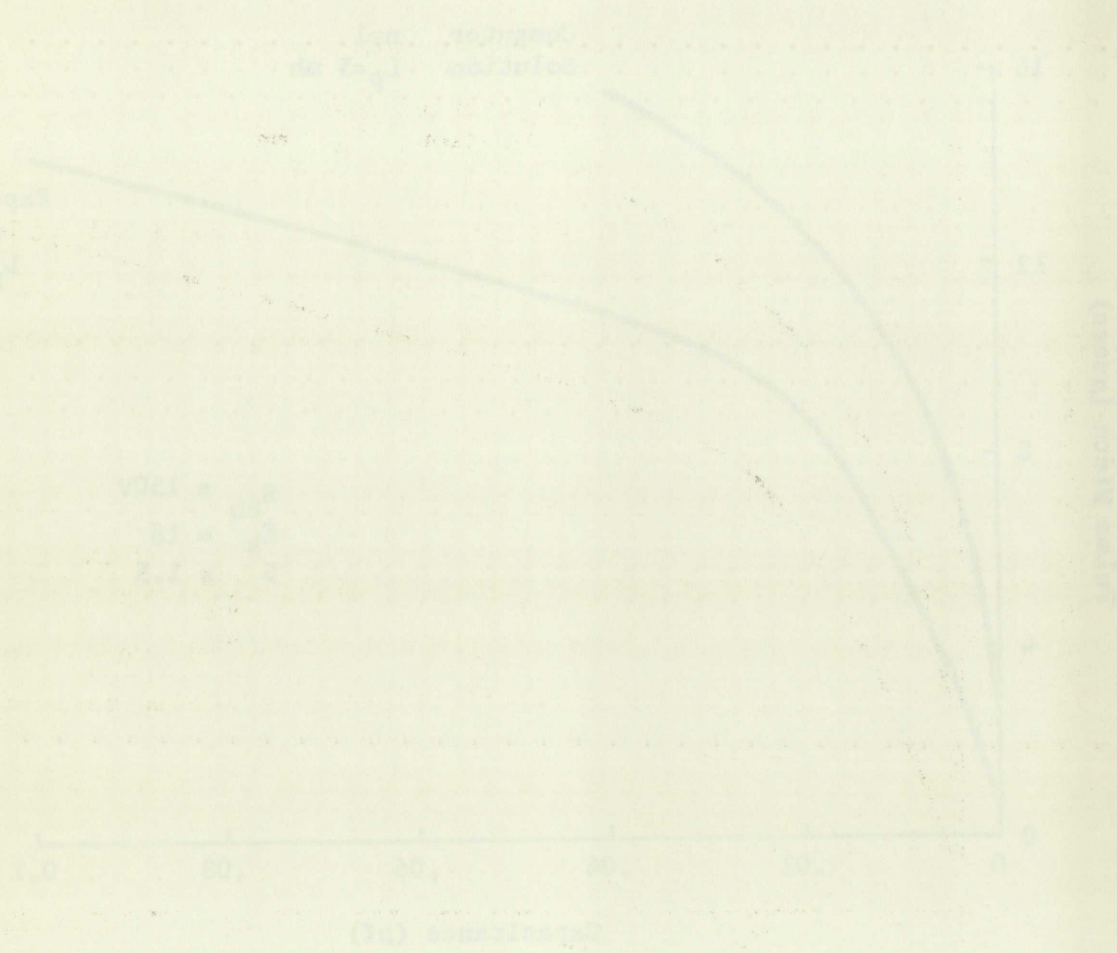


Figure 2. The Effect of the First Harmonic on Pulse Width

## Grid-Plate Diode

A diode may be connected between the grid and the plate such that the diode will conduct when the grid voltage tries to exceed the plate voltage. The objective in adding this diode is twofold: (1) The output pulse amplitude is held more nearly constant; and (2) Any tendency for Barkhausen oscillations is reduced or eliminated.

Except for the capacitance of the diode, the presence of the diode will have no effect on the rise time and recovery intervals. During the main part of the pulse, however, the plate and grid voltages will be practically equal as long as the diode is conducting. Equating the plate and grid voltages in Equations (1) and (2), and solving for the output pulse, results in:

$$E_o = \frac{n}{n+1} E_{bb} \text{ for } E_p = E_g = \frac{E_{bb}}{n+1} - E_k \quad (35)$$

Points on the paths of operation corresponding to Equation (35) are designated by D in Figure 8. Since the plate current is the sum of the diode current, the reflected grid current and the magnetizing current, the diode current is then

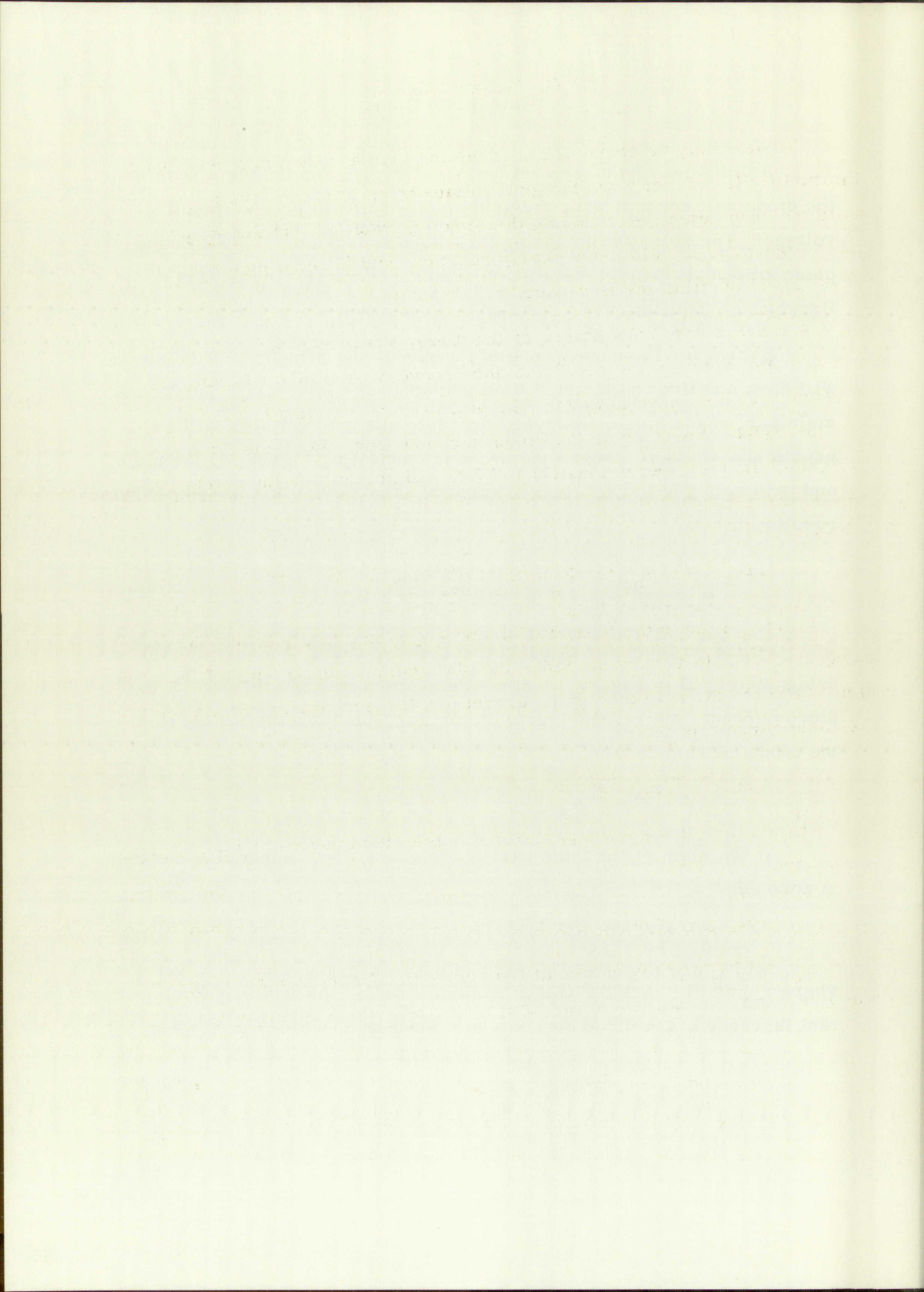
$$i_d = I_p - i_m - I_g/n.$$

At the start of the main part of the pulse, the magnetizing current is zero and

$$I_d = I_{pd} - I_{gd}/n \quad (36)$$

where  $I_{pd}$  and  $I_{gd}$  are the values at the points D. As the magnetizing current increases, the diode current decreases and becomes zero when

$$I_m = I_{pd} - \frac{I_{gd}}{n} \quad (37)$$



Thus, the presence of the grid-plate diode gives the effect of a constant magnetizing current. As the magnetizing current increases from zero, the position on the path of operation remains stationary at the points D until the magnetizing current exceeds the value given by Equation (37). As the magnetizing current increases further, the diode becomes reverse-biased and the diode current remains at zero; the remaining portion of the pulse is not, then, affected by the diode.

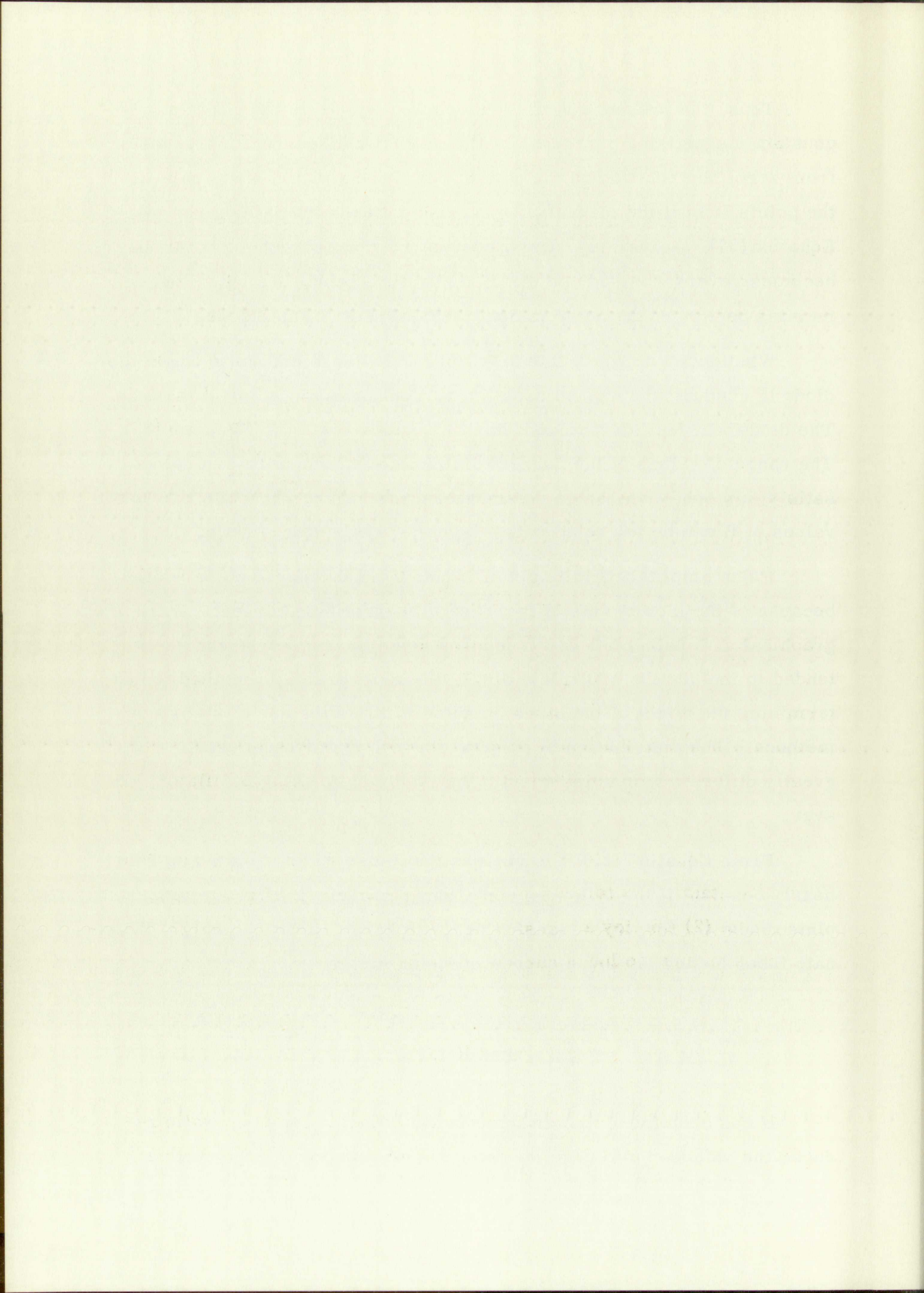
Whether or not the pulse amplitudes are large enough to cause the diode to conduct will depend upon the current division factor of the tube. The diode will just start to conduct if  $E_1$  equals the  $E_0$  in Equation (35). The range of values of the current division factor which do and do not satisfy this condition can be determined from Figure 28. Note that lower values of B can be tolerated with a higher effective turns ratio.

Pulse amplitude limiting will result in an increased pulse width because of the slower rate of increase in magnetizing current. While the graphical and mathematical procedures given in Chapter IV can be extended to include the grid-plate diode, the most practical method for determining the effect of the diode on pulse width is the use of statistical methods. The distribution of pulse width with the diode is usually not greatly different than obtained with the intrinsic blocking oscillator, however.

From Equation (30) it is obvious that pulse width can also be held nearly constant if the following conditions are met: (1) Use the grid-plate diode; (2) Employ a transformer with hard saturation; and (3) Eliminate tubes having too low a current division factor.

#### Grid Resistor

It has been found that an increase in the effective turns ratio reduces the cathode current in the intrinsic blocking oscillator, with a





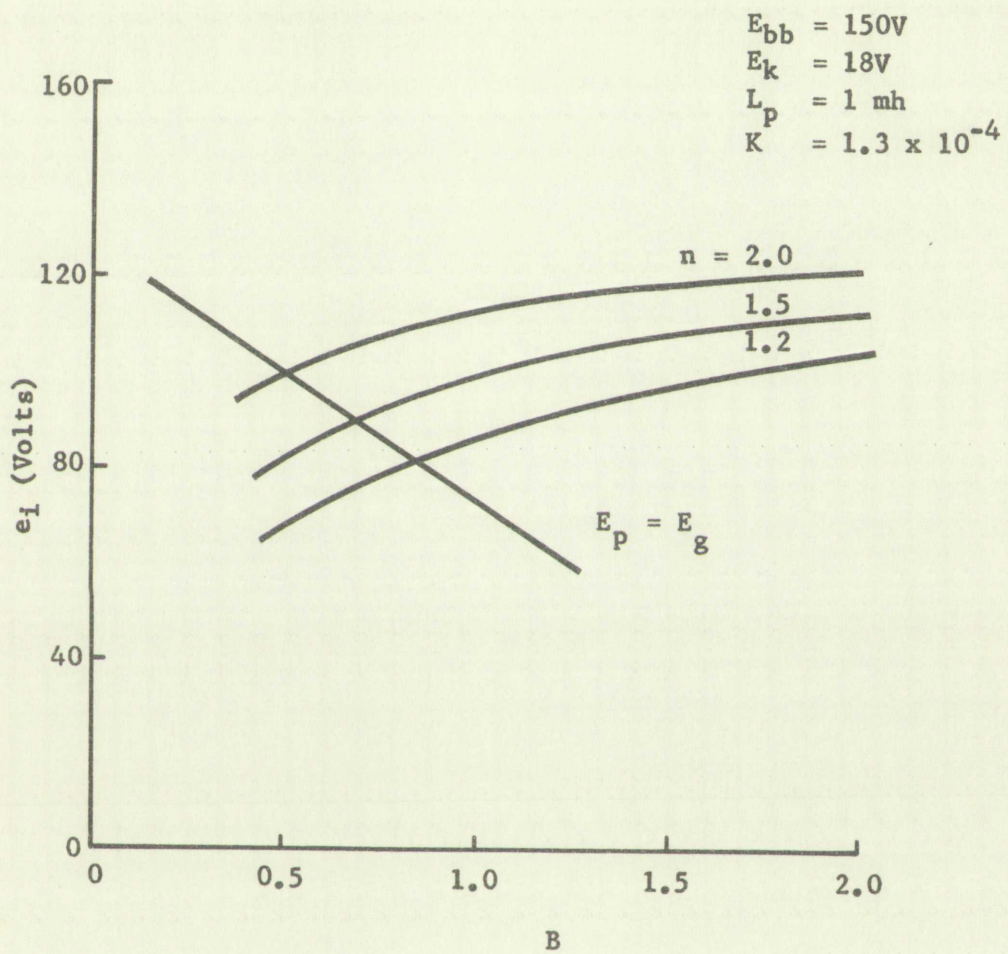
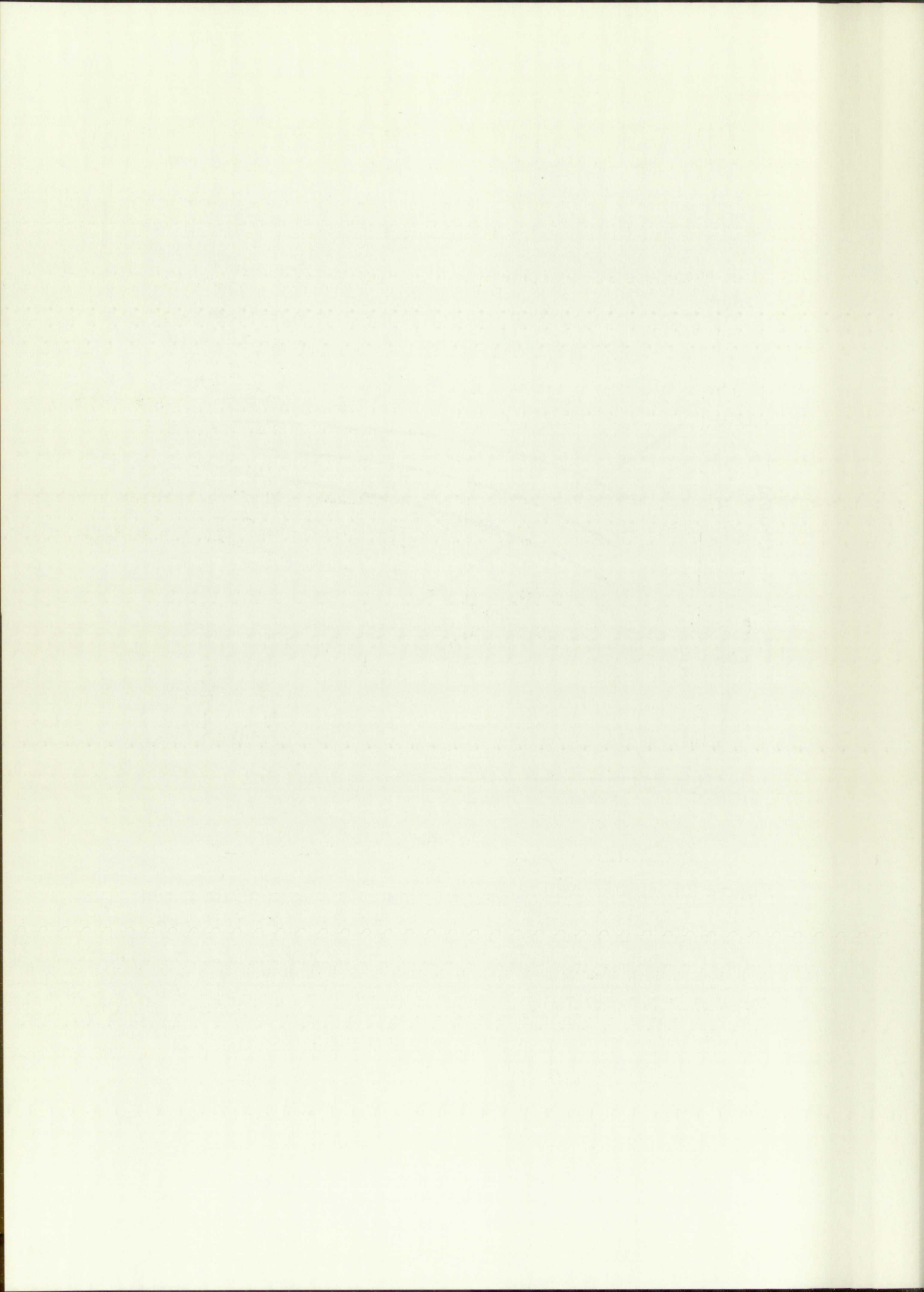


Figure 28. Pulse Amplitude Limiting with a Grid-Plate Diode



consequent increase in operating life. This decrease in cathode current results from the reduced grid voltage. Similar effects can be obtained by inserting additional resistance in series with the grid circuit. Thus, the desirable properties of a higher turns ratio can be simulated with the more commonly available unity turns ratio transformers.

It is evident that a mathematical analysis of this circuit can be made. The equations would be similar to those obtained for the grid capacitor circuit and would require solution on a computer.

A combination of grid resistor and grid-plate diode can be employed as shown in Figure 29. When both components are used, there is an additional method of connection as shown in Figure 30. A not so obvious advantage of this latter circuit is the lesser possibility of Barkhausen oscillations since the grid voltage is limited to less than the plate voltage.

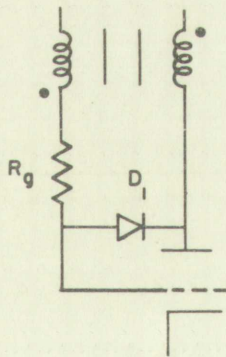


Figure 29. Combination of Grid Resistor and Diode

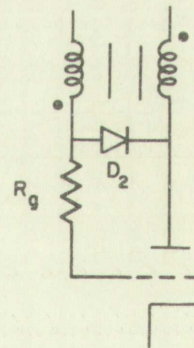
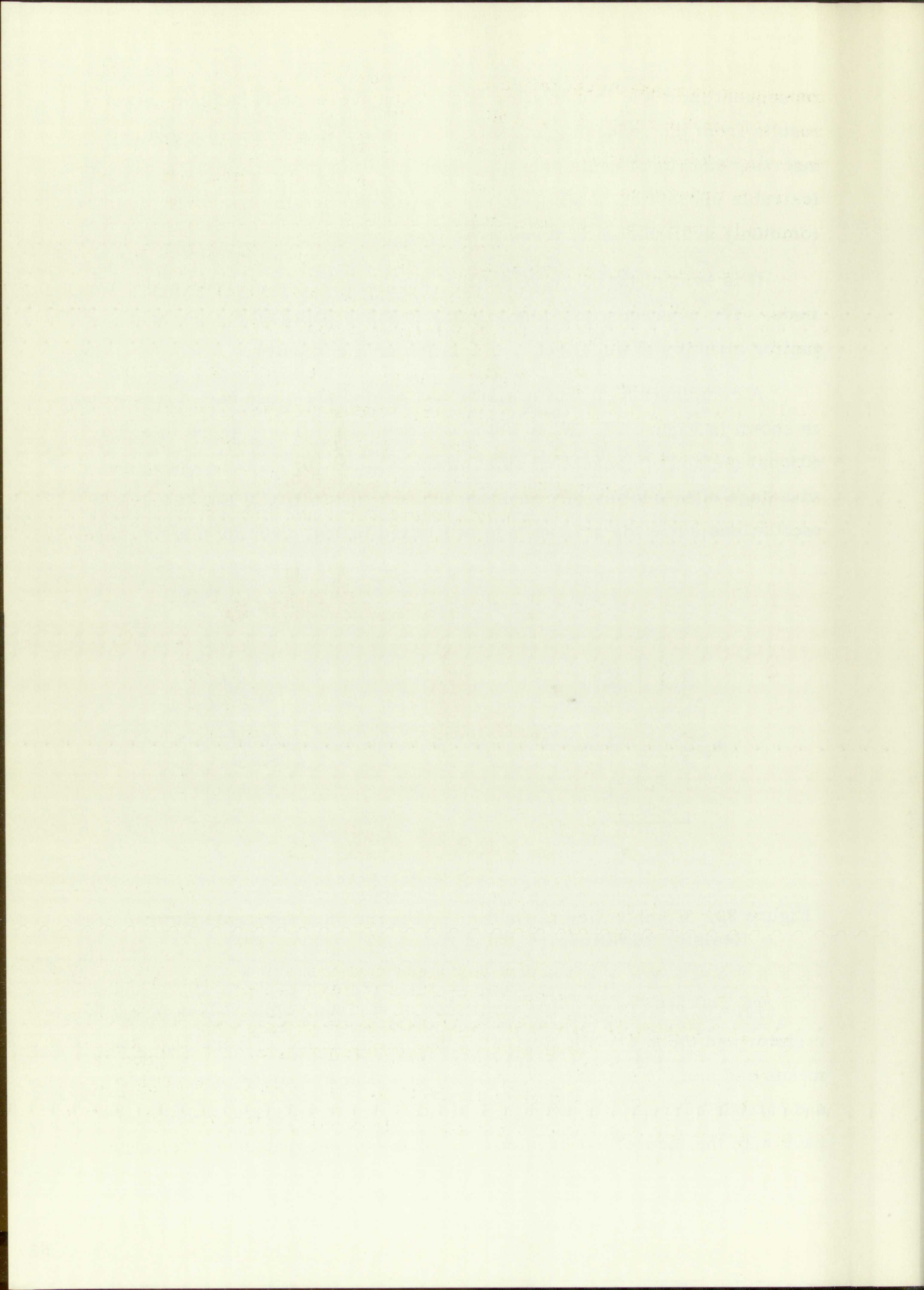


Figure 30. Alternate Combination

Typical effects on pulse amplitude of various combinations of a grid resistor and diode are illustrated by the histograms in Figure 31. The means and sample standard deviations for pulse amplitude, pulse width, and cathode current are given in Table II. The results are in good agreement with the theoretical predictions. It is evident that the combination



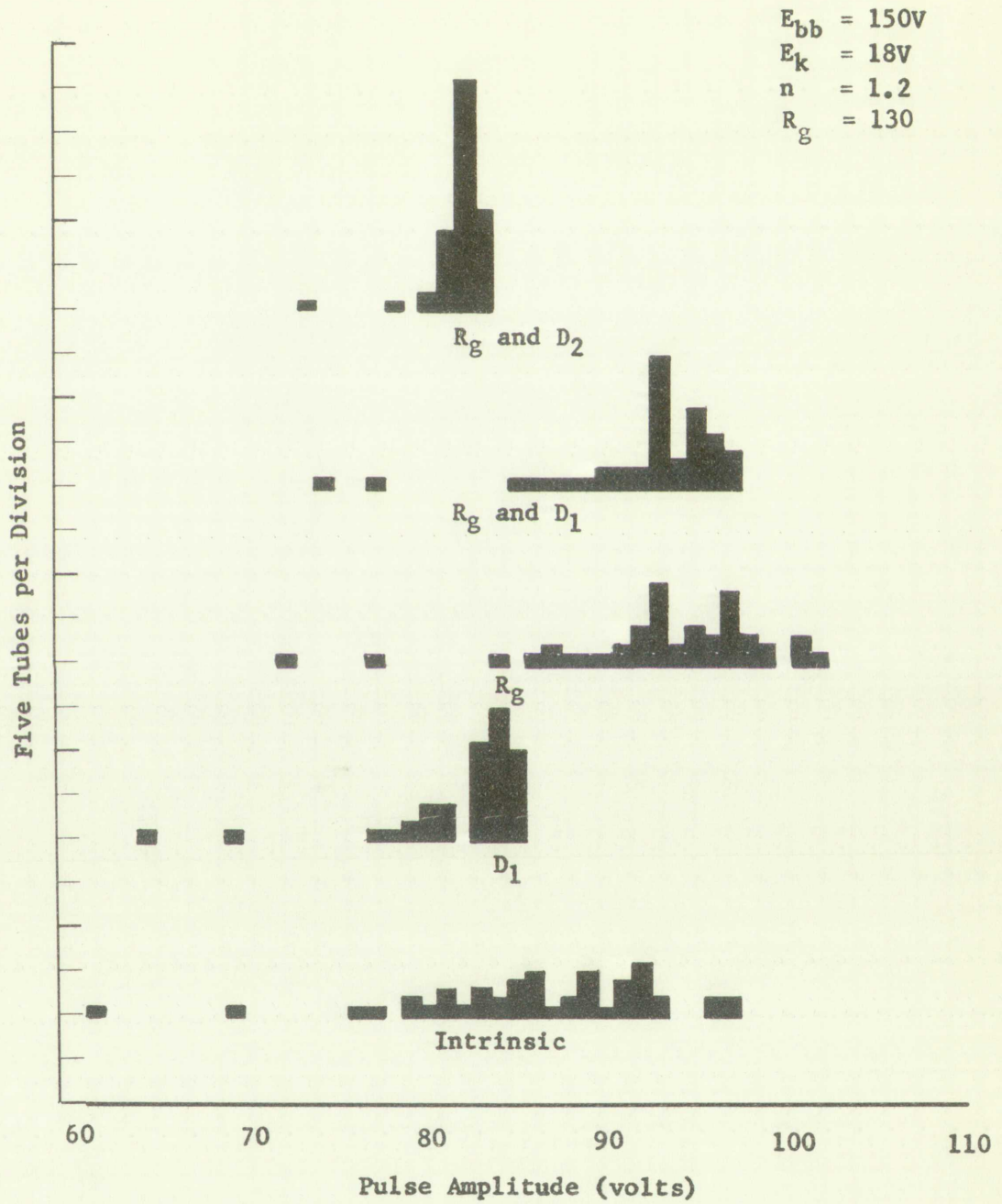
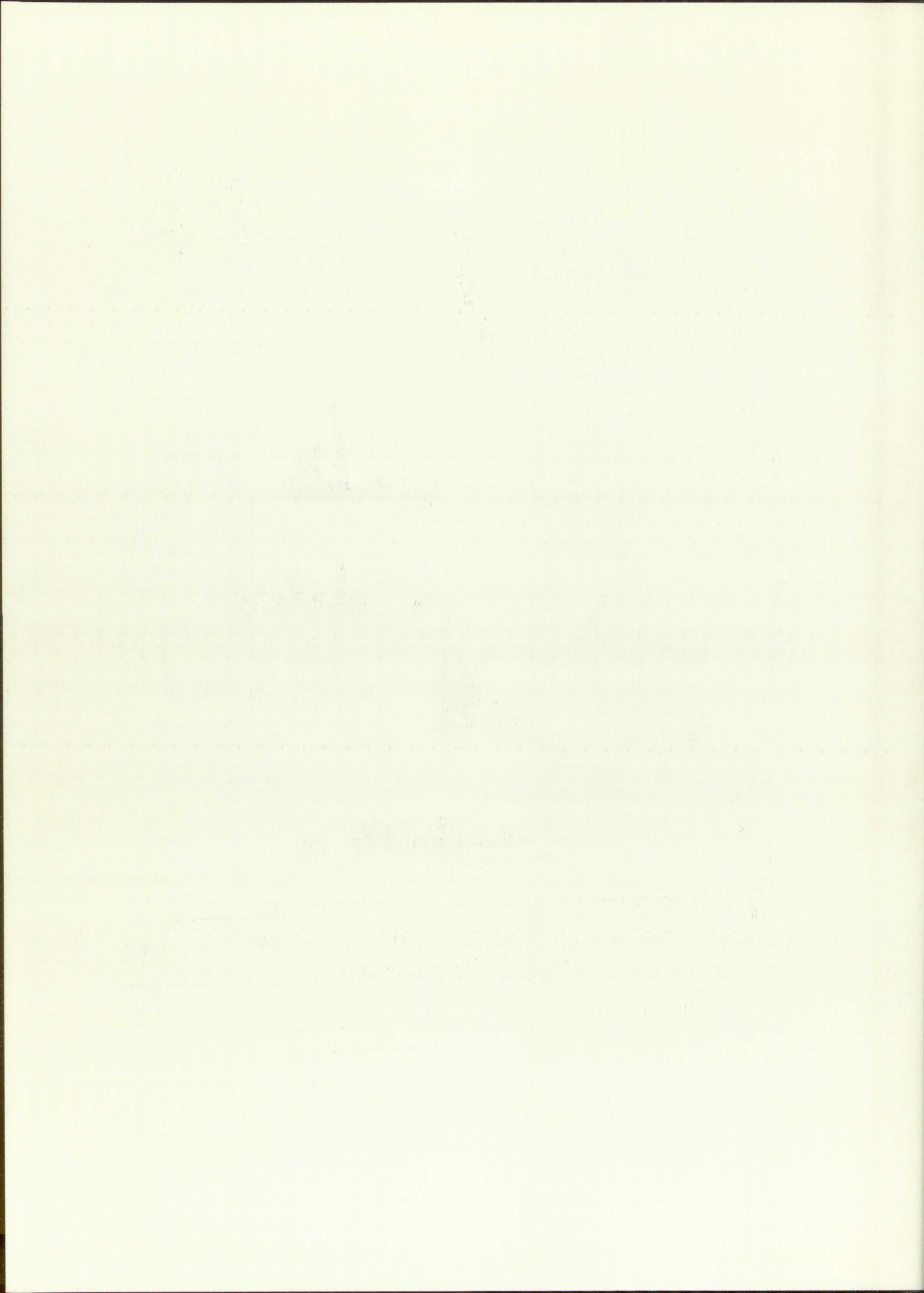


Figure 31. Distributions of Pulse Amplitude with Various Circuit Modifications



of  $R_g$  and  $D_2$  results in both a drastic reduction in the spread of pulse amplitude and a reduction of cathode current. Note that neither the modifications in Table II nor the variations in  $n$  in Table I have much effect on the variations in pulse width; since the pulse width is relatively independent of  $B$ , the spread in pulse width is primarily due to the distribution of  $K$ , shown in Figure 20.

TABLE II

The Effects of Circuit Modifications

Circuit*	Pulse amplitude (volts)		Pulse width ( $\mu s$ )		Cathode current (ma)	
	$\bar{X}$	S	$\bar{X}$	S	$\bar{X}$	S
Intrinsic	86	6.8	6.0	0.43	680	71
$D_1$	81	3.8	6.1	0.44	660	60
$R_g$	93	5.6	4.1	0.33	480	33
$R_g$ and $D_1$	92	4.6	4.2	0.33	480	32
$R_g$ and $D_2$	81	1.6	4.7	0.50	440	30

\* Conditions:  $E_{bb} = 150v$ ,  $E_k = 18v$ ,  $L_p = 2.2$  mh,  $n = 1.2$ ,  
 $R_g = 130$  ohms

The two tubes having low amplitude values in Figure 31 are seen by Figure 21 to have low values of  $B$ . The elimination of these low  $B$  tubes would result in improved distributions. The elimination of these low  $B$  tubes and the use of  $R_g$ ,  $D_2$ , and a saturating transformer will result in nearly constant pulse amplitude and width, a long operating life, and little possibility of Barkhausen oscillations. In addition, these modifications do not alter the ability to generate high repetition rate nonperiodic

of  $\sigma$  and  $\tau$  results in both a dynamic reduction in the spread of noise...  
 contribution and a reduction of balance current...  
 variation in Table II and the variation in Table I have been...  
 the variation in noise with noise...  
 percent of  $\sigma$  has spread in noise with is primarily due to the...  
 portion of  $\sigma$  shown in Figure 10.

TABLE II

The Effect of Circuit Modifications

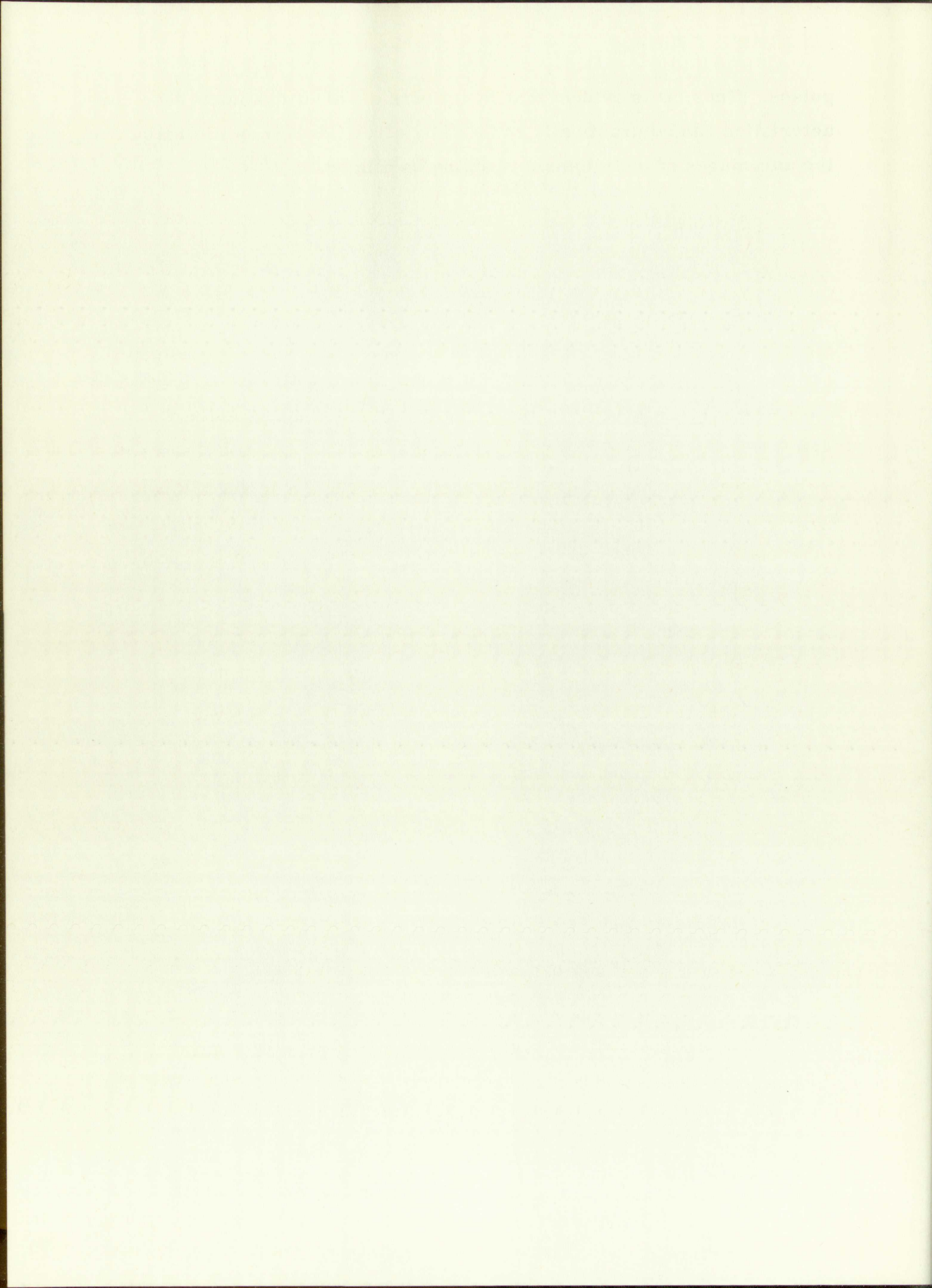
Circuit Number	Noise Amplitude ( $\mu V$ )		Noise Width ( $\mu s$ )		Circuit Current ( $\mu A$ )
	$\bar{X}$	$\sigma$	$\bar{X}$	$\sigma$	
11	38	0.8	0.9	0.45	500
12	34	0.8	0.7	0.45	500
13	32	0.8	0.7	0.45	500
14	30	0.8	0.7	0.45	500
15	31	0.8	0.7	0.45	500

Conditions:  $R_1 = 150 \text{ ohms}$ ,  $R_2 = 150 \text{ ohms}$ ,  $R_3 = 150 \text{ ohms}$ ,  $R_4 = 150 \text{ ohms}$ ,  $R_5 = 150 \text{ ohms}$ ,  $R_6 = 150 \text{ ohms}$ ,  $R_7 = 150 \text{ ohms}$ ,  $R_8 = 150 \text{ ohms}$ ,  $R_9 = 150 \text{ ohms}$ ,  $R_{10} = 150 \text{ ohms}$ ,  $R_{11} = 150 \text{ ohms}$ ,  $R_{12} = 150 \text{ ohms}$ ,  $R_{13} = 150 \text{ ohms}$ ,  $R_{14} = 150 \text{ ohms}$ ,  $R_{15} = 150 \text{ ohms}$ .

The two cases having low resistance values in Figure 11 are shown...  
 Figure 11 to have low values of  $\sigma$ . The elimination of these low  $\sigma$ ...  
 noise level is improved... The elimination of these low  $\sigma$ ...  
 noise and the use of  $R_1$ ,  $R_2$ , and a capacitor...  
 is nearly constant... with a long operating...  
 noise... In addition, these...  
 allow it to be able to generate high repetition rate...  
 noise...



pulses. Thus, it is evident that the effects of variations in the tube characteristics can be drastically reduced by circuit design, while maintaining the advantages of the intrinsic blocking oscillator.



## CHAPTER VI -- TRANSISTOR BLOCKING OSCILLATORS

### General Considerations

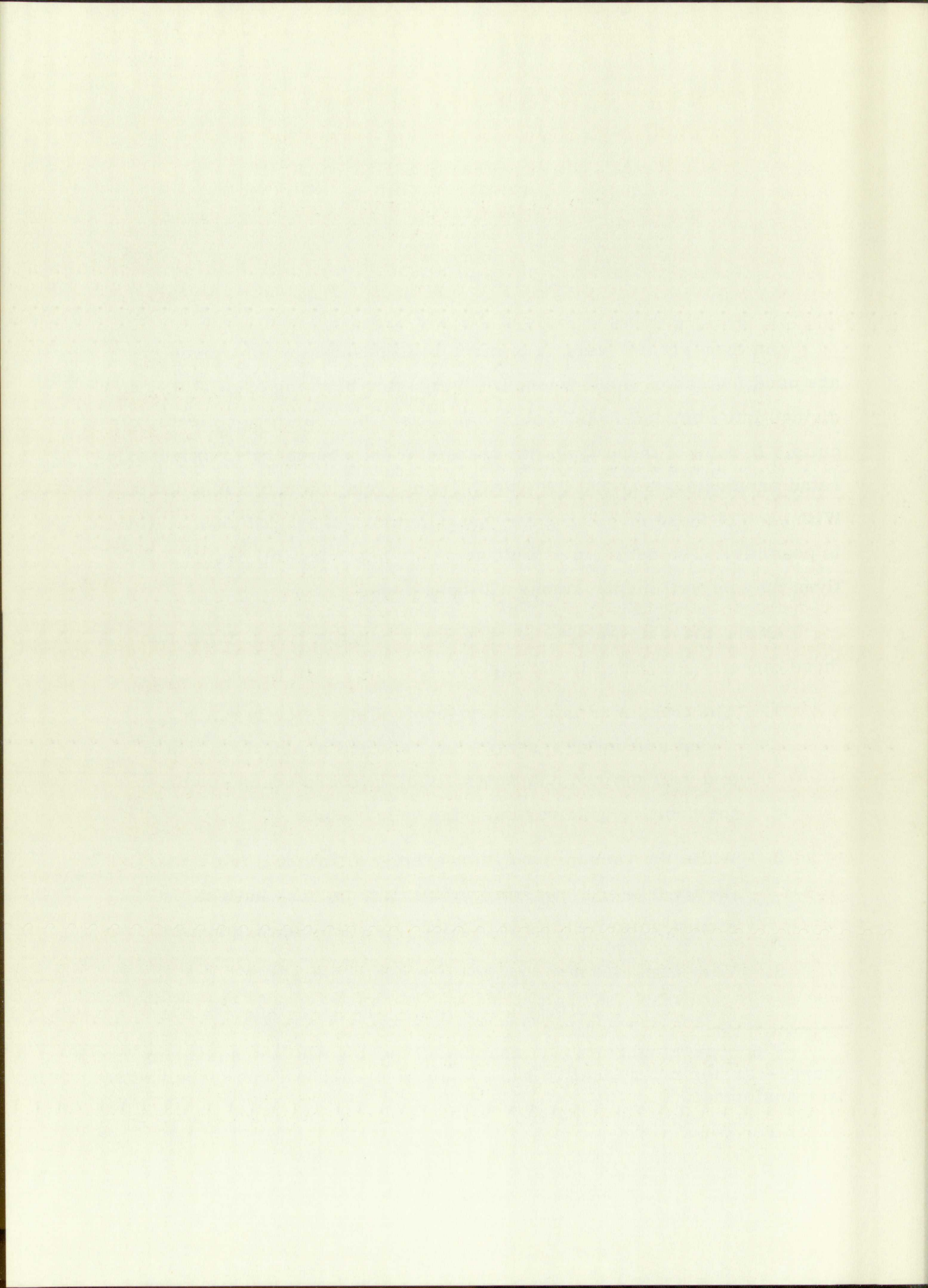
An even greater variety of circuits is possible when transistors are used instead of vacuum tubes. Transistor blocking oscillators can be divided into common-base, common-emitter, and common-collector circuits. In each of these types the transistor may be operated either saturated or unsaturated, and the transformer<sup>12</sup> may or may not saturate. With each of these circuits a very large number of circuit modifications is possible. The optimum circuit design to best meet all design objectives may be well hidden among all these possibilities.

Of the many advantages afforded by the use of transistors, some of those directly affecting circuit design are:

1. The transistor is a current-controlled device in which a vast amount of research has resulted in relatively linear and well-defined characteristics, in sharp contrast with the positive-grid region of the vacuum tube.
2. While the vacuum tube is inherently a limited-life device, the transistor, operating within ratings, may have an almost unlimited life with fairly constant characteristics.
3. Very high efficiency pulse circuits are possible.

---

<sup>12</sup>Schenkel and Statz [9] describe a blocking oscillator utilizing charge-carrier multiplication and avalanche breakdown in a circuit with no transformer.

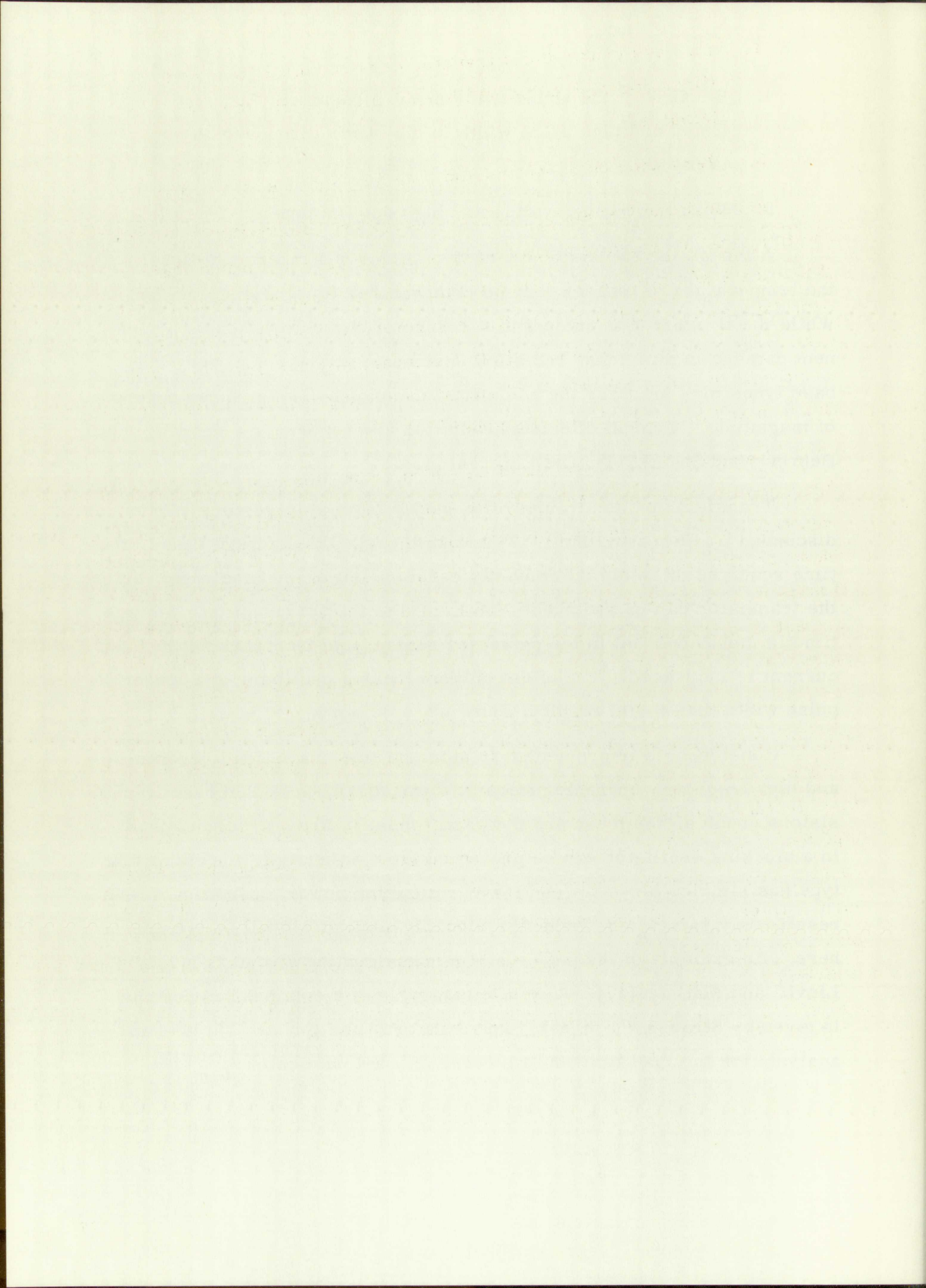


4. Because of the small transformers required, fast rise times and high pulse width to rise time ratios are obtainable.
5. Very wide pulse widths and high duty factors are feasible.

Although the transistor characteristics are temperature-sensitive, the temperature variations may be compensated for by circuit design. While the transistor is subject to a change in characteristics or permanent damage in an intense radiation environment, the use of very thin base types may increase the radiation tolerance by two or three orders of magnitude. Typical effects of radiation are reported by Messenger [10], Behrens and Shaul [11], and Loferski [12].

Transistor pulse circuits often suffer from storage-time effects, as discussed by Ebers and Moll [13] and Moll [14]. The storage time is the time required to sweep the minority carriers out of the base region before the transistor can be switched from the On to the Off condition. Storage time is most apparent in the saturated region, and increases as the base current is increased. The effect on the blocking oscillator is a longer pulse width than would result if there were no storage effects.

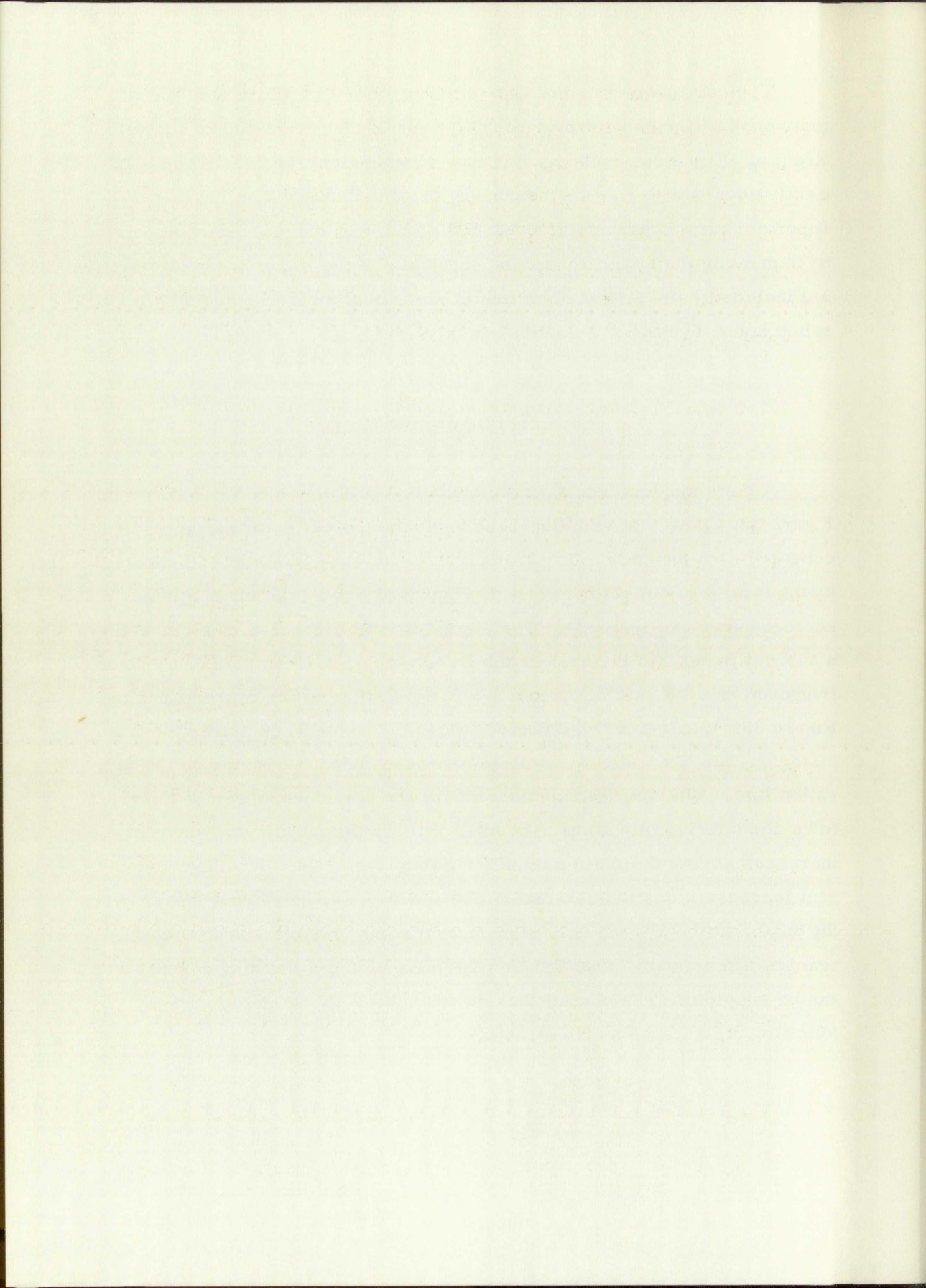
Considerable improvement in storage time, radiation tolerance, and high frequency characteristics is obtained with very thin base transistors, such as the mesa and epitaxial types. Although the transistor in a blocking oscillator can be prevented from saturating, the saturating type has simpler circuitry and lower transistor power dissipation. As a result, only saturating-transistor blocking oscillators will be considered here. An example of the analysis of a nonsaturating circuit is given by Linvill and Mattson [15]. A detailed analysis of a common base circuit is given by Strauss [7, p. 357], and Senatorov and Guzhov [16] give an analysis for the rise time and recovery characteristics.



Typical analysis and design procedures will be illustrated for two common-emitter saturating circuits by use of piecewise-linear equivalent circuits. For most designs, this type of equivalent circuit will be sufficiently accurate to give the necessary design equations and identify the important circuit parameters. Greater accuracy can of course be obtained by improving the approximations, especially if the important nonlinearities are included. As with vacuum tubes, statistical methods should be heavily relied upon, even with a nonlinear analysis.

### Saturated Equivalent Circuit

A common-emitter intrinsic blocking oscillator circuit is shown in Figure 32. Note that common-base and common-collector intrinsic circuits are also possible. The transistor's characteristics are illustrated by the family of collector curves in Figure 33 and by the input voltage-current curve of Figure 34. The circuit may be triggered on by inserting a current pulse into the base of the transistor by various methods. When triggered on, the path of operation will be similar to the dashed lines in Figure 33. During the rise period, the positive feedback drives the transistor on, and the collector voltage decreases until it bottoms on the saturation line. The magnetizing current for the transformer can be assumed to be zero during this short rise interval. As the magnetizing current increases during the main part of the pulse, the collector voltage and current increase along the saturation line, and the base drive decreases. At the base current  $I_{bx}$  the collector current comes out of saturation and reaches a maximum, thus limiting the maximum magnetizing current that can be supplied. The circuit then switches back to the stable state by following a path such as illustrated.





A linear approximation for the transistor characteristics during the main part of the pulse is the equivalent circuit shown in Figure 35. The saturation resistance  $R_s$  is the reciprocal of the slope of a straight line drawn through the origin and approximating the slope of the saturating line,  $B$  is the static current gain, and the collector saturation diode accounts for the excess current generated in the collector. The input portion of the equivalent circuit is obtained from the approximations shown in Figure 34.

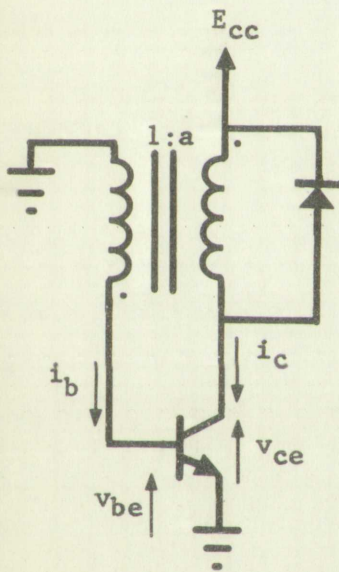


Figure 32. Common-Emitter Intrinsic Blocking Oscillator

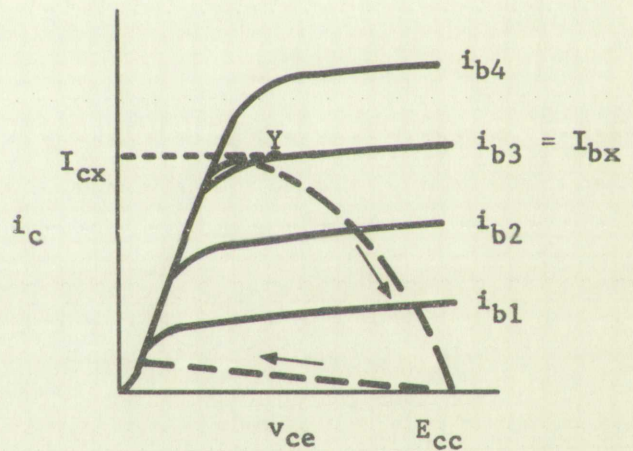


Figure 33. Typical Collector Characteristic and Path of Operation

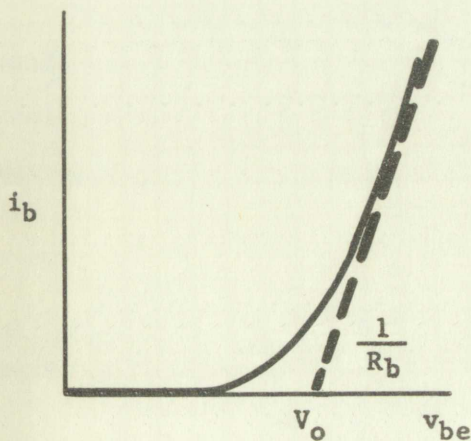


Figure 34. Input Characteristics and Linear Approximation

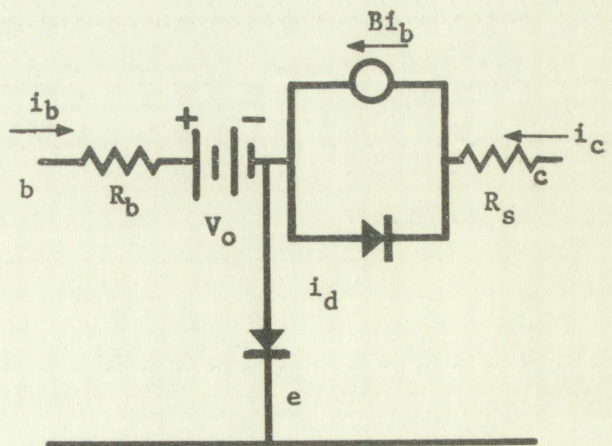
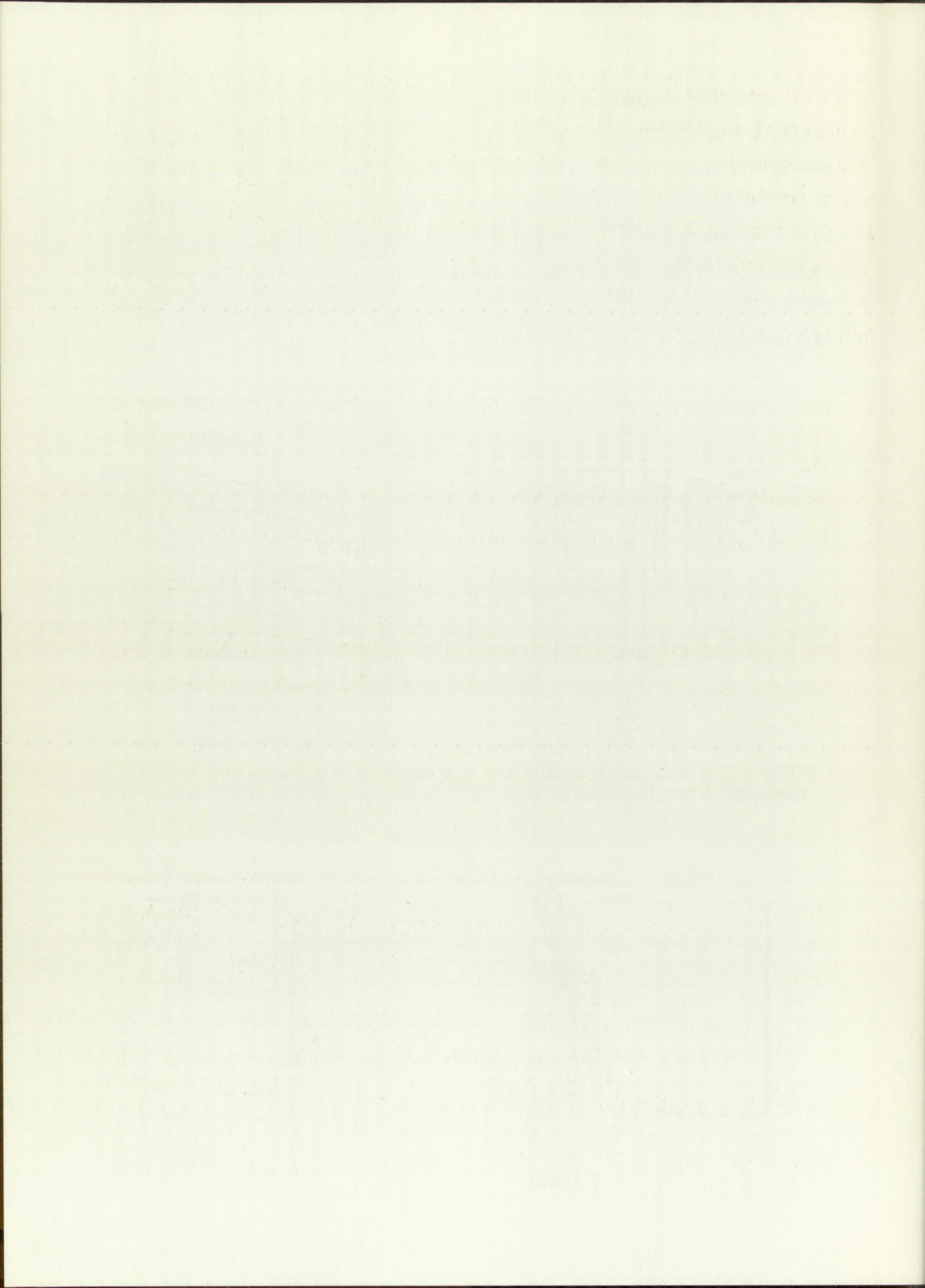


Figure 35. Saturated Transistor Equivalent Circuit



The evaluation of B near the saturation line can be somewhat arbitrary because of the curvature of the collector curves as the transistor comes out of saturation. More consistent results can be obtained by determining B in the active region where the collector current curves become more nearly flat parallel lines, such as point Y in Figure 33. At this point the current gain<sup>13</sup> is

$$B = \frac{I_{cx}}{I_{bx}} \quad (38)$$

Because the current gain varies slowly with base and collector current in the active region, the actual point of measurement is not critical. The result of this approximation will be a somewhat higher maximum collector current than actually occurs, but the equivalent circuit is in terms of easily measurable parameters.

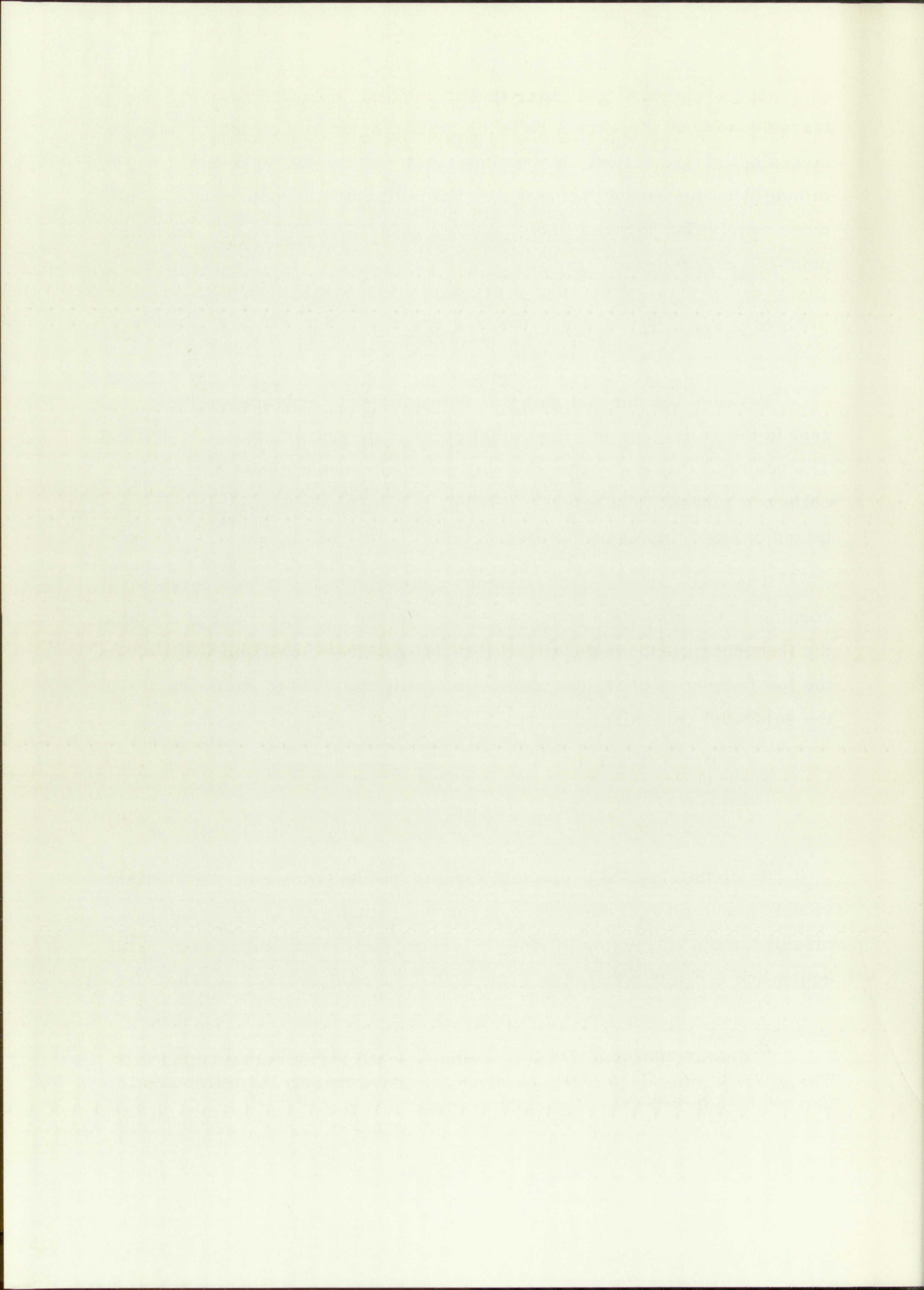
The transistor's high frequency characteristics are selected according to the rise time requirements. During the main part of the pulse, the frequency components will then be of relatively low frequency. Thus, the low frequency characteristics can usually be used to obtain values for the saturated equivalent circuit.

### Intrinsic Circuit Analysis

By combining the equivalent circuit for the transistor with the previously assumed equivalent circuit for the transformer, the equivalent circuit for the saturating intrinsic blocking oscillator is obtained. This equivalent circuit is shown in Figure 36. An analysis of a similar circuit,

---

<sup>13</sup> Another commonly used symbol for the static current gain is  $h_{FE}$ . The present symbol is used, however, since it has already been used to denote the current gain of vacuum tubes.



with and without an input capacitor, is given by Zimmermann and Mason [17, p. 467] with a more idealized equivalent circuit using small-signal parameters.

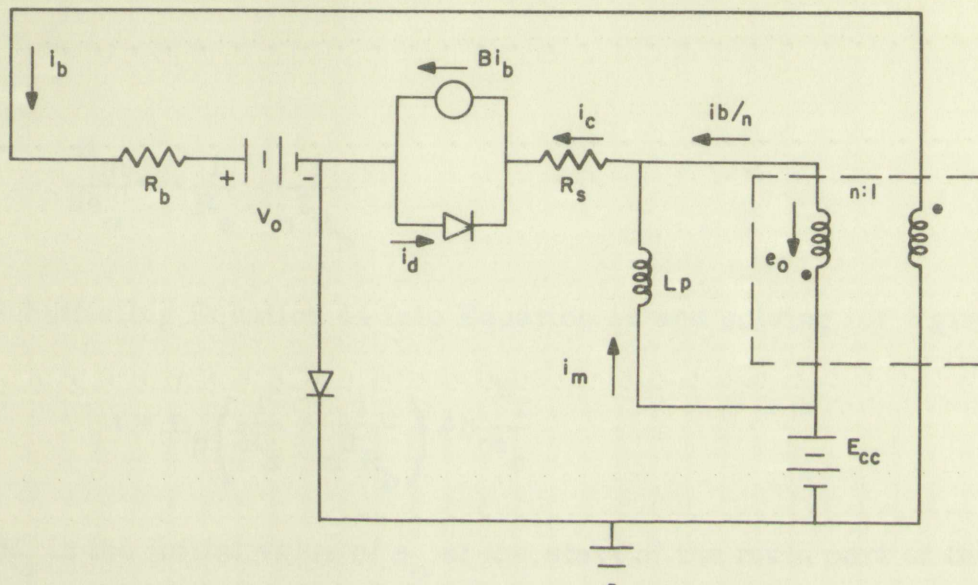


Figure 36. Equivalent Circuit for the Intrinsic Blocking Oscillator

The equations for this equivalent circuit<sup>14</sup> are

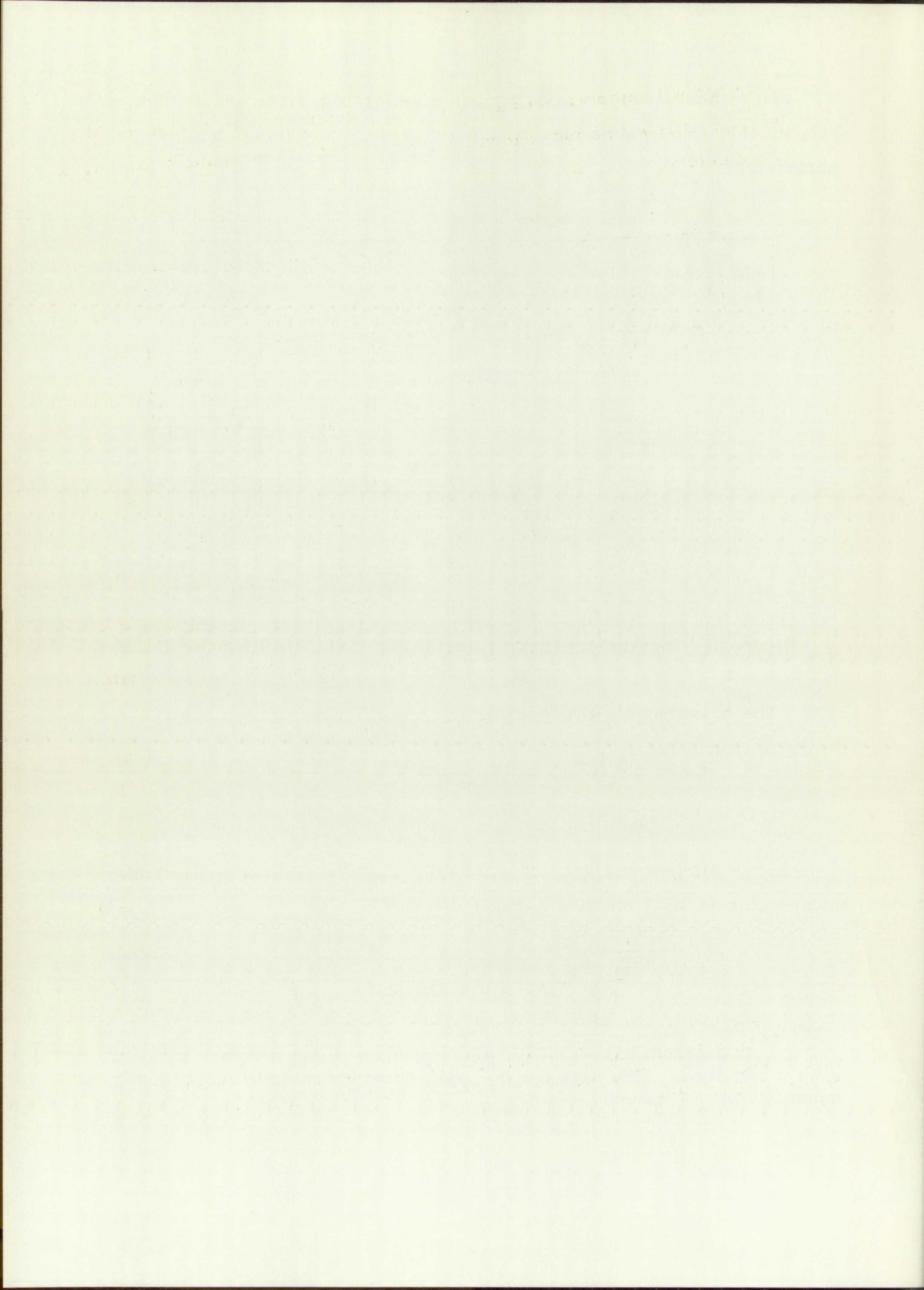
$$E_{cc} = e_o + i_c R_s \quad (39)$$

$$i_c = i_m + i_b/n \quad (40)$$

$$Bi_b = i_c + i_d \quad (41)$$

$$i_b = \frac{e_o}{nR_b} - \frac{V_o}{R_b} \quad (42)$$

<sup>14</sup>An external base-emitter bias has been neglected since it is not always required. This bias can be easily inserted into the subsequent equations when desired.



From these equations the magnetizing current as a function of  $e_o$  is found to be

$$i_m = \frac{E_{cc} - e_o}{R_s} - \frac{e_o}{n^2 R_b} + \frac{V_o}{R_b} \quad (43)$$

and

$$\frac{di_m}{de_o} = -\frac{1}{R_s} - \frac{1}{n^2 R_b} \quad (44)$$

Substituting Equation 44 into Equation 14 and solving for t gives

$$t = L_p \left( \frac{1}{R_s} + \frac{1}{n^2 R_b} \right) \ell \eta \frac{E_i}{e_o} \quad (45)$$

where  $E_i$  is the initial value of  $e_o$  at the start of the main part of the pulse.

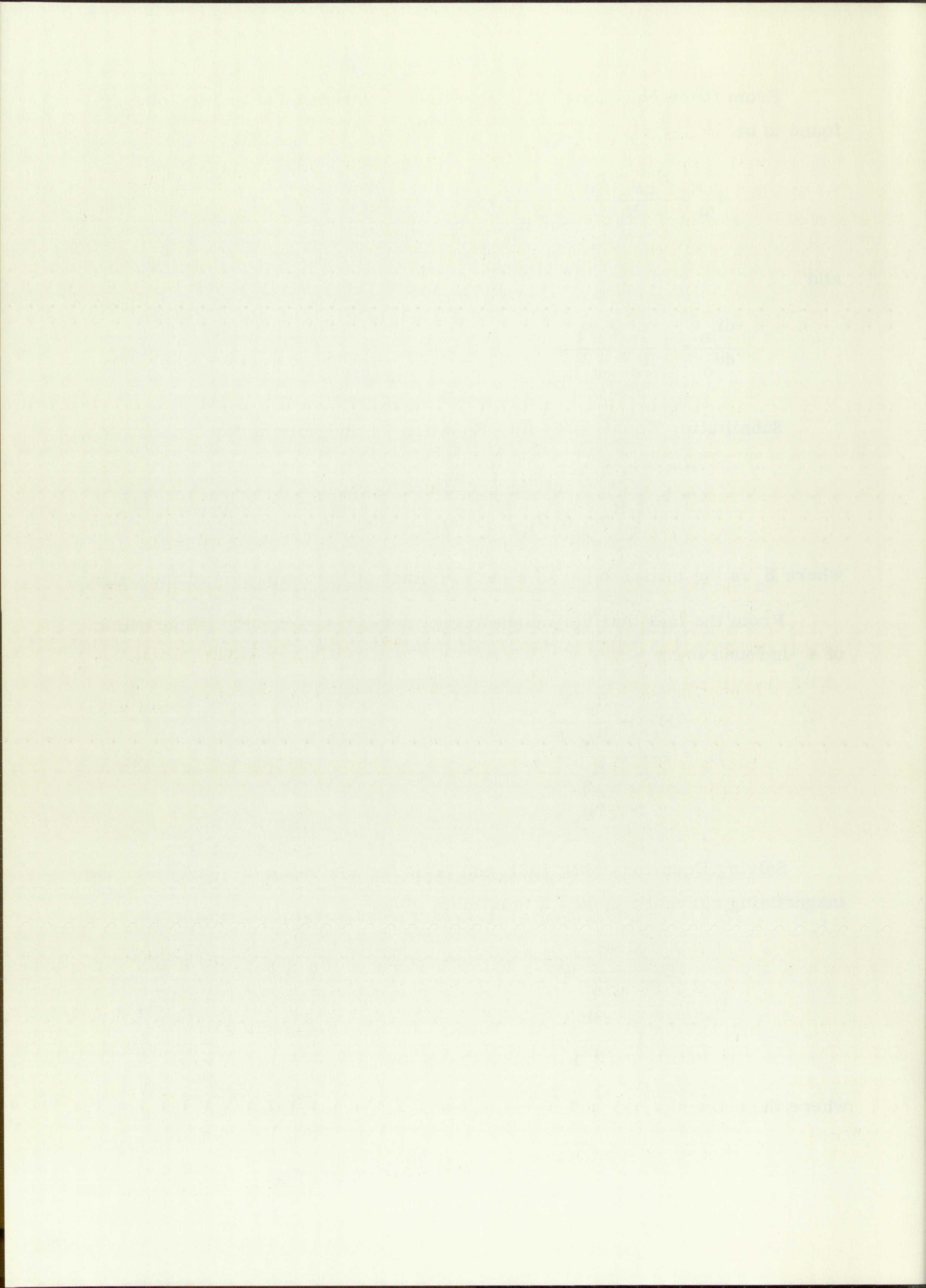
From the fact that the magnetizing current is zero, the initial value of  $e_o$  is found to be

$$E_i = \frac{E_{cc} + \frac{R_s}{R_b} \frac{V_o}{n}}{1 + \frac{R_s}{n^2 R_b}} \quad (46)$$

Solving Equations (38), (39), and (42), for the value of  $e_o$  at which the magnetizing current reaches a maximum gives

$$E_x = \frac{E_{cc} - \frac{R_s}{R_b} BV_o}{1 + \frac{R_s}{nR_b}} \quad (47)$$

where the subscript, x, refers to the value at the termination of the pulse.





The values of  $I_{bx}$  and  $I_{mx}$  can be shown to be

$$I_{bx} = \frac{E_x}{nR_b} - \frac{V_o}{R_b} \quad (48)$$

and

$$I_{mx} = I_{bx} \left( B - \frac{1}{n} \right) \quad (49)$$

Considering the duration of the main part of the pulse as the pulse width, the pulse width is given by

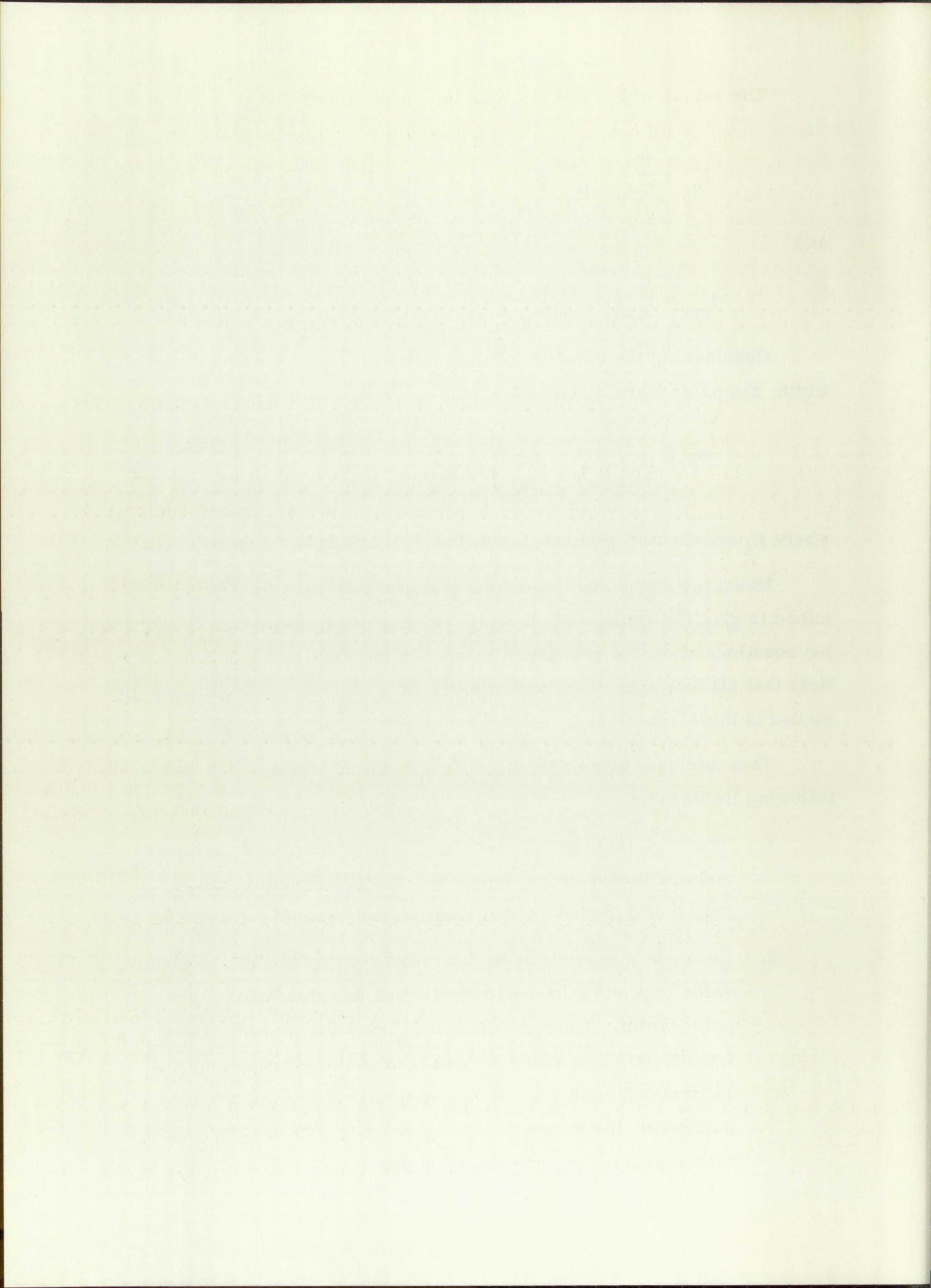
$$PW = L_p \left( \frac{1}{R_s} + \frac{1}{n^2 R_b} \right) \ell \eta \frac{E_i}{E_x} \quad (50)$$

where  $E_i$  and  $E_x$  are given by Equations (46) and (47), respectively.

Using the above equations, the transformer parameters can be determined to give the desired pulse width for a given transistor. In addition, the equations show the relationships among the various circuit parameters. Note that all four transistor parameters ( $R_s$ ,  $R_b$ ,  $V_o$ , and  $B$ ), are included in these equations.

This intrinsic circuit is of limited practical interest because of the following limitations:

1. The transistor parameters have manufacturing tolerances and are temperature-sensitive, and the resulting distribution of pulse width will have a considerable spread.
2. Because of the relatively low values of  $R_b$  and  $V_o$ , a high value of  $n$  and a low value of  $L_p$  are necessary for a given pulse width. The low value of  $L_p$  may present a difficult transformer design problem in preventing transformer saturation, especially if  $E_{cc}$  is high. If the transformer saturates, the magnetizing current may reach damagingly high levels during the storage time.



While the vacuum tube intrinsic blocking oscillator has been shown to be of great practical value, this transistor intrinsic blocking oscillator is primarily of academic interest. Many modifications are possible for improving this transistor circuit. One such circuit having greatly improved characteristics will be considered next.

### Current-Limited Blocking Oscillator

#### Analysis

A blocking oscillator circuit which has the maximum collector current limited by a relatively large resistance in the collector circuit is shown in Figure 37. An extensive analysis of a similar circuit has been made by Narud and Aaron [18], with particular emphasis on the rise time and triggering characteristics. The equivalent circuit for the saturation region is given in Figure 38.

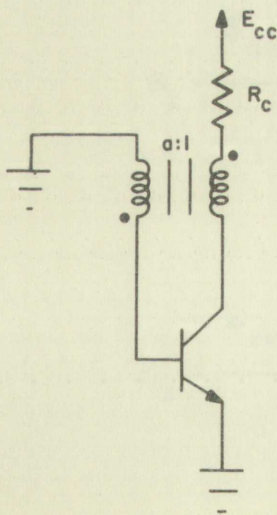


Figure 37. Current-Limited Blocking Oscillator

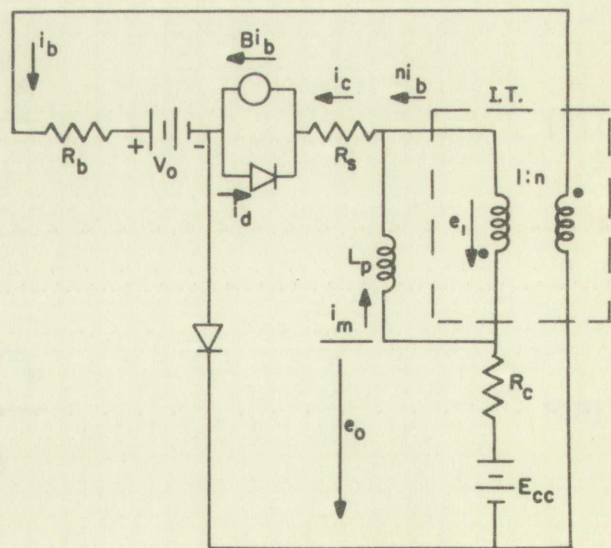


Figure 38. Equivalent Circuit



From Figure 38 the circuit equations are

$$E_{cc} = e_1 + i_c (R_c + R_s) \quad (51)$$

$$i_c = i_m + ni_b \quad (52)$$

$$Bi_b = i_c + i_d \quad (41)$$

$$i_b = \frac{ne_1 - V_o}{R_b} \quad (53)$$

The following equations may now be derived

$$I_{bx} = \frac{nE_x - V_o}{R_b} \quad (54)$$

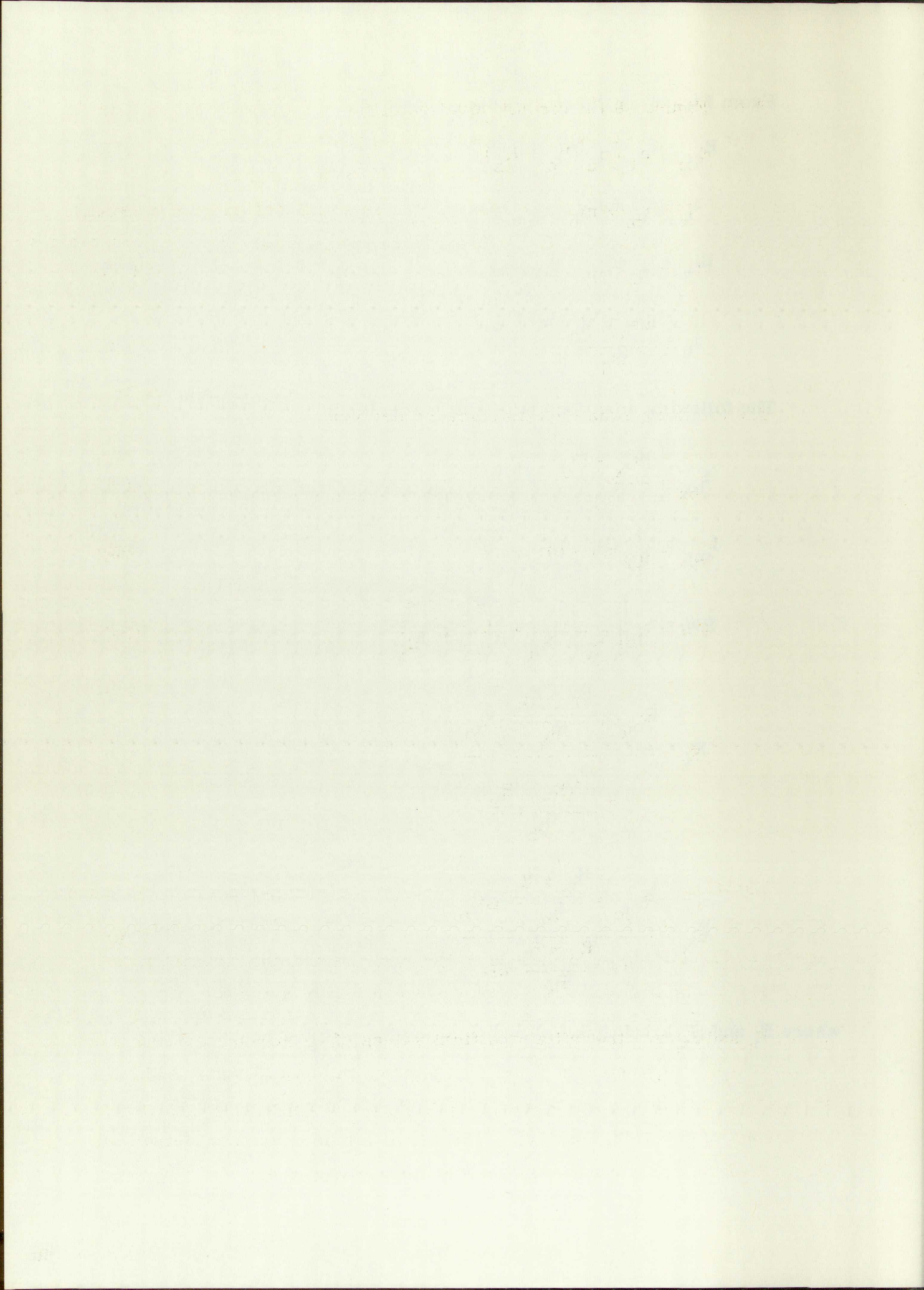
$$I_{mx} = I_{bx} (B - n) \quad (55)$$

$$PW = L_p \left[ \frac{1}{R_c + R_s} + \frac{n^2}{R_b} \right] \ell \eta \frac{E_i}{E_x} \quad (56)$$

$$E_i = \frac{E_{cc} + \frac{R_c + R_s}{R_b} nV_o}{1 + \frac{n^2(R_c + R_s)}{R_b}} \quad (57)$$

$$E_x = \frac{E_{cc} + \frac{R_c + R_s}{R_b} BV_o}{1 + \frac{R_c + R_s}{R_b} nB} \quad (58)$$

where  $E_i$  and  $E_x$  are the initial and final values of  $e_1$ , respectively.



From Equation (55) a necessary condition for a quasi-stable state is  $B > n$  since the magnetizing current must be positive and reach a value greater than zero. Normally,  $R_c \gg R_s$ ,  $R_c > R_b$ , and  $n > 1$ , and Equations (57) and (58) indicate that  $e_1$  will be small and most of the pulse voltage will appear across  $R_c$ . Under the condition that

$$R_c \gg \frac{R_b}{n},$$

then Equations (57) and (58) may be simplified with very little error to

$$E_i = \frac{R_b}{R_c} \frac{E_{cc}}{n} + \frac{V_o}{n} \quad (59)$$

$$E_x = \frac{R_b}{R_c} \frac{E_{cc}}{nB} + \frac{V_o}{n} \quad (60)$$

Equation (56) may then be reduced to

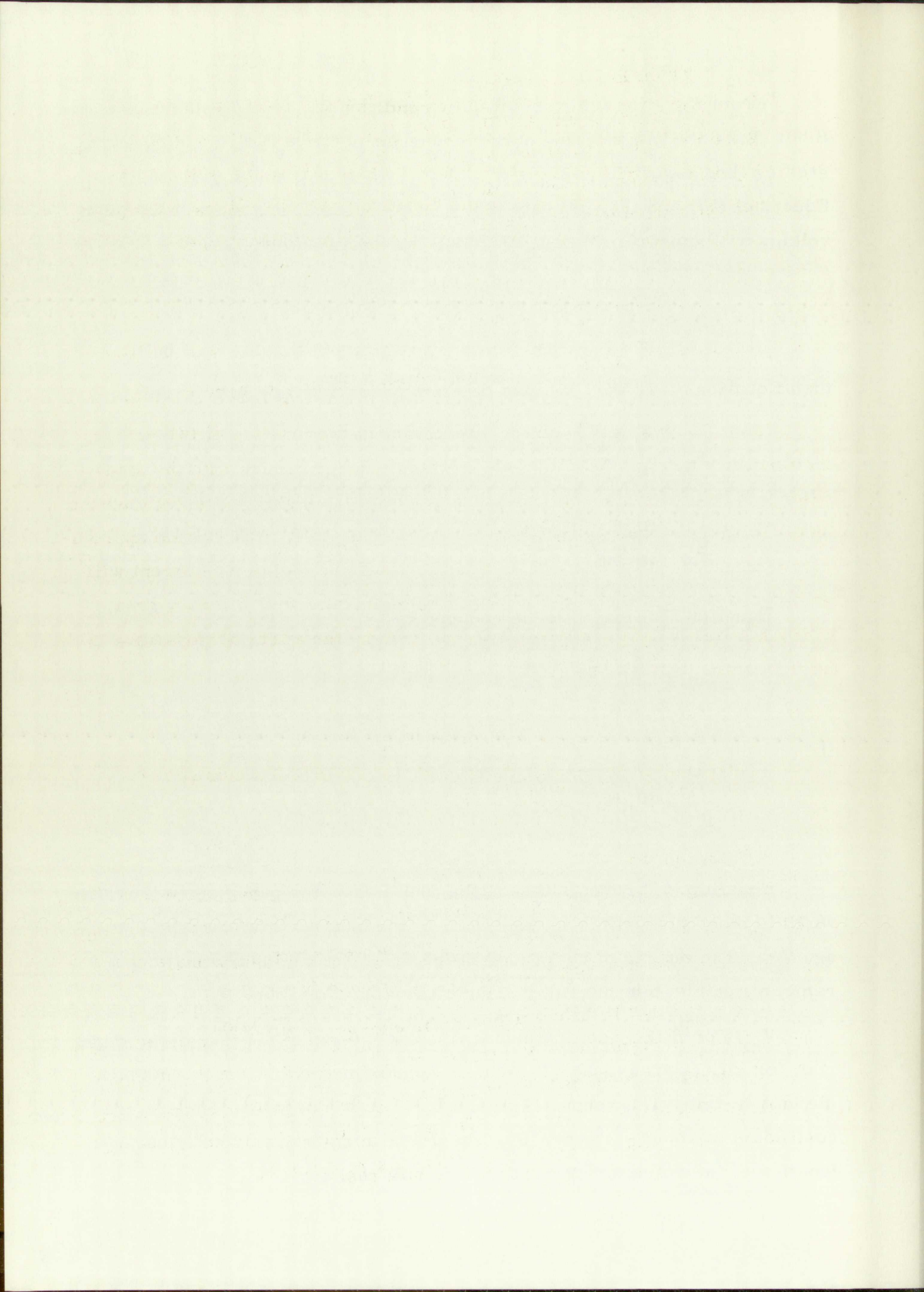
$$PW \cong \frac{nL_p (B - n) E_{cc}}{R_c B V_o} \quad (61)$$

if

$$R_c > \frac{5R_b E_{cc}}{V_o} \left( \frac{B - n}{nB} \right).$$

Equation (61) reveals that of the four transistor parameters the pulse width is most susceptible to variations in the base-emitter threshold voltage  $V_o$ . The effects of variations in the three remaining transistor parameters can be minimized by using high values for  $B$  and  $R_c$ .

$V_o$  is primarily determined by the energy gap of the transistor material; for silicon transistors  $V_o$  will be approximately 0.7 volt. Although the unit-to-unit variations will be small,  $V_o$  has a negative temperature coefficient of about  $-2.5 \text{ mv}/^\circ\text{C}$ . The actual temperature coefficient is a function of the collector current and the bulk resistance.





Resistor  $R_c$  may be considered as the parallel combination of the actual collector resistor and any external load resistance. The choice of value of collector resistor must be based on considerations of the source impedance desired, and the maximum collector current rating of the transistor, and also upon the fact that the transistor parameters are a function of the collector current.

Example

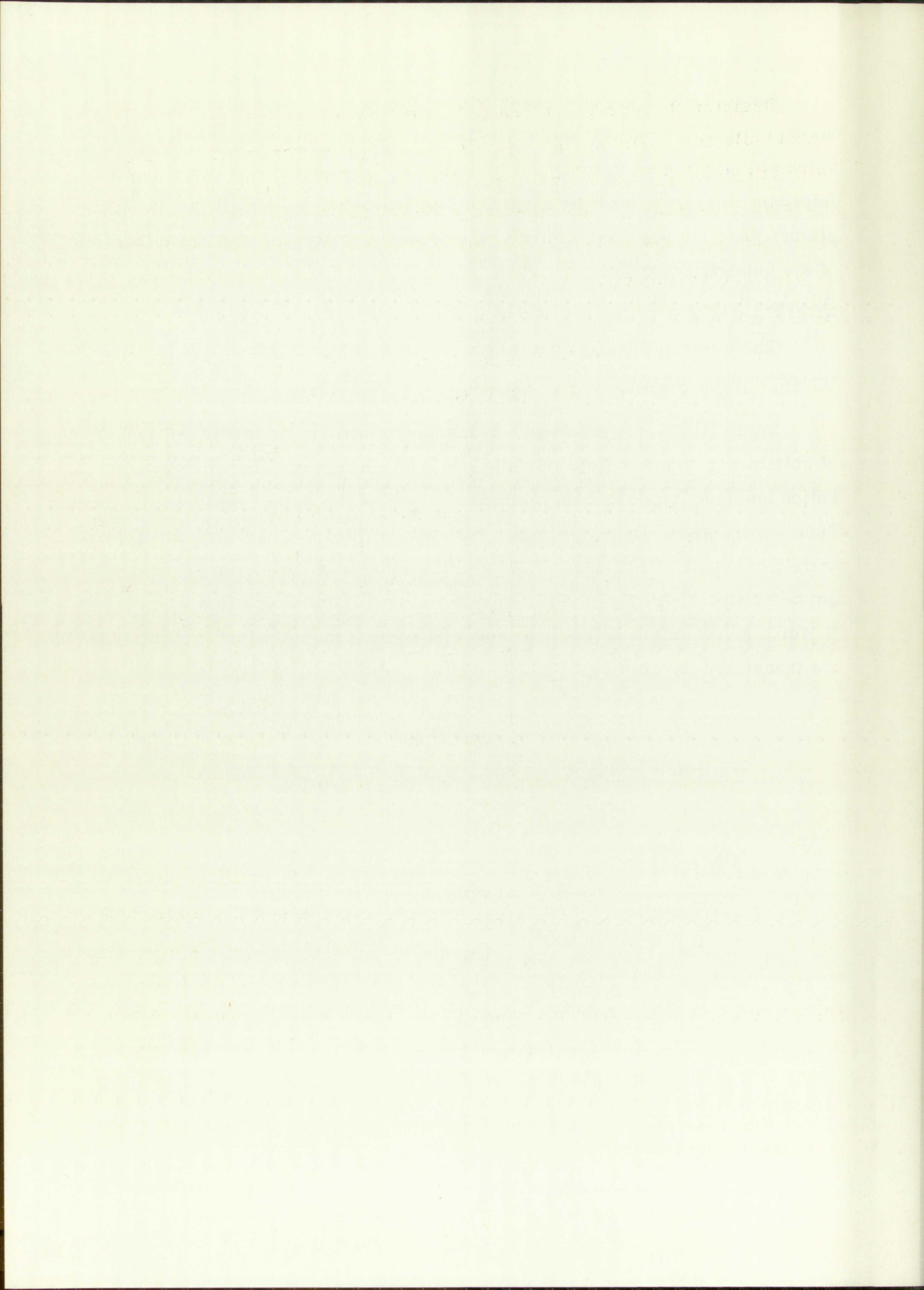
The effects of variations in the transistor parameters will be illustrated by data obtained with Type 2N1613 transistors.

Table III gives the average transistor characteristics at two values of collector current. Note that the greatest change occurs with the saturation and base resistances, both decreased at the higher collector current. Since, for a given supply voltage, the ratio of  $R_c$  to  $R_b$  will remain approximately constant, the values of  $R_c$  and the maximum collector current will not be critical. An increase in supply voltage, however, allows a greater  $R_c$  for a given collector current and will reduce the effect of variations in the transistor parameters.

TABLE III  
Parameter Means for Sample of Ten 2N1613 Transistors

Parameter	$I_c = 15 \text{ ma}$	$I_c = 200 \text{ ma}$
	$\bar{X}$	$\bar{X}$
B	74	71*
$R_s$	21 ohms	6 ohms
$V_o$	0.64 v	0.75 v
$R_b$	200 ohms	24 ohms

\*From a sample of 30



Results of pulse width measurements are given in Table IV for two values of collector resistance. From the sample of transistors the coefficient of variation of B was measured as 18 percent. The coefficient of variation of pulse width for the high collector resistance was 13 percent, from Table IV, as a result of the distributions of all four transistor parameters. Thus, it is evident that the effects of transistor variations have been attenuated.

The small spread in pulse width, with the low collector resistance, results from transformer saturation. Use of saturating transformers is very attractive in this circuit, since the maximum magnetizing current is limited by  $R_c$ .

TABLE IV  
Measurements\* on Sample of 30-2N1613

<u>Pulse Width</u>	<u><math>R_c = 1.5 \text{ k}</math></u>	<u><math>R_c = 100 \text{ ohms}</math></u>
$\bar{X}$	6.3 $\mu\text{s}$	22 $\mu\text{s}$
$\sigma$	0.82 $\mu\text{s}$	0.1 $\mu\text{s}$
V	13%	0.5%

\* Conditions:  $E_{cc} = 22 \text{ v}$ ,  $L_p = 75 \mu\text{h}$ ,  $a = 4$

Various means of temperature compensation, primarily to correct for the negative temperature coefficient of  $V_o$ , are possible. An obvious method from Equation (61) is to use a positive temperature coefficient resistance for  $R_c$ . Typical compensated and uncompensated variations of pulse width with temperature are shown in Figure 39. Temperature compensation was obtained by using a silicon resistor.<sup>15</sup> Since the temperature

<sup>15</sup> Manufactured by Texas Instruments, Incorporated, and given the trade name, Sensistor.

Results of a few runs with a constant  $\alpha$  are given in Table IV for two values of the temperature coefficient  $\beta$ . From the values of  $\beta$  and the constant  $\alpha$  of equation (1) we can calculate  $\beta$  as a function of  $\alpha$ . The condition of variation of  $\beta$  with  $\alpha$  for the sign collector circuit was 13 percent from Table IV, as a result of the distribution of all four transistors in parallel. This is evident from the values of  $\beta$  in Table IV.

The small spread in gain with the low collector resistances is due to the fact that the gain is not very sensitive to the variation of  $\beta$  in this circuit. The maximum gain variation is about 1 percent.

TABLE IV

Measurement conditions:  $V_{CC} = 10$  V,  $R_{C1} = R_{C2} = 10$  k $\Omega$ ,  $R_{E1} = R_{E2} = 10$  k $\Omega$ ,  $R_{B1} = R_{B2} = 10$  k $\Omega$ ,  $R_{B3} = 10$  k $\Omega$ ,  $R_{B4} = 10$  k $\Omega$ ,  $R_{B5} = 10$  k $\Omega$ ,  $R_{B6} = 10$  k $\Omega$ ,  $R_{B7} = 10$  k $\Omega$ ,  $R_{B8} = 10$  k $\Omega$ ,  $R_{B9} = 10$  k $\Omega$ ,  $R_{B10} = 10$  k $\Omega$ ,  $R_{B11} = 10$  k $\Omega$ ,  $R_{B12} = 10$  k $\Omega$ ,  $R_{B13} = 10$  k $\Omega$ ,  $R_{B14} = 10$  k $\Omega$ ,  $R_{B15} = 10$  k $\Omega$ ,  $R_{B16} = 10$  k $\Omega$ ,  $R_{B17} = 10$  k $\Omega$ ,  $R_{B18} = 10$  k $\Omega$ ,  $R_{B19} = 10$  k $\Omega$ ,  $R_{B20} = 10$  k $\Omega$ ,  $R_{B21} = 10$  k $\Omega$ ,  $R_{B22} = 10$  k $\Omega$ ,  $R_{B23} = 10$  k $\Omega$ ,  $R_{B24} = 10$  k $\Omega$ ,  $R_{B25} = 10$  k $\Omega$ ,  $R_{B26} = 10$  k $\Omega$ ,  $R_{B27} = 10$  k $\Omega$ ,  $R_{B28} = 10$  k $\Omega$ ,  $R_{B29} = 10$  k $\Omega$ ,  $R_{B30} = 10$  k $\Omega$ ,  $R_{B31} = 10$  k $\Omega$ ,  $R_{B32} = 10$  k $\Omega$ ,  $R_{B33} = 10$  k $\Omega$ ,  $R_{B34} = 10$  k $\Omega$ ,  $R_{B35} = 10$  k $\Omega$ ,  $R_{B36} = 10$  k $\Omega$ ,  $R_{B37} = 10$  k $\Omega$ ,  $R_{B38} = 10$  k $\Omega$ ,  $R_{B39} = 10$  k $\Omega$ ,  $R_{B40} = 10$  k $\Omega$ ,  $R_{B41} = 10$  k $\Omega$ ,  $R_{B42} = 10$  k $\Omega$ ,  $R_{B43} = 10$  k $\Omega$ ,  $R_{B44} = 10$  k $\Omega$ ,  $R_{B45} = 10$  k $\Omega$ ,  $R_{B46} = 10$  k $\Omega$ ,  $R_{B47} = 10$  k $\Omega$ ,  $R_{B48} = 10$  k $\Omega$ ,  $R_{B49} = 10$  k $\Omega$ ,  $R_{B50} = 10$  k $\Omega$ ,  $R_{B51} = 10$  k $\Omega$ ,  $R_{B52} = 10$  k $\Omega$ ,  $R_{B53} = 10$  k $\Omega$ ,  $R_{B54} = 10$  k $\Omega$ ,  $R_{B55} = 10$  k $\Omega$ ,  $R_{B56} = 10$  k $\Omega$ ,  $R_{B57} = 10$  k $\Omega$ ,  $R_{B58} = 10$  k $\Omega$ ,  $R_{B59} = 10$  k $\Omega$ ,  $R_{B60} = 10$  k $\Omega$ ,  $R_{B61} = 10$  k $\Omega$ ,  $R_{B62} = 10$  k $\Omega$ ,  $R_{B63} = 10$  k $\Omega$ ,  $R_{B64} = 10$  k $\Omega$ ,  $R_{B65} = 10$  k $\Omega$ ,  $R_{B66} = 10$  k $\Omega$ ,  $R_{B67} = 10$  k $\Omega$ ,  $R_{B68} = 10$  k $\Omega$ ,  $R_{B69} = 10$  k $\Omega$ ,  $R_{B70} = 10$  k $\Omega$ ,  $R_{B71} = 10$  k $\Omega$ ,  $R_{B72} = 10$  k $\Omega$ ,  $R_{B73} = 10$  k $\Omega$ ,  $R_{B74} = 10$  k $\Omega$ ,  $R_{B75} = 10$  k $\Omega$ ,  $R_{B76} = 10$  k $\Omega$ ,  $R_{B77} = 10$  k $\Omega$ ,  $R_{B78} = 10$  k $\Omega$ ,  $R_{B79} = 10$  k $\Omega$ ,  $R_{B80} = 10$  k $\Omega$ ,  $R_{B81} = 10$  k $\Omega$ ,  $R_{B82} = 10$  k $\Omega$ ,  $R_{B83} = 10$  k $\Omega$ ,  $R_{B84} = 10$  k $\Omega$ ,  $R_{B85} = 10$  k $\Omega$ ,  $R_{B86} = 10$  k $\Omega$ ,  $R_{B87} = 10$  k $\Omega$ ,  $R_{B88} = 10$  k $\Omega$ ,  $R_{B89} = 10$  k $\Omega$ ,  $R_{B90} = 10$  k $\Omega$ ,  $R_{B91} = 10$  k $\Omega$ ,  $R_{B92} = 10$  k $\Omega$ ,  $R_{B93} = 10$  k $\Omega$ ,  $R_{B94} = 10$  k $\Omega$ ,  $R_{B95} = 10$  k $\Omega$ ,  $R_{B96} = 10$  k $\Omega$ ,  $R_{B97} = 10$  k $\Omega$ ,  $R_{B98} = 10$  k $\Omega$ ,  $R_{B99} = 10$  k $\Omega$ ,  $R_{B100} = 10$  k $\Omega$ .

Further means of temperature compensation, primarily to correct for the negative temperature coefficient of  $\beta$ , are discussed in the following section. Figure 10 shows a positive temperature coefficient circuit for  $\beta$ . Typical operating and temperature stability data for this circuit are shown in Figure 11. Temperature compensation was obtained by using a silicon resistor. From the temperature

characteristics of these resistors, indicated in Figure 12, and from the

coefficient of silicon resistors is  $+0.7\% / ^\circ\text{C}$ , the desired temperature coefficient can be obtained by combining the silicon resistor with ordinary resistors; the network used in this example was a 510-ohm carbon resistor in series with an 820-ohm silicon resistor.

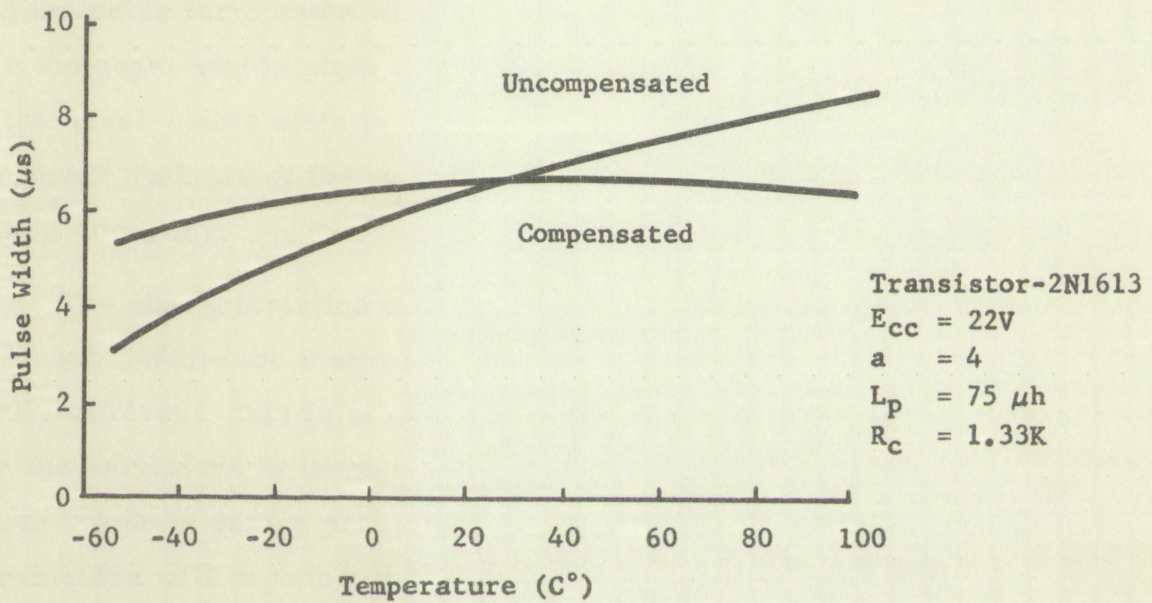
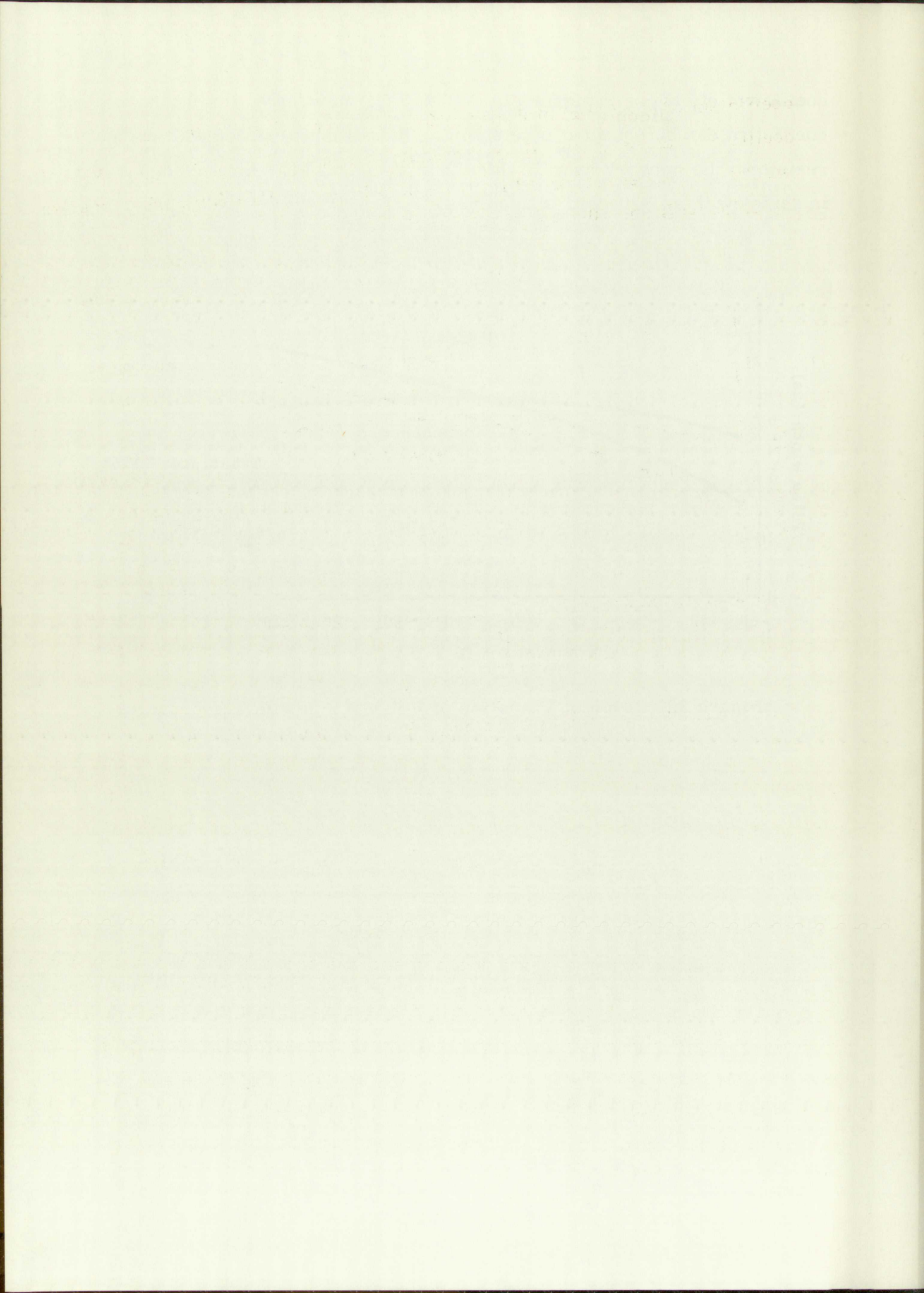


Figure 39. Typical Variation of Pulse Width with Temperature



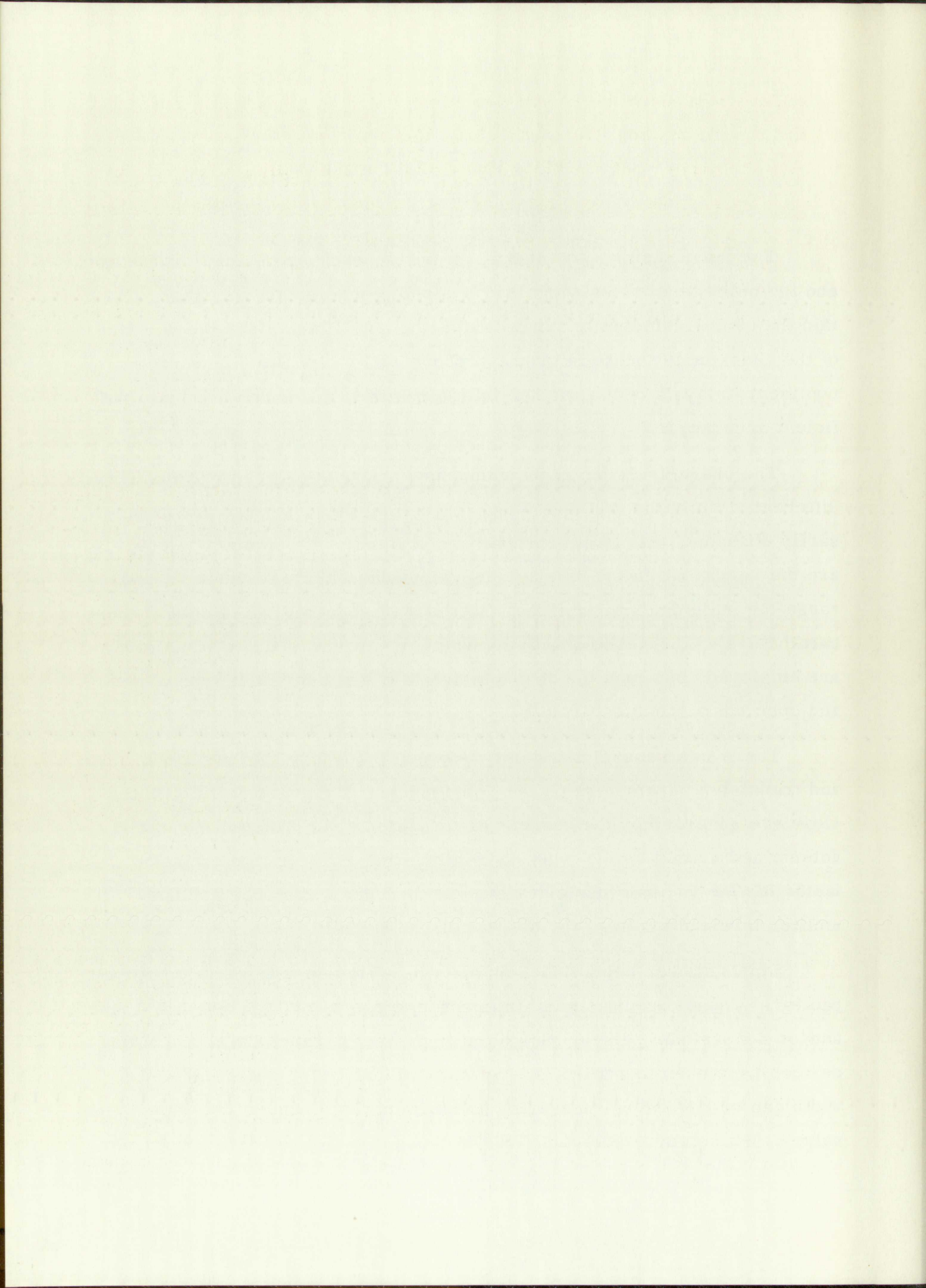
## CHAPTER VII -- CONCLUSIONS

The magnetizing current that the active device can supply is limited, and the pulse terminates when the physical requirements necessary to sustain the quasi-stable state can no longer be satisfied. Since the duration of the quasi-stable state is greatly influenced by circuit nonlinearities, a nonlinear analysis of the vacuum tube circuits is necessary to obtain sufficient accuracy.

The characteristics of vacuum tubes and transistors are considerably different. While the methods of approximating these devices are necessarily different, this is of secondary importance. Of primary interest are the variations in the parameters, since the effects of these variations cause the main design problems. Methods of reducing the effects of these parameters will depend not only on whether vacuum tubes or transistors are employed, but upon the characteristics of the particular type of device and upon the particular circuit.

There is a general similarity between the effects of the vacuum tube and transistor parameters on the pulse shape. The pulse amplitude and slope are governed by the current gain parameters. The pulse width is determined mainly by the input characteristics—the current emission factor for the vacuum tube circuits, and the base resistance and base-emitter threshold voltage for the transistor circuits.

Emphasis has been placed on circuits which do not use an input capacitor. These circuits are of interest for generating high repetition rate and/or nonperiodic pulses. Since the important parameters of the active devices have been identified, the spreads in both pulse amplitude and width can be limited by measuring and eliminating those units with extreme values. Pulse amplitude variations in these circuits can also be reduced



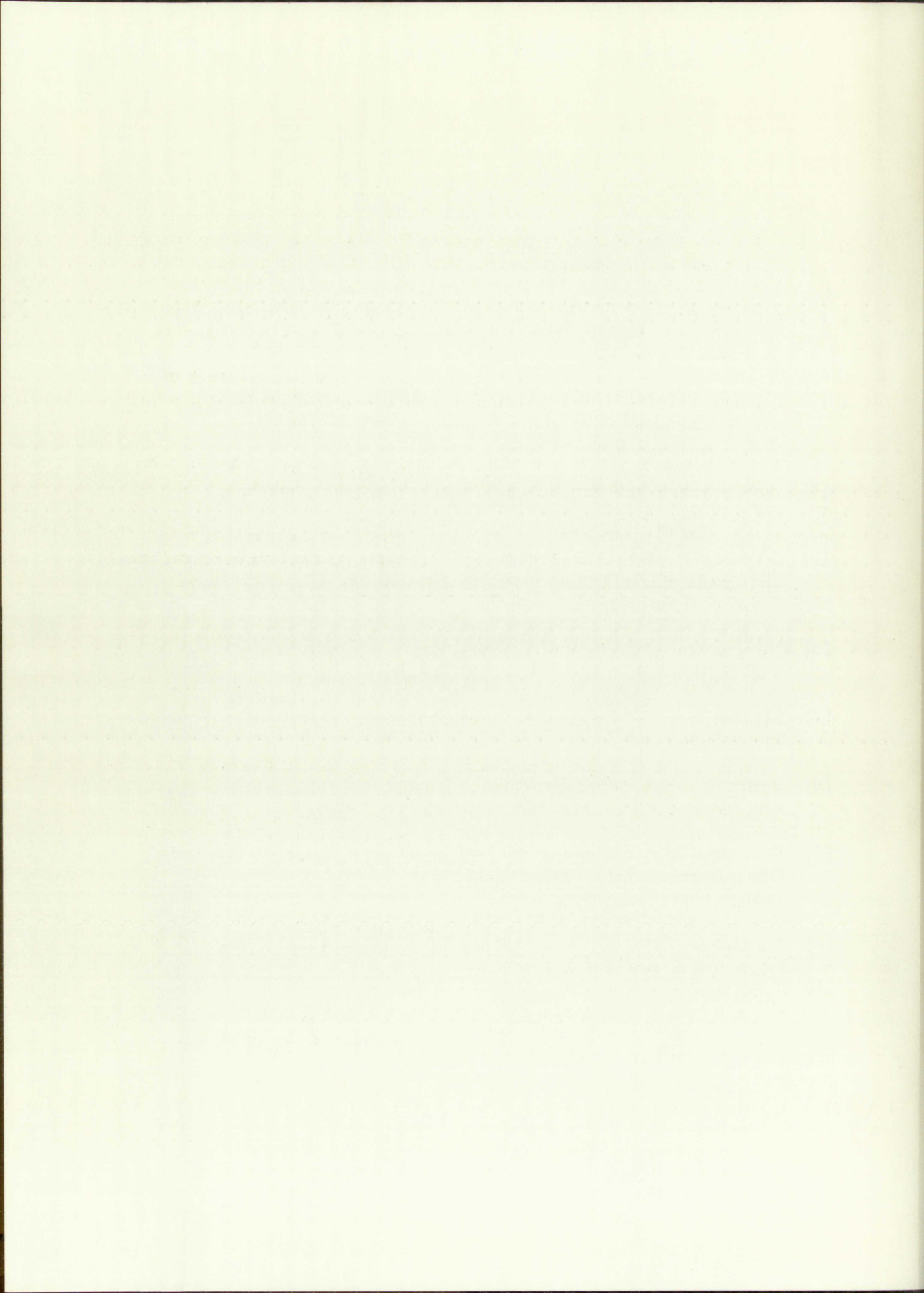


by the methods which have been described, or by amplitude limiting with a Zener diode or other fixed potential. The only feasible means of controlling the pulse width to very close limits, without using either an external turnoff pulse or an input capacitor, appears to be a combination of amplitude control and the use of a saturating transformer.

by the method which has been described or by another method with a factor which is other than unity. The only possible method of such a kind is to use a factor which is other than unity. It appears to be a combination of small factors or an exact equality. It appears to be a combination of small factors and the use of a saturating reagent.

## LIST OF REFERENCES

- [1] Lee, R., Electronic Transformers and Circuits, 2nd Ed., John Wiley and Sons, Inc., New York, N. Y., 1955.
- [2] Owens, C. D., "A Survey of the Properties and Applications of Ferrites Below Microwave Frequencies," Proc. IRE, Vol. 44, pp. 1234-1248, October 1956.
- [3] Lange, H., "Current Division in Triodes and its Significance in the Determination of Contact Potential," Zeitschrift für Hochfrequenz, Vol. 31, pp. 105-196, 1928.
- [4] Spangenberg, K. R., Vacuum Tubes, McGraw-Hill Book Co., Inc., New York, N. Y., 1948.
- [5] Jonker, J. H. L., and Tellegen, B. D. H., "Current to a Positive Grid in Electron Tubes," Phillips Research Reprints, Vol. 1, pp. 13-32, October 1945.
- [6] Nergaard, L. S., "Studies of the Oxide Cathode," R. C. A. Review, Vol. 13, pp. 464-545, 1952.
- [7] Strauss, L., Wave Generation and Shaping, McGraw-Hill Book Co., Inc., 1960.
- [8] Smith, J. M., "Millimicrosecond Blocking Oscillators," Electronic Eng, Vol. 29, pp. 184-186, April 1957.
- [9] Schenkel, H., and Statz, H., "Junction Transistors with Alpha Greater than Unity," Proc. IRE, Vol. 44, pp. 360-371, March 1956.
- [10] Messenger, G. C., "The Effects of Neutron Irradiation on Germanium and Silicon," Proc. IRE, Vol. 46, pp. 1038-1044, June 1958.
- [11] Behrens, W. V., and Shaul, J. M., "The Effects of Short-Duration Neutron Radiation on Semiconductor Devices," Proc. IRE, Vol. 46, pp. 601-605, March 1958.



- [12] Loferski, J. J., "Analysis of the Effects of Nuclear Radiation on Transistors," J. Appl. Phys., Vol. 29, pp. 35-40, January 1958.
- [13] Ebers, J. J., and Moll, J. L., "Large-Signal Behavior of Junction Transistors," Proc. IRE, Vol. 42, pp. 1761-1772, December 1954.
- [14] Moll, J. L., "Large-Signal Transient Response of Junction Transistors," Proc. IRE, Vol. 42, pp. 1773-1784, December 1954.
- [15] Linvill, J. C. and Mattson, R. H., "Junction Transistor Blocking Oscillators," Proc. IRE, Vol. 43, pp. 1632-1638, November 1955.
- [16] Senatorov, K. Ya., and Guzhov, V. P., "On the Analysis of Processes in Transistor Blocking Oscillators," Radio-tehnika i Elektronika, Vol. 2, No. 9, pp. 1119-1126, 1957.
- [17] Zimmermann, H. J., and Mason, S. J., Electronic Circuit Theory, John Wiley and Sons, Inc., New York, N. Y., 1959.
- [18] Narud, J. A., and Aaron, M. R., "Analysis and Design of a Transistor Blocking Oscillator Including Inherent Nonlinearities," Bell System Tech. J., Vol. 38, No. 3, pp. 785-852, 1959.

118] Lohr, J. L. "Analysis of the Effects of the First Reaction on  
 Transients." IEEE Trans. on Power Apparatus and Systems, Vol. 82, No. 1, January 1963.

119] Egan, J. J., and Holt, J. L. "Large-Signal Behavior of the  
 Transient." Proc. IRE, Vol. 53, pp. 1771-1773, December 1965.

120] Holt, J. L. "Large-Signal Transient Response of Junction Trans-  
 istors." Proc. IRE, Vol. 53, pp. 1764-1766, December 1965.

121] Holt, J. L., and Egan, J. J. "Transient Behavior of Junction  
 Transistors." IEEE Trans. on Power Apparatus and Systems, Vol. 82, No. 11, November 1963.

122] Benoit, R. J., and Egan, J. J. "The Analysis of  
 Transients in Transistor Switching Circuits." IEEE Trans. on  
 Electrical Engineering, Vol. 82, pp. 1119-1120, 1963.

123] Egan, J. J., and Holt, J. L. "The First-Cut-Off Theory  
 of Junction Transistors." IEEE Trans. on Power Apparatus and  
 Systems, Vol. 82, No. 1, January 1963.

124] Holt, J. L., and Egan, J. J. "Analysis and Design of  
 Transistor Switching Circuits." IEEE Trans. on Power Apparatus and  
 Systems, Vol. 82, No. 1, January 1963.

## APPENDIX A

### TUBE CURVE PLOTTER

Vacuum tubes may be permanently damaged by operation at high current densities in the positive grid region for periods exceeding a few milliseconds. Pulse techniques are therefore necessary to obtain tube data in this region.

A circuit to plot the characteristic curves by means of an X-Y plotter is shown in Figure A-1. A low impedance pulse generator supplies the grid voltage pulse, and the VTVM is used to measure the pulse amplitude. A sweep generator drives a triode to sweep the plate voltage over the desired range, and this voltage is also supplied to the horizontal axis of the plotter through a voltage divider.

The plate and grid current pulses are converted into a DC voltage by the transformers and networks shown, and the switch selects the voltage to be applied to the vertical axis. The transformers use a large step-up turns ratio so that the load reflected into the plate and grid circuits will be small, and so that an output voltage much greater than the diode threshold is available. The primary inductance of the transformers must be high in relation to the reflected load, so that appreciable current is not shunted from the load; this necessitates a relatively large core area.

The threshold of the diodes results in no output for the first 50 milliamperes of plate and grid current. The output voltage at higher currents is very linear, however. The error due to the diodes is compensated for by offsetting the vertical axis of the plotter an equivalent of the 50-milliamperere error. While the writing speed is limited by the response of the plotter, a set of curves, such as was shown in Figure 8, can easily be obtained in ten minutes.

THEORY OF THE ...

The first part of the theory is concerned with the ...

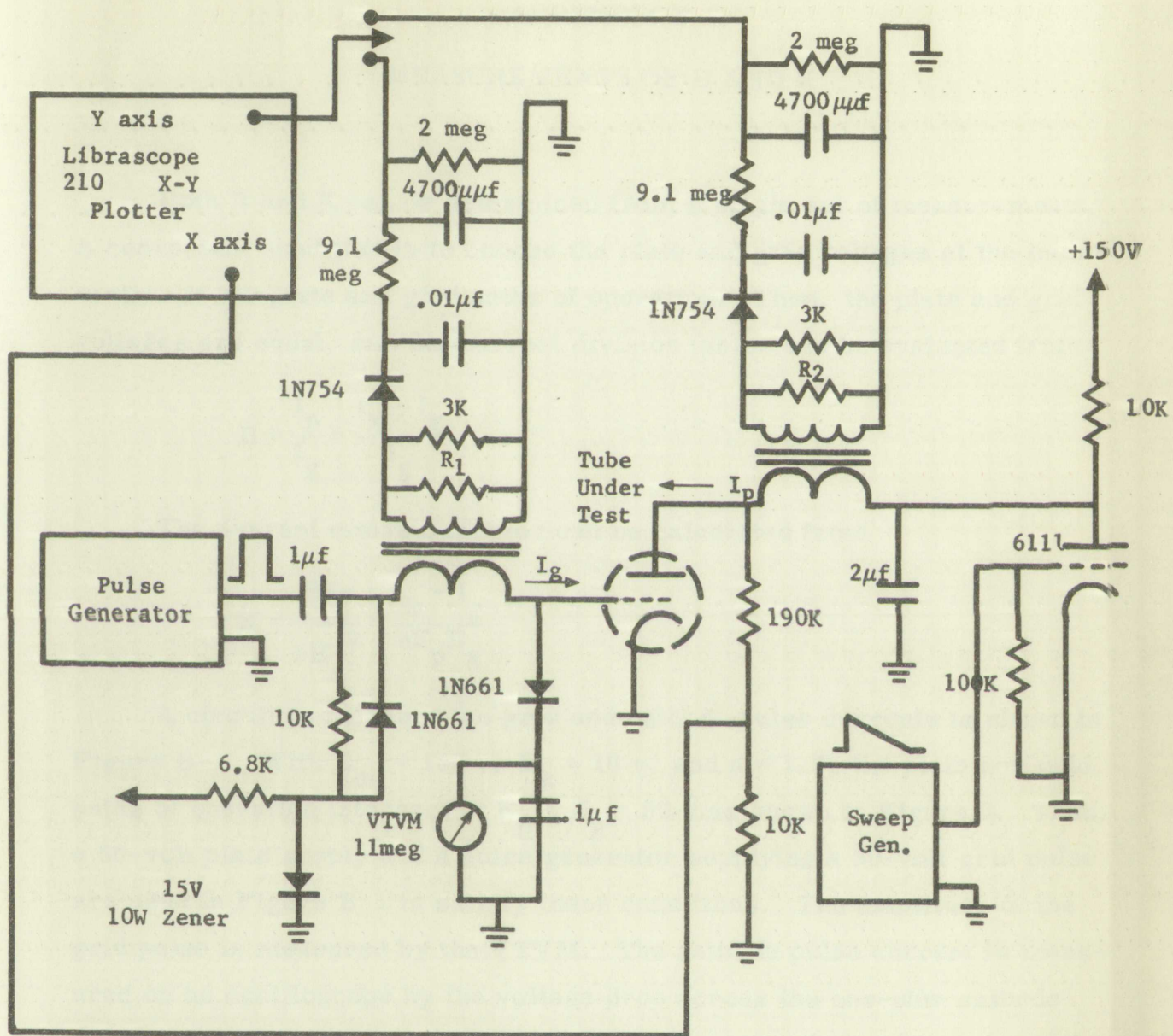
A further part of the theory is concerned with the ...

The third and last part of the theory is concerned with the ...

It is clear that the theory is concerned with the ...

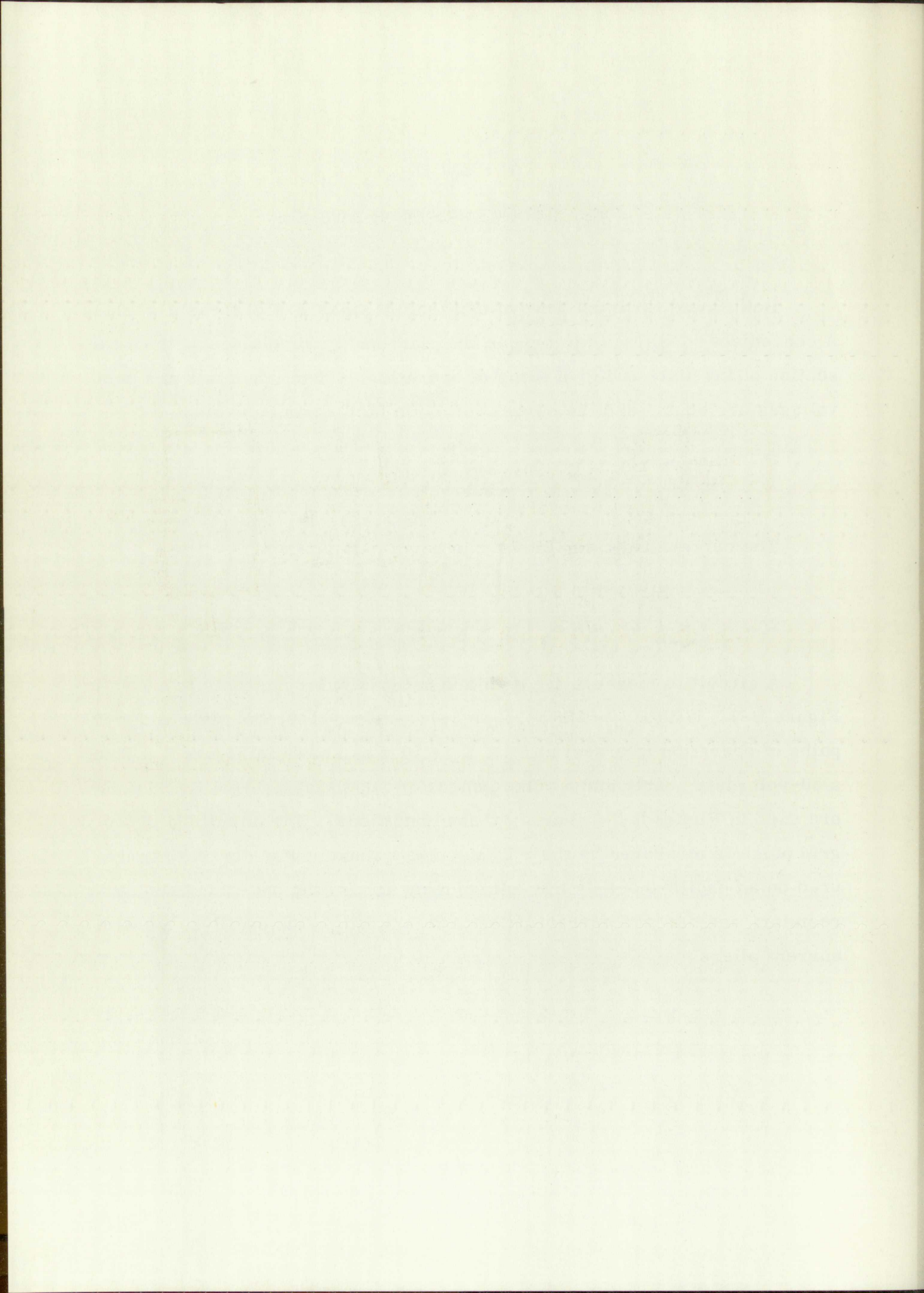
The theory is concerned with the ...





$R_1$  and  $R_2$  are calibration resistors  
 $R_1 = 10\text{K}$   
 $R_2 = 8.2\text{K}$

Figure A-1. Circuit for Plotting the Positive-Grid Characteristics



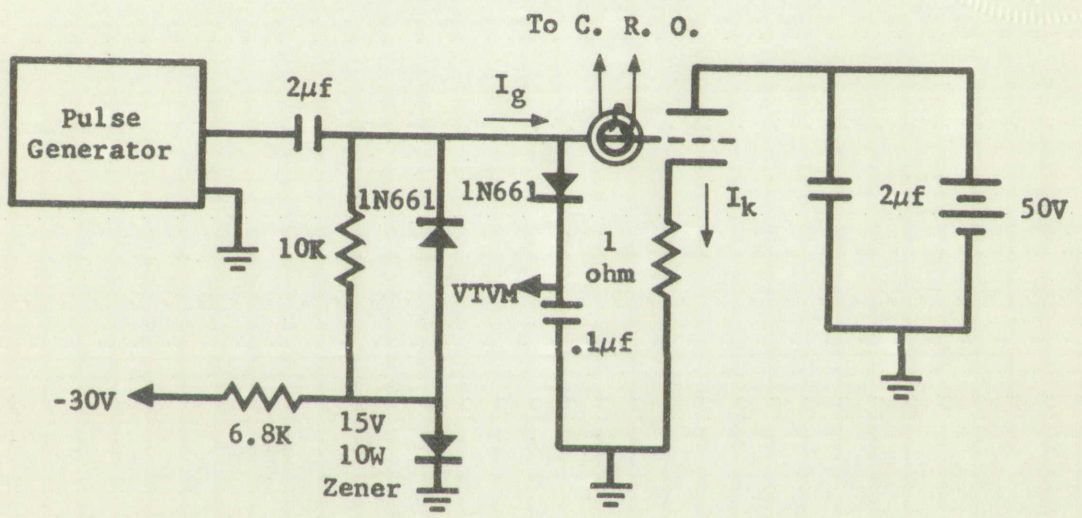


Figure B-1. Circuit for Measuring B and K

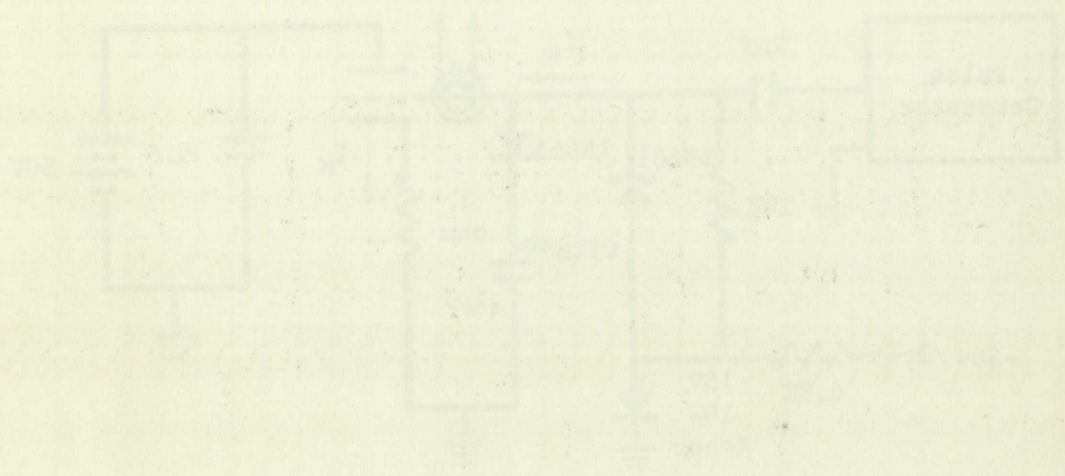
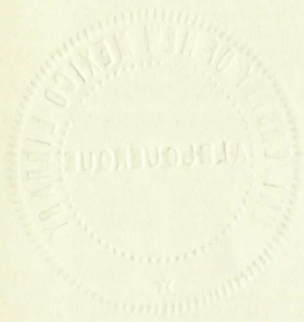


Figure 1. Circuit for measuring  $\beta$  and  $X$

UNIVERSITY OF TORONTO  
LIBRARY  
130 St. George Street  
Toronto, Ontario  
M5S 1A5

THE  
AMERICAN  
COPYRIGHT  
BOARD  
INCORPORATED  
NEW YORK

